



Norwegian University of
Science and Technology

A thermogravimetric and kinetic study on devolatilization of biomass

Thanh Nguyen Cong

Master of Energy and Environmental Engineering

Submission date: June 2018

Supervisor: Terese Løvås, EPT

Co-supervisor: Liang Wang, Sintef

Norwegian University of Science and Technology
Department of Energy and Process Engineering

Table of Contents

Acknowledgements.....	4
Abstract.....	5
Research objectives.....	6
List of abbreviations	7
Biomass and waste resources for energy production/purposes.....	8
Biomass composition.....	13
Cellulose	13
Hemicellulose	14
Lignin.....	15
Protein.....	16
Lipids	17
Other carbohydrates.....	17
Biomass conversion technologies	18
Thermochemical conversion.....	20
Pyrolysis.....	20
Types of pyrolysis processes.....	22
Slow pyrolysis.....	22
Fast pyrolysis	22
Flash pyrolysis	23
Carbonization.....	24
Intermediate pyrolysis.....	24
Ultra-rapid pyrolysis	25
Vacuum pyrolysis	25
Hydropyrolysis.....	25
Combustion	26
Gasification.....	28
Hydrothermal Liquefaction.....	31

Pretreatment techniques	33
Biological pretreatment.....	34
Physical pretreatment.....	35
Milling.....	35
Extrusion.....	36
Ultrasound pretreatment.....	36
Hydrodynamic cavitation.....	37
Microwave pretreatment.....	37
Chemical and physicochemical pretreatment.....	38
Torrefaction.....	38
Steam explosion.....	38
Liquid hot water treatment.....	39
Acid hydrolysis.....	39
Alkaline hydrolysis.....	40
Wet oxidation.....	41
CO ₂ explosion.....	41
Pyrolysis reactor and configurations.....	42
Fixed bed reactors.....	43
Fluidized bed reactors – BFB and CFB.....	43
Ablative pyrolysis reactors.....	46
Auger/screw reactors.....	47
Rotating cone reactors.....	48
Ultra-rapid reactors.....	49
Vacuum pyrolysis reactor.....	49
Analytical techniques for organic matter devolatilization investigations.....	50
Thermogravimetric analysis (TG/TGA).....	51
Mass spectrometry (MS).....	53
Fourier Transform Infrared Spectroscopy (FTIR).....	57
Gas chromatography (GC).....	58

Chemistry of lignocellulosic biomass decomposition.....	59
Reactions occurring during devolatilization and potential products.....	59
Biomass devolatilization kinetic modeling and evaluation.....	67
Effect of pyrolysis parameters on the process performance	74
Effect of biomass constituents	75
Effect of temperature and heating rate.....	76
Effect of particle size	77
Effect of residence time	78
Effect of pressure	78
Experimental procedure	79
Materials	79
TGA procedure	79
Results and discussion	80
TGA	80
Blank tests.....	80
General decomposition behaviours of spruce and birch wood sample	84
Kinetic evaluation	94
Conclusions.....	97
List of tables and figures.....	98
References.....	100

EPT-M-2018-120

MASTER THESIS

for

Student Nguyen Cong Thanh

Spring 2018

A thermogravimetric and kinetic study on devolatilization of biomass

Background and objective

Biomass has a great potential to be used for energy purpose. However, conversion behaviors of biomass materials are significantly different than for fossil fuel such as coal and can vary in a wide range depending on the raw material properties. In addition, the conversion process conditions, such as temperature, heating rate and atmosphere, have great effects on the thermal conversion behavior and the efficiency of biomass and waste materials conversion processes. Devolatilization is a very important primary step during thermal conversion of biomass materials with high volatile matter content. Reactions occurring during devolatilization of biomass materials, conversion degree of the raw feedstock, distribution of gas and solid products, further reactions of volatiles and degradation of char etc. are important aspects. Thermogravimetric analysis (TGA) is an efficient and useful tool to characterize devolatilization behaviors of biomass materials under conditions. The objective of this project is to investigate devolatilization behaviors of selected biomass under different conditions via thermogravimetric analyzer (TGA). Devolatilization of representative biomass materials are studied by using a thermogravimetric analyzer (TGA) for studying decomposition behaviors and possible reaction mechanisms of two biomass feedstocks under different conditions.

The following tasks are to be considered:

1. Literature study
 - a. Biomass for energy production
 - b. Devolatilization behaviours and reactions of biomass
 - c. Analytical techniques for studying devolatilization of biomass
 - d. Biomass devolatilization kinetic modelling and evaluation
2. Experimental study
 - a. General characterization of selected biomass materials
 - b. TG study on devolatilization of selected biomass materials
 - c. Kinetic evaluation of devolatilization of the studied biomass materials
3. Data processing and evaluation
4. Report writing

-- ” --

Within 14 days of receiving the written text on the master thesis, the candidate shall submit a research plan for his project to the department.

When the thesis is evaluated, emphasis is put on processing of the results, and that they are presented in tabular and/or graphic form in a clear manner, and that they are analyzed carefully.

The thesis should be formulated as a research report with summary both in English and Norwegian, conclusion, literature references, table of contents etc. During the preparation of the text, the candidate should make an effort to produce a well-structured and easily readable report. In order to ease the evaluation of the thesis, it is important that the cross-references are correct. In the making of the report, strong emphasis should be placed on both a thorough discussion of the results and an orderly presentation.

The candidate is requested to initiate and keep close contact with his/her academic supervisor(s) throughout the working period. The candidate must follow the rules and regulations of NTNU as well as passive directions given by the Department of Energy and Process Engineering.

Risk assessment of the candidate's work shall be carried out according to the department's procedures. The risk assessment must be documented and included as part of the final report. Events related to the candidate's work adversely affecting the health, safety or security, must be documented and included as part of the final report. If the documentation on risk assessment represents a large number of pages, the full version is to be submitted electronically to the supervisor and an excerpt is included in the report.

Pursuant to “Regulations concerning the supplementary provisions to the technology study program/Master of Science” at NTNU §20, the Department reserves the permission to utilize all the results and data for teaching and research purposes as well as in future publications.

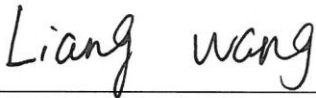
The final report is to be submitted digitally in DAIM. An executive summary of the thesis including title, student's name, supervisor's name, year, department name, and NTNU's logo and name, shall be submitted to the department as a separate pdf file. Based on an agreement with the supervisor, the final report and other material and documents may be given to the supervisor in digital format.

- Work to be done in lab (Water power lab, Fluids engineering lab, Thermal engineering lab)
 Field work

Department of Energy and Process Engineering, 2. February 2018



Terese Løvås
Academic Supervisor



Liang Wang, SINTEF Energy
Research Advisor

Acknowledgements

Support for the project work from the Research Council of Norway and industry partners through the project GrateCFD is gratefully acknowledged.

I would also like to express my deep gratitude and profound indebtedness to dr Liang Wang, Research Scientist, SINTEF, Norway, Trondheim for his guidance and invaluable suggestion which enabled us to accomplish this project. His association and constructive criticism and encouragement have all been a valuable part of my learning experience.

Abstract

The rapid industrialization, high growth rates of population and urbanization, and the developments in transportation contributed to accelerate the use of fossil fuels. This has resulted in doubling the energy demand from 1970 to 2000 and increase by 26% from 2000 to 2010. Nowadays, ca. 82% of world's energy consumption is satisfied mostly by oil, coal and natural gas [Bilgili et al., 2017]. Taking those facts into account, expenditure of fossil fuels and environment pollution would grow with appalling rate. Hence, the United Nations decided to aim for reduction of greenhouse gases by 50-80% by 2050 [Bhaskar and Dhyani, 2017]. Achieving this goal relies on searching for clean, renewable, and sustainable resources, and developing and optimizing processes which allows extracting energy from them. One of the potential clean energy sources is biomass. Unlike fuels such as oil, coal and gas, biomass is globally available and is not concentrated only in restricted geographical areas. . Bioenergy can be produced from the biomass through different thermochemical and biochemical conversion paths including pyrolysis, gasification, combustion, aerobic digestion, and fermentation [Mamvura et al., 2017; Dai et al., 2017].

This study focuses on the effect of conversion parameters and fuel property on devolatilization behaviors of woody biomass. The research can aid in determining the more suitable and economically reasonable way of thermal transformation of waste biomass in order to maximize overall efficiency and productivity of its conversion process.

Research objectives

The depletion of fossil energy sources, environmental pollutions and government restrictions has led to exploiting and utilization of new, sustainable and renewable energy resources such as biomass. Studying and understanding of the conversion behaviors of biomass during thermal decomposition processes is necessary to increase the efficiency of its application in energy-generating sector. The first objective of this experimental investigation is to study devolatilization behaviors of spruce and birch wood. For this purpose, experimental work is conducted using thermogravimetric analysis (TGA). For the spruce and birch wood, experiments are conducted with varying heat rate (5, 20 and 50 K/min) and sample size (0.063-0.1 mm and 0.2-0.3 mm). The pyrolysis process was subdivided into four stages at a rate of 5, 20 and 50 K/min, varying from 30 to 600 °C. Below 170 °C, a mass loss occurred for drying and preheating the sample and a significant mass loss occurred between 230-420 °C.

The second objective of this thesis is to mathematic evaluation of chemical kinetic parameters of studied spruce and birch wood. The results obtained during the TGA measurements allow to estimate the kinetic parameters using the Coats-Redfern method. The estimation of kinetic parameters for the temperature range of 150-600 °C resulted in obtaining values of activation energies between 54.48-66.76 kJ/mol and 50.03-65.04 kJ/mol for spruce and birch, respectively.

List of abbreviations

MSW	municipal solid wastes
GHG	greenhouse gas
GHGP	Greenhouse Gas Protocol
CHP	Combined Heat and power
BIGCC	Biomass Integrated Gasification Combined Cycle
HTL	hydrothermal liquefaction
HHV	higher heating value
LHW	liquid hot water
AFEX	ammonia fiber explosion
ILs	ionic liquids
BFB	bubbling fluidized bed
CFB	circulating fluidized bed
EGA	evolved gas analysis
MS	mass spectrometer/spectrometry
FTIR	Fourier transform infrared
EI	electron-impact ionization
CI	chemical ionization
MALDI	matrix-assisted laser desorption/ionization
ESI	electrospray ionization
DC	direct current
AC	alternating current
LC-MS	liquid chromatography-mass spectrometry
RF	radio frequency
GC	gas chromatography
LGA	levoglucosan
LMWC	low molecular weight compounds
PAH	polyaromatic hydrocarbons
FR	Friedman differential method
OFW	Ozawa-Flynn-Wall linear integral method
KAS	Kissinger-Akahira-Sunose linear method
ANL	the advanced Vyazovkin nonlinear integral method
NL	the Vyazovkin nonlinear integral method
DAEM	distributed activation energy model
EIPR	extended independent parallel reaction model

Biomass and waste resources for energy production/purposes

Biomass, as a renewable energy source, is defined as biological material from living, or recently living organism, most often referring to plants or plant-derived materials [Jia et al., 2013]. Biomass is generated through photosynthesis. During that process, carbon dioxide from air and water from ground is combined to produce carbohydrates, which form the biochemical structure of biomass. The solar energy absorbed by plant during photosynthesis is stored in chemical bonds of the carbohydrates and other molecules which are present in biomass. If the cultivation and harvest of biomass is carried out in a way that allows further growth without depleting nutrient and water resources, it is considered as a renewable resource that can be used to generate energy on demand, with little or none additional contributions to global greenhouse gas emissions [Kurchania, 2012]. This phenomenon is defined as carbon-neutrality and refers to achieving net zero carbon emission. This means that plants from which biomass is formed, balances measure amount of carbon compounds released during combustion process by absorbing carbon dioxide during their life cycle. [Chiueh et al., 2017; Mamvura et al., 2017; Sedjo, 2011].

It is interesting to note that out of the total global biomass production, forests contribute largest option of biomass reservoir and has the greatest potential in terms of the return of energy. Among other different alternatives the potential of their growth and productivity stands out with relatively high rate [Maurya et al., 2018]. Latest statistics estimate that trees present in forests cover ca. 4 billion hectares world-wide and that is roughly 30% of the total land area [Rödl, 2018].

Biomass is considered to be energy safe. Energy safety is connected with satisfying energy demand via continuous use of different types of energy at convenient price without causing negative and intolerable effects on economy and environment. Energy price variation also called as energy price shocks may cause break down of the trade balances of countries, because of disproportionate distribution of energy sources across them. With the provision of energy safety, economy would become stronger against energy price shocks and thus the development of energy sector would accelerate as well [Bilgili et al., 2017]. The crux lies in evaluation of limiting factors of biomass availability, which is a supply of

carbon dioxide, water, nutrients, solar energy and land area. Since the photosynthetic efficiency under natural conditions varies around 1%, it translates into low area-specific yields and consequently into an inefficient use of land. Therefore, the production of biomass is very area-demanding and assessment of biomass potentials should be based on the sustainable availability of suitable land [Batteiger et al., 2018].

Biomass is used to meet a variety of energy needs, including generating electricity, heating homes, fueling vehicles, and providing process heat for many industrial facilities [Alidrisi and Demirbas, 2016]. It can be converted to many different types of final energy, e.g., charcoal, electricity, producer gas, ethanol, methanol, biodiesel, additive for reformulated gasoline, etc. [Demirbas, 2007]. The production of electricity by direct combustion of biomass, advanced gasification and pyrolysis technologies are almost ready for commercial scale use [Demirbas, 2004].

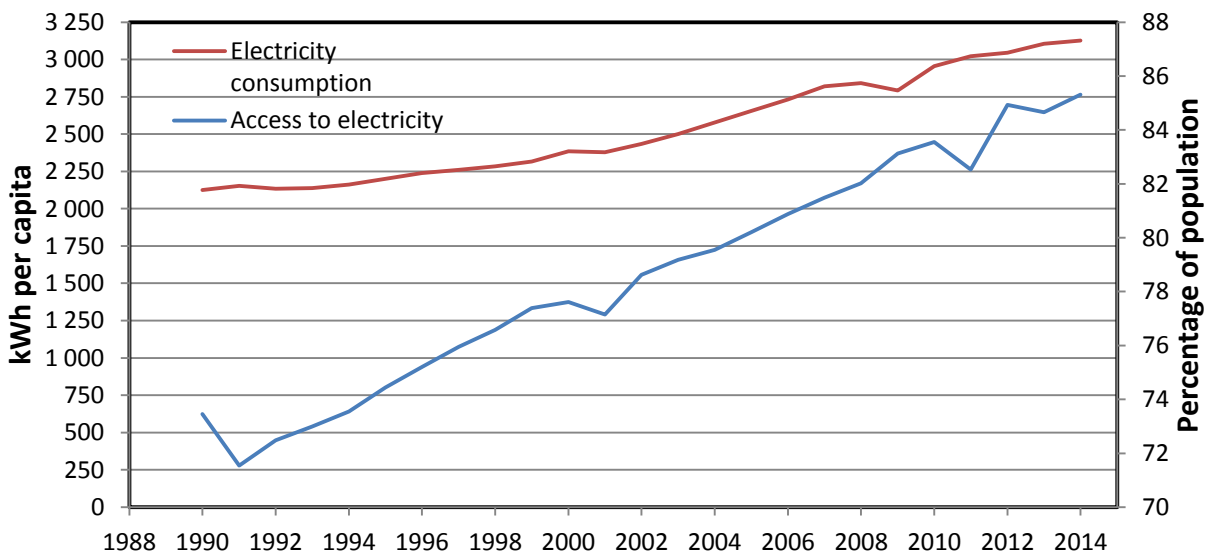


Figure 1. The change of electricity consumption and access to electricity of population over the years [World Bank, 2018].

Over the past few decades, the correlation between energy consumption and economic growth along with economic growth and carbon dioxide emissions has been one of the most intense subject matters of research. The relentless increase in energy consumption has uncompromisingly intensified environmental degradation. With the

increase of energy consumption, more environmental problems will take place such as climate changes, GHG emissions, and global warming. These aspects will probably slow down the planning process of the economic development if there is an absence of government intervention in controlling the energy consumption and carbon dioxide emissions together with other GHG emissions [Hilfa et al., 2016].

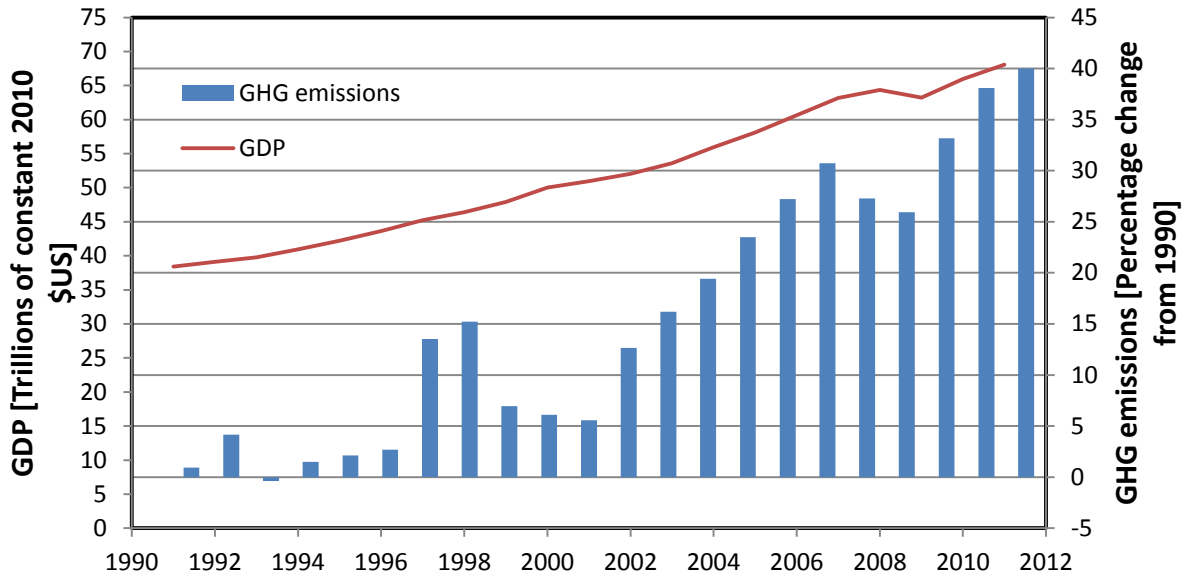


Figure 2. GDP and GHG emissions change over the years [World Bank, 2018].

Demand for biomass and other resources for energy production increased not only due to depleting of fossil fuel resources, but also for climate protection. This concern represents a challenge of central importance for mankind in twenty-first century. At the 2015 United Nations Climate Change Conference (COP 21) held in Paris, the parties agreed on the long-term target of limiting global warming to “well below 2 °C” compared to pre-industrial levels and also “pursuing efforts to” limit the temperature increase to 1.5 °C. According to some scientists, the 1.5 °C goal would require zero emissions sometime between 2030 and 2050 [Le Quere, 2016]. In order to achieve this, we should reach the peaking of GHG emissions as soon as it is possible and seek to rapid reductions afterwards towards an essentially carbon-neutral global society and economy after 2050 [UNFCC, 2015]. This requires substantial contributions from all sectors which generate GHG

emissions. A shift from fossil to renewable energy base will be crucial in this context [Batteiger et al., 2018].

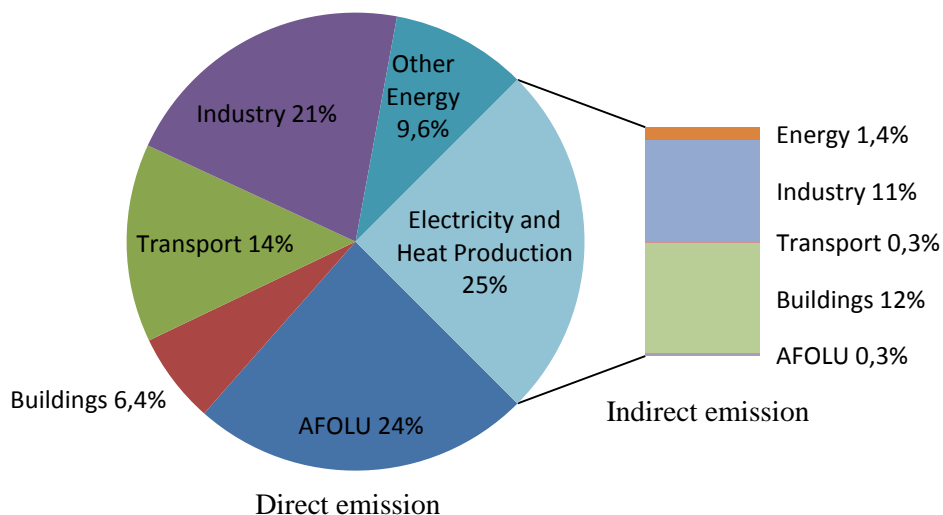


Figure 3. GHG emissions by sector [GHG Protocol, 2018; EPA, 2018].

Figure 3. shows contributions of each sector to the emission of GHG. According to GHG Protocol (GHGP), emissions are divided into two main types: direct and indirect. Direct GHG emissions are emissions from sources that are owned or controlled by the reporting entity and indirect GHG emissions are those that are a consequence of the activities of the reporting entity, but occur at sources owned or controlled by another entity [GHG Protocol, 2018]

Data from IPCC suggest that the main sectors responsible for largest GHG emissions are respectively [EPA, 2018; IPCC, 2014]:

- **Electricity and Heat Production** – generated the largest share of 2010 global GHG emissions from burning coal, natural gas and oil,
- **Agriculture, Forestry and Other Land Use (AFOLU)** – GHG emissions from this sector comes mostly from cultivation of crops and livestock (agricultural soils, rice productions, cows),

- **Industry** – this sector produces GHG primarily from burning fossil fuels on site at facilities for energy and from certain chemical reactions of raw materials processing,
- **Transport** – GHG mostly from diesel and gasoline burning for road, rail, air and marine transportation,
- **Buildings** – GHG from energy generation and burning fuels for cooking and heat in buildings. Emissions from electricity use in this sector are excluded and are instead covered in the Electricity and Heat Production sector,
- **Other Energy** – emissions of GHG from this sector refers to emissions from energy sector which are not associated with electricity or heat production.

According to data from [World Bank, 2018] electricity production from renewables tends to increase rapidly for the last two decades (**figure 4.**) and in view of the above facts, it is obvious that development of technologies related to biomass and waste processing is necessary.

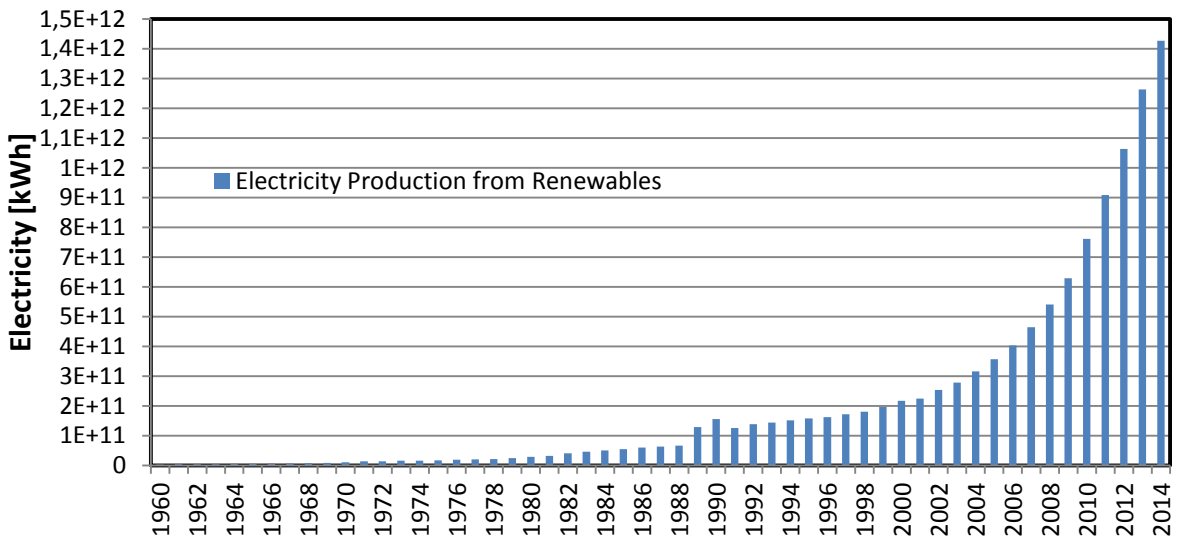


Figure 4. Amount of electricity produced from renewables over the years [World Bank, 2018].

Biomass composition

Biomass refers to a wide range of materials, including various natural and derived materials, such as woody and herbaceous species, woody wastes (e.g. from forest thinning and harvesting, timber production and carpentry residues), agricultural and industrial residues. The main biomass components are carbohydrates (mainly cellulose, hemicellulose), lignin, protein and lipids. The composition of these constituents varies from one plant species to another and their ratios depend on the type and source of the biomass. For instance, hardwoods are abundant in cellulose, whereas leaves and wheat straw have more hemicellulose [Bajpai, 2016; Hoffmann et al., 2014]. The relative contents of biomass' main components are the key factors in determining the optimum conversion route for each type of biomass [Basu, 2013].

The elemental composition of biomass comprises mainly carbon, hydrogen, oxygen, and nitrogen, but for example animal wastes may also have small amounts of chlorine and sulfur. The latter is rarely present except for secondary sources like demolition woods [Fantini, 2017]. Carbon, as the most important elemental constituent of biomass comes from the atmospheric CO₂ during photosynthesis and represents the major contribution to the overall heating value. Another major elemental constituent, hydrogen, is abundant in chemical structures of carbohydrates and phenolic polymers and also contributes to the overall heating value significantly. Nitrogen constitutes the vital nutrient form for plants and its presence contributes to the degradation in biochemical processes, e.g. fermentation or digestion [Gu et al., 2017; Hayes, 2013].

Cellulose

Cellulose is the main structural component of cell walls in biomass and functions as the rigid, load-bearing component [Brunner, 2013]. It is the most abundant biogenic polymer with estimates of 324 billion m³ available globally with an annual production of around 100 billion tons [Hayes, 2013]. Its content for most plants is around 33% except for the cotton in which this value reaches even up to 90%. Cellulose is a linear

homopolysaccharide composed exclusively of β -D-anhydro-glucopyranose units, which are linked together by β -(1,4)-glycosidic bonds, represented by the generic formula $(C_6H_{10}O_5)_n$. It is characterized by very high degree of polymerization ($DP < 10\,000$) [Basu, 2013; Meincken and Tyhoda, 2014]. The β -(1,4)-glycosidic bonds have high tendency to form strong intra- and intermolecular hydrogen bonds, leading to formation of either a highly ordered crystalline structure or less ordered amorphous region. The crystalline three-dimensional structure renders it insoluble in water and resistant to attack by enzymes or acids [Brunner, 2013; Hoffmann et al., 2014]. This makes it difficult to be treated via non-pyrolytic upgrading processes. The glucan chains require harsh conditions such as heating at $320\text{ }^\circ\text{C}$ under pressure of 25 MPa to be dissociated and become amorphous [Dyer et al., 2013; Faik, 2013].

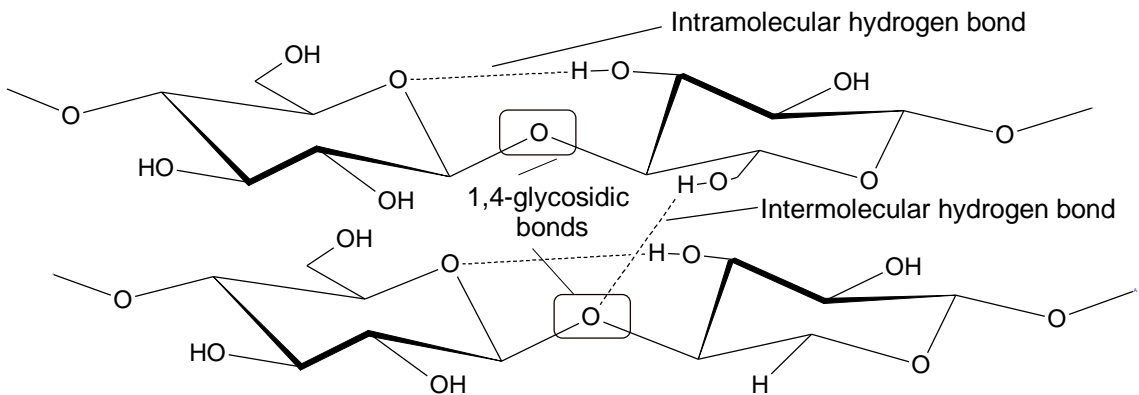


Figure 5. The glucopyranoside residues and the inter-, intra-, and glycosidic bonding of cellulose [Cornejo et al., 2013; Hayes, 2013].

Hemicellulose

Hemicellulose is present along with cellulose in almost all terrestrial plant cell walls and it is the second most abundant chemical constituent of grassy and woody biomass [Dyer et al., 2013]. The term “hemicellulose” represents variety of carbohydrate polymers that are mostly resistant to hot water, but unlike cellulose, are soluble in weak alkaline solutions and are easily hydrolyzed by dilute acid or base [Hayes, 2013]. The generic formula of hemicellulose is $(C_5H_8O_4)_n$ and it consists of a group of carbohydrates representing quite low degree of polymerization as compared to cellulose. It has a branched, weaker amorphous structure than cellulose and there is a significant variation in its composition

among different types of biomass [Basu, 2013]. However, most of hemicelluloses are built up by 100-200 units [Rafiqul et al., 2017] of pentoses like D-xylose and L-arabinose, and hexoses like D-galactose, D-glucose, D-mannose [Meincken and Tyhoda, 2014]. Hemicellulose, among the key components of lignocellulosics is the most thermochemically sensitive and tends to form inhibitory compounds like furfural and formic acids during degradation processes [Bajpaj, 2016; D. Rana and V. Rana, 2017]. As compared to cellulose, hemicellulose yields more gases and less tar in thermal conversions [Basu, 2013]. In biomass, hemicellulose and cellulose are connected via hydrogen-bonding interactions and they together build structural matrix that is further bound to lignin and results in formation of lignocellulosic complex [Rafiqul et al., 2017].

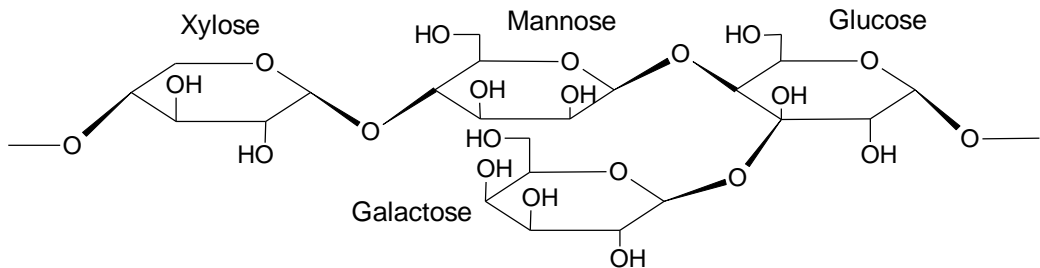


Figure 6. Molecular structure of typical hemicellulose composed of xylose, mannose, glucose and galactose linked together via 1,4-glycosidic bonds [Basu, 2013; Vaz, 2016].

Lignin

Lignin is a high-molecular, branched, polyphenolic, and complex compound with a highly random structure and together with cellulose and hemicellulose is a major component of plant materials. The lignin content varies among species of biomass and even among morphological parts of a plant. It is most stable component of biomass and is considered to be responsible for mechanical support, resistance to variety of pathogens and transport of water [Abramson et al., 2013; Dyer et al., 2013]. The characteristics of amorphous form of lignin is similar to that of hemicellulose, whereas solubility to that of cellulose. Furthermore, it possesses binding capacity of stem cells and fibrous contents of plants which is the reason for strong structure. As compared to the other two main compounds of biomass, lignin stores more energy content, hence products of its conversion

have higher heating value of about 23 MJ/kg [Gu et al., 2017; Meincken and Tyhoda, 2014].

Lignin has a network structure and lacks a defined primary structure [Meincken and Tyhoda, 2014]. The main building units of lignin are three monomeric blocks: coumaryl-, coniferyl-, and sinapyl alcohol [Hoffmann et al., 2014]. These are the relatives of carbohydrates produced via dehydration and cyclization of sugars [Hayes, 2013]. The aromatic matrix of lignin makes it highly thermally stable, thus conversion of biomass that is abundant in lignin require much harsher conditions which may cause some complications during processing [Dyer et al., 2013]. Structure of lignin is not identical for different plants and all the proposed structures in various sources are just approximations [Cornejo et al., 2013].

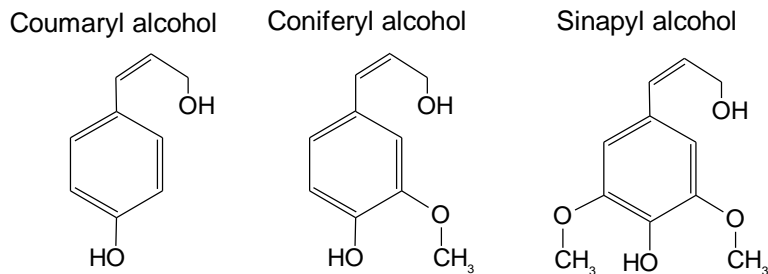


Figure 7. Monomeric lignin building units [Hayes, 2013; Hoffmann et al., 2014].

Protein

Proteins, as fundamental building blocks of living cells, consist of carbon, hydrogen, oxygen, nitrogen, and sulfur. Their structure includes number of amino acids connected by peptide bonding to polymers. Amino acids are highly heterogeneous and hence the complexity in degrading them is challenging. There are only about 20 amino acids that are found regularly in naturally occurring proteins [Hayes, 2013]. Peptide bonds of proteins are considered to be much more stable than glycosidic bonds that were mentioned in case of cellulose and starch. Thus, below 230 °C, only slow hydrolysis can occur [Hoffmann et al., 2014]. Hydrothermal liquefaction of proteins leads to the formation of amines, hydrocarbons, aldehydes, and acids like carboxylic, acetic, propionic and some butyric acids [Gu et al., 2017]. The content of proteins in plants is usually determined via

combustion methods by determining the content of nitrogen and multiplying it by so called conversion factor (6.25 is most commonly used) [Aden et al., 2017]

Lipids

Lipids are generally defined as compounds that are insoluble in water, but are soluble in organic solvents like alcohol, benzene. However, hydrolysis of lipids is possible in harsher environment with hot and compressed water, because of the fact, that dielectric constant of water significantly decreases at subcritical conditions [Hoffmann et al., 2014]. Lipids are a very heterogeneous group consisting of number of hydrophobic molecules synthesized by several biochemical pathways and serving multiple physiological roles [Behrendt et al., 2018]. They include fats, oils, waxes, sterols, fat-soluble vitamins (A, D, E and K), phospholipids, mono-, di-, and triglycerides [Favaro et al., 2018]. Lipids constitute a reservoir of chemical energy, which is of crucial importance when it comes for production of biofuels. One of the biomass sources, that has is characterized by abundance in lipid content is microalgae. It consists mainly of triglycerides which were found to yield bio-oil that is completely different in terms of benzene content as compared to the one derived from lignocellulosic materials [Dyer et al., 2013].

Other carbohydrates

Carbohydrates are divided into monosaccharides, disaccharides and oligosaccharides, and polysaccharides. From the latter, apart from cellulose and hemicellulose, starch and pectin are also worth mentioning. Starch, the simplest of glucans in many plants functions as a sugar store. It is a mixture of two polysaccharides: linear amylose and branched amylopectin [Cornejo et al., 2013]. Amylose has an approximate degree of polymerization of 2000 and forms a helix containing six glucose units in every turn. It consists of α -(1,4)-glycosidic bonds. The alpha-nature of the bond results in lower strength and abundance of intermolecular hydrogen bonds between amylose molecules, thus the overall structure of starch is weaker than that of cellulose [Hayes, 2013]. However, amylose is generally a minor component of most starches, with amylopectin being the major constituent. The content of amylose varies from 20 to 30%, whereas that of amylopectin

from 70 to 80% [Brunner, 2013]. Amylopectin mostly contains glucose units linked via α -(1,4) bonds, but there are also α -(1,6) branches that occur every 24-30 glucose units. Its DP reaches even up to 200 000 in potatoes and is certainly much higher than that of amylose. Unlike amylose, it does not form helix and does not present intermolecular alignment, and hence no significant hydrogen bonding. This means, that it is much more soluble as compared to cellulose [Hayes, 2013].

Pectins are heterogeneous mixtures of polysaccharides that mainly consists of α -(1,4)-linked D-galacturonic acid (GalA) residues. GalA, a negatively charged monosaccharide makes pectin easy to solubilize in hot water [Faik, 2013]. Pectin is a part of primary cell walls of terrestrial plants and is responsible for porosity, cell wall adhesion, environmental response, and structural integrity [Abramson et al., 2013]. It is considered to be the most branched polysaccharide and can be found in significant quantities in vegetables, fruits, and some food wastes, like apple pomace [Hayes, 2013].

Biomass conversion technologies

There are a number of conversion routes for producing energy from biomass. Conversion technologies may release energy from biomass by using it direct as a solid fuel or by synthesizing intermediate and final conversion products for production of useful liquid fuels and chemicals.

The main routes of biomass conversion are the thermochemical conversion and biochemical conversion. Generally, the biomass can be converted into charcoal, liquid fuels (mainly transportation) and gaseous fuels (e.g. hydrogen, producer gas, bio gas) [Kurchania, 2012]. Unlike biochemical conversion process, which acts mainly on cellulose, thermochemical conversion operates on most of the components of biomass material and has much higher throughputs when compared to biochemical conversion processes [Atnaw et al., 2017]. Thermochemical conversion efficiency of biomass greatly depends on the properties and composition of biomass. Physicochemical characterization is critical for evaluating suitability and grade of biomass and selection of further proper thermochemical

conversion processes. Physicochemical characterization of biomass normally includes measurement and determination of:

- particle size
- bulk density
- proximate analyses including
 - moisture content
 - volatile matter
 - fixed carbon content
 - ash content
- ultimate analyses for measuring content of:
 - carbon
 - hydrogen
 - Nitrogen
 - Sulphur
- ash fusion temperature,
- calorific value,
- biochemical composition (cellulose, hemicellulose and lignin)

The thermochemical methods are more amenable to commercialization, because there are based on technologies that are mature and established over years. On the other hand, biochemical methods have greater potential for cost reduction and are less harmful to the environment. These processes are mainly used to convert organic wastes, both MSW and agricultural, which are relatively difficult to process because of handling barriers and low energy density [Baskar et al., 2012].

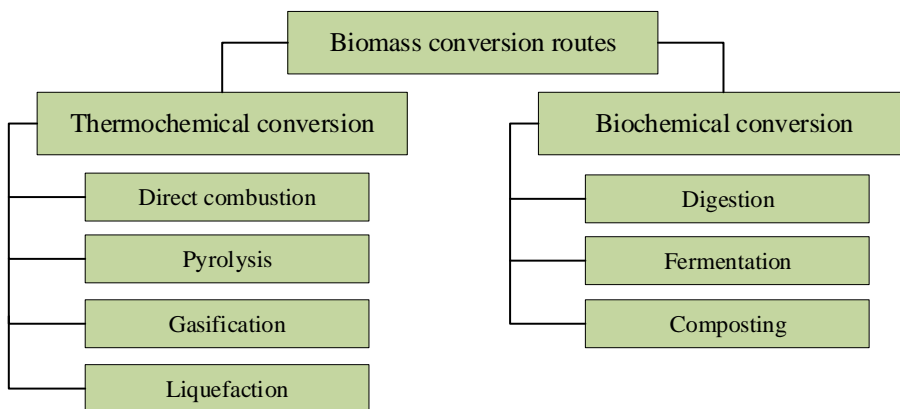


Figure 8. Biomass conversion routes diagram [Agbontalor, 2007; Atnaw et al., 2017; Baskar et al., 2012].

Thermochemical conversion

Pyrolysis

Pyrolysis is defined as the irreversible thermochemical decomposition of organic materials at elevated temperature in the absence of oxygen, water, or any other reagents [Aden et al., 2017; Agbontalor, 2007]. It starts at 180 °C [Agbontalor, 2007] preceding the combustion and gasification processes and is followed by partial or complete oxidation of primary products [Mohee et al., 2018].

Pyrolysis can efficiently and successfully convert a wide variety of biomass to commercially viable biofuels and chemical feedstock. Unlike combustion, pyrolysis is endothermic reaction and requires to be supplied for the process. The liquid products generated via pyrolysis include oils and water. Gaseous products are generally carbon monoxide, carbon dioxide and methane, whereas carbonaceous solid residue is known as charcoal. The liquid product (bio-oil) can be used for heating, power generation, as a transportation fuel if upgraded properly, and for conversion into other suitable chemicals. Upgrading is achieved through catalytic pyrolysis. Bio-oil is most preferred product as a cleaner and more stable intermediate energy carrier. The gas produced can be used directly as a heat resource for the pyrolyzer after combustion in a gas burner or can be processed through gas turbines or gas boilers for production of electricity [Baskar et al., 2012; Mohee

et al., 2018]. Charcoal can be used for heating or as a feedstock to prepare activated carbon, used for soil remediation purposes [Arumugasamy et al., 2017].

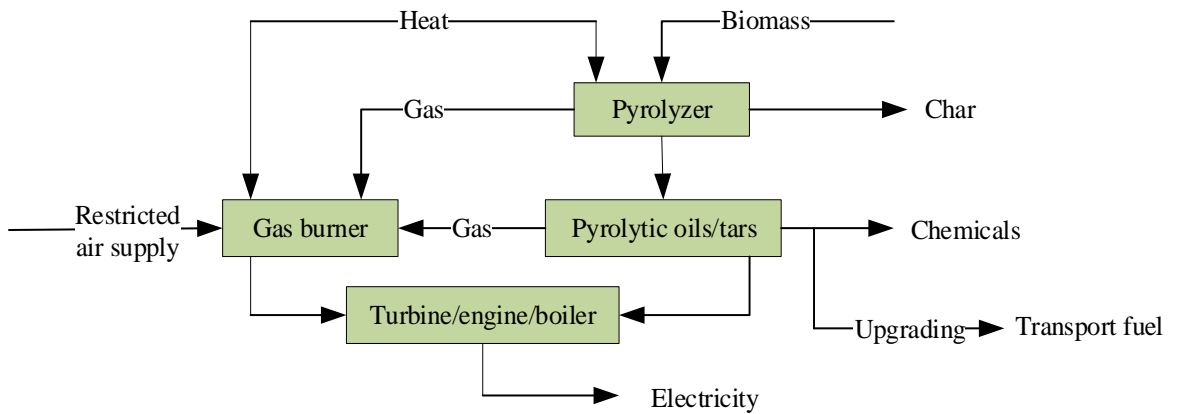


Figure 9. Simplified layout of a pyrolysis plant [Basu, 2013].

As one can see on **figure 9.**, in the typical pyrolysis plant biomass fed to the chamber is transformed into condensable and non-condensable vapors released in the pyrolysis process. These vapors leave the chamber containing part of produced solid biochar, while the rest of it remains in the chamber. Char is later separated and collected, whereas gas is cooled downstream of the reactor. The condensable vapor forms bio-oil in the gas condenser and the non-condensable vapor leaves as a product or can be returned as a heat carrier to the chamber, since it is free of oxygen and does not lead to combustion process [Aden, et al., 2017; Basu, 2013]

Types of pyrolysis processes

Pyrolysis processes can be conducted in various ways differing in reaction conditions such as temperature, residence time, particle size, type of feedstock, etc. however the main parameter on which the most common classification is based is heating rate. Hence, three major pyrolysis processes are divided as follows: slow/conventional, fast, and flash pyrolysis. Apart from these, there are also other types mentioned in various literatures, which are: torrefaction, carbonization, intermediate pyrolysis, ultra-rapid pyrolysis, vacuum pyrolysis, hydrolysis, methano-pyrolysis [Basu, 2013; Baskar et al., 2012; Bridgwater, 2017].

Slow pyrolysis

Slow pyrolysis is used when the main objective is to produce biochar and non-condensable gases. It has the highest biomass to biochar conversion ratio, which is around 35% [Arumugasamy et al., 2017] and involves slow heating of the biomass over long periods of time. The long residence times inside the reactor tend to promote secondary reactions of the pyrolysis vapors, thus resulting in higher proportion of biochar [Pizarro de Oro and Thormann, 2018]. Slow pyrolysis can be additionally divided into torrefaction and carbonization.

Fast pyrolysis

Fast pyrolysis is a promising technology for generation of liquid biofuels from lignocellulosic biomass. It is characterized by high heating rates and very short residence times (to minimize secondary reactions) which lead to obtaining mostly bio-oil. The maximum amount of bio-oil yield which is around 75% can be achieved at ca. 500 °C [Bhuyan et al., 2018]. Higher heating rate favors production of liquids before they can react to form undesired biochar. Bio-oil yields highly depend on the parameters of pyrolysis and properties of processed feedstock. Generally, highest yields are obtained for woody biomass, because they are more abundant in cellulose and hemicellulose content as compared to e.g. agricultural residues or energy crops [Pizarro de Oro and Thormann,

2018]. The particle size of feedstock is also very important issue. Bigger particles have lower heat transfer rate which results in decrease of bio-oil yield and increase of char yield instead. Thus, smaller particles are preferred. The produced bio-oil in fast pyrolysis process has low pH value and is highly corrosive. Additionally, its heating value is relatively low (approximately two times lower) as compared to crude oil, hence the necessity of upgrading of bio-oil [Bhuyan et al., 2018; Bridgwater, 2017].

Flash pyrolysis

Flash pyrolysis which is still in research phase is an improved and modified form of fast pyrolysis. The temperatures in flash pyrolysis varies from 900 °C to 1200 °C with a heating rate of 1000 °C or even higher and a very short residence time of vapors in the range of 0.1-1 s [Bhattacharyya et al., 2018]. The idea of this process is same as in the fast pyrolysis, since combination of rapid heating rate, high temperatures, and short vapor residence time favor high liquid yield. However, there are some important limitations of flash pyrolysis process, e.g. stability and quality of the bio-oil affected by the char present in the product. Additionally, its application on industrial scale still needs to be studied, because configuration of reactor for flash pyrolysis, in which input biomass is treated by very high temperature for such a short period of time is a huge challenge [Baskar et al., 2012; Bhuyan et al., 2018].

Table 2. Operating parameters and characteristics of main pyrolysis types [Atnaw et al., 2017; Mohee et al., 2018].

Type	Temp. [°C]	Heating rate [°C/s]	Residence time [s]	Particle size [mm]	Characteristics
Slow	300-700	0.1-1	45-550	5- 50	char formation higher than liquid and gaseous products; energy intensive (low heat transfer)
Fast	600-1000	10-200	0.5-10	< 1	60-75 wt% of liquid bio-oil; 15-25 wt% of solid biochar; 10-20 wt% of non-condensable gases; high energy efficiencies; low investment cost
Flash	800-1050	> 1000	< 0.5	< 0.2	research stage; bio-oil yield of 75%

Carbonization

Carbonization is a process by which solid residues with increasing content of carbon are formed. It is a derivative of pyrolysis where biomass is heated slowly to temperature around 400 °C in the absence of oxygen as well. This process is maintained for several days. Long duration allows sufficient time to transform condensable vapors into char and non-condensable gases [Aroca et al., 2018; Baskar et al., 2012]. Generally, carbonization refers to processes in which char is the main product of interest derived from processing of wood. The optimal temperature of carbonization, that is roughly 400 °C as it was mentioned before, allows obtaining the highest yield of char production in this process [Demirbas, 2009]. Carbon accumulates due to gradual reduction of oxygen and hydrogen contained in wood. The wood is processed in numerous physicochemical conversions with the increase of temperature. It is considered that between 100 °C and 170 °C most of the water is evaporated. The further increase up to 270 °C leads to formation of condensable gases, whereas between 270 °C and 280 °C, an exothermic reaction takes place which can be detected by sudden heat generation [Kurchania, 2012].

Intermediate pyrolysis

Intermediate pyrolysis operates at moderate temperatures and residence time. It is usually conducted in order to obtain similar proportions of liquid and solid products. The operating conditions of intermediate pyrolysis are set in such way to prevent formation of high molecular weight tars and to produce dry char that can be applied to soil in agricultural fields or used for energy generation along with bio-oil [Bhuyan et al., 2018; Ferdiosian and Xu, 2017]. The typical temperature and residence time is in the range of 350-450 °C and 5-10 min, respectively [Pizarro de Oro and Thormann, 2018]. However, there are plenty of different conditions reported in other sources, e.g. according to Bhuyan et al. (2018) the temperature is in the range of 500-650 °C, whereas residence time 5-15 min.

Ultra-rapid pyrolysis

In ultra-rapid pyrolysis, which gives predominantly gaseous products the heating is done by using a heat carrier solid such as sand. Thus, it is capable of conducting extremely fast heating of feedstock, surpassing values of fast and flash pyrolysis. Since the output of reactor is a mixture of solid heat carrier and non-condensable gases and primary product vapors a gas-solid separator is required in order to recycle the heat carrier [Pizarro de Oro and Thormann, 2018; Nachenius et al., 2013]

Vacuum pyrolysis

Vacuum pyrolysis process is characterized by heating rates similar to those of slow pyrolysis and rapid removal of pyrolysis products as in e.g. fast pyrolysis. The temperature ranges between 450 °C and 600 °C with total pressure around 0.05-0.20 MPa [Anatunović et al., 2017]. The technology of vacuum pyrolysis allows for processing larger biomass particles as compared to fast pyrolysis. Total liquid yields are relatively lower and varies from 60% to 65%. Additionally, their properties are different (e.g. higher heating value) as compared to those produced via fast pyrolysis. It is due to vacuum that allows for decomposition of the organic components under lower temperatures. It was also observed that vacuum conditions leads to obtaining biochar with more porous structure [Baskar et al., 2012; Bhuyan et al., 2018; Nachenius et al., 2013].

Hydropyrolysis

Hydropyrolysis is a process in which a thermal decomposition of biomass it carried out in an atmosphere of high-pressure (5-20 MPa) hydrogen/hydrogen-based materials. Heat transfer rate, residence time, and temperature are kept approximately similar to that of the fast pyrolysis, thus it is hydropyrolysis is often considered as fast pyrolysis under high pressure condition. Hydrogen reduces the oxygen content in the produced bio-oil and lowers the yield of char [Basu, 2013; Nachenius et al., 2013]. Hydrogen-pyrolysis also enhances the content of hydrogen in liquid products. It is due to use of two stage system. The first stage involves treating biomass with hydrogen at 200-300 °C under pressure,

whereas the second stage involves cracking of the hydrocarbon produced in the first stage into lighter hydrocarbon at around 500 °C [Baskar et al., 2012]. There are often catalysts used in order to increase the removal of water, O₂, and CO_x from bio-oil and to reduce depolymerization and coking reactions [Bhuyan et al., 2018].

Combustion

The most widely applied thermal conversion route for producing energy from biomass is combustion [Abdulrahman and Huisingh, 2018]. Combustion is burning of biomass in the air and results in the generation of heat [Maurya et al., 2018]. Total combustion process is divided into four stages:

1. heating and drying,
2. distillation of volatiles,
3. combustion of volatiles,
4. residual fixed carbon combustion.

During the drying phase most of the water within the biofuel is evaporated at temperatures below 150 °C. Vaporization of the water is an endothermic reaction and requires energy released from combustion process. Therefore, this step lowers the temperature in the combustion chamber and slows down the whole combustion process. It is estimated that in case of exceeding a certain percentage of water content (ca. 60%), biomass would require too much energy to evaporate the moisture and would not result in sustain combustion. Apart from moisture content, the size of feed particles also plays an important role for conversion of biomass material. Most of biomass used for combustion applications are woody biomasses. The woody biomass does not have good thermal conductivity, the bigger the size of particles, the lower the rate of heat transmission through the feed bed [Baskar et al., 2012; Wiese, 2017]. Therefore, the woody biomasses are normally shredded and milled before fed into the combustion chamber for realizing complete combustion of the fuel particles and overall conversion efficiency.

The second stage of biomass combustion normally occurs between 150 °C and 600 °C and is defined as devolatilization of fuel particles [Wiese, 2017]. During devolatilization,

a large fraction of biomass is decomposed with formation of gases (CO, CO₂, H₂O, methane) and, tars and residual char. Conversion of biomass fuel particles in this stage generally depends on the heating rate and final temperature. Slow heating rates favor formation of tar and char and low molecular weight gases. Whereas, fast heating rates provide products that are liquid under normal conditions [Jones et al., 2014].

The ignition of volatiles normally takes place in the temperature range between 630 °C and 730 °C. The combustion involves an exothermic reaction of combination of volatiles and oxygen. Ratio of amount of oxygen to volatiles, moisture content and biomass composition determine the temperature of flame. The excess of oxygen is normally preferred in order to avoid forming soot which absorbs volatiles and results in generation of tar [Baskar et al., 2012].

In parallel to devolatilization, oxidation of residual fixed carbon also takes place. The combustion of residual char is often affected by 1) mixing of char with oxidizing gas, and 2) residence time of char at combustion temperature [Wiese, 2017].

The efficiency of the overall combustions process is described as combustion efficiency. It is a ratio of the heat energy generated during combustion and the heating value of the fuel. Apart from physical losses which are described as a heat exchange with environment, there are also chemical losses which occur due to incomplete oxidation. In this situation, the energy is still contained in un-oxidized components, which are released with the flue gas to the atmosphere. Nowadays, power plants or combined heat and power plants (CHP) are capable of achieving up to 98% of combustion efficiency however the performance of combustion process is not expressed in terms of efficiency, but is controlled by analysis of the ash and flue gases [Wiese, 2017]. The issue of ash generated due to combustion of biomass is also an essential topic to discuss about. These amounts are significant, for 50 MW power plant has to deal with up to 20 tons of ash per day [Maurya et al., 2018].

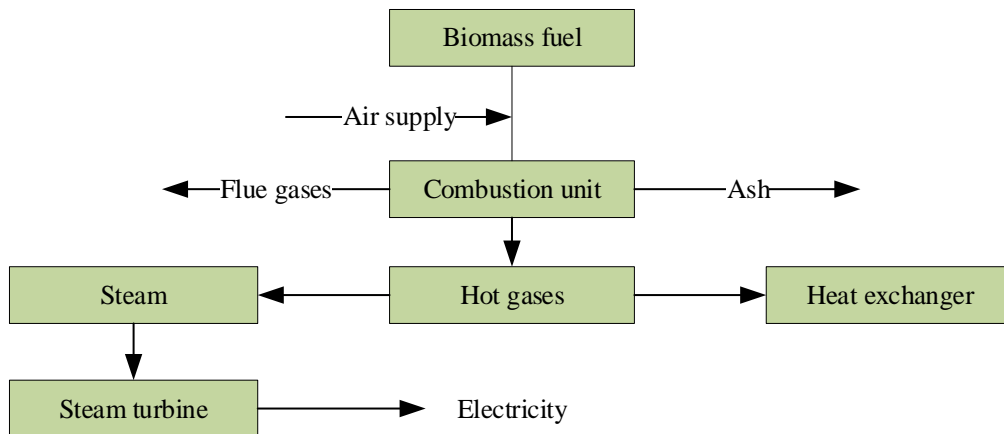


Figure 10. Combustion of biomass for heat and power generation [Baskar et al., 2012; Jones et al., 2014].

Gasification

Biomass gasification refers to a controlled process involving heat, steam and oxygen to convert biomass to mixture of gas products and solid residue [Luque and Speight, 2015]. This useful and convenient mixture of produced gases is often called syngas that can be directly burned to release energy or can be used for production of value-added chemicals. Combustion and gasification are two thermochemical processes which are closely related to each other, but there is a significant difference between them. While combustion breaks chemical bonds to release the energy, gasification is the process that packs energy into chemical bonds in the product gas to form compounds with higher hydrogen-to-carbon (H/C) ratio [Basu, 2013]. The use of syngas is more efficient as compared to direct combustion fuels, because it can be [Jenkins, 2015; Luque and Speight, 2015]:

- Combusted at higher temperatures,
- Used in fuel cells,
- Used as a feedstock for methanol and hydrogen production,
- Transformed into a wide range of synthesis liquid fuels, e.g. via Fischer-Tropsch (FT) process.

Hence, gasification finds application in converting biomass to useful carbon- and hydrogen-rich fuel gas which is more suitable to handle and utilize in various processes [At Naw et al., 2017; Baskar et al., 2012]. This process can also be used for producing heat and electricity,

obtaining up to 50% efficiency with respect to electricity generation in so called Biomass Integrated Gasification Combined Cycle (BIGCC).

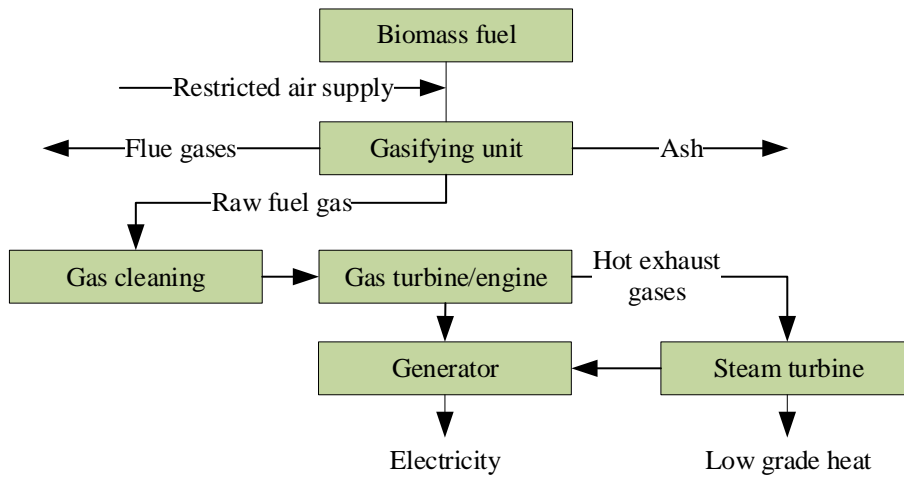


Figure 11. Biomass Integrated Gasification Combined Cycle (BIGCC) [Baskar et al., 2012].

Gasification process consists of various chemical reactions that include homogeneous as well as heterogeneous reactions which generally follows the sequence of: preheating and drying, pyrolysis and combustion, and char gasification.

The drying stage is when the moisture of the biomass is reduced or totally removed and released as a vapor. The initial moisture content of biomass feedstock can reach up to 70% or even more, while every kilogram of water in biomass requires about 2242 kJ to be vaporized. Therefore, the biomass feedstock is normally dried before gasification process. The moisture content of the biomass used for the gasification varies in the range of 5-25% to reduce energy losses [Atnaw et al., 2017].

The second stage is responsible for the release of volatile components of biomass feedstock. It involves the thermal breakdown of larger hydrocarbon molecules into smaller gas molecules with no major chemical reaction with any gasifying medium. During devolatilization process, the most important product is the tar. At the same time, partial combustion of solid carbon and gas products takes place with a limited air/oxygen supply to provide heat for biomass gasification process. To prevent complete combustion, an amount of delivered air/oxygen is lower than the amount that would be calculated from stoichiometry [Luque and Speight, 2015]. The equivalence ratio varies in the range of 0.2-

0.4 [Atnaw et al., 2017]. The generated heat is used for the endothermic reactions which take place during pyrolysis.

Part of the char produced during devolatilization react towards to gasification agent (i.e., air, oxygen, steam or carbon dioxide) to form a gas mixture of carbon monoxide, hydrogen, methane, carbon dioxide as well as hydrocarbons such as ethane and propane.

Biomass gasification as a complex process can be affected by many factors, mainly biomass characteristics (e.g. moisture content), operating conditions reactor configuration and gasifying medium (agent). The influence of these parameters can be seen in **table 1.** and **table 2.**

Table 1. Heating values of product gas and characteristics of gasification processes basing on gasifying medium [Atnaw et al., 2017; Basu, 2013].

Medium	Heating value [MJ/Nm ³]	Characteristics
Air	3-7	low heating value of syngas due to dilution high amount of nitrogen present in air, low investment costs
Steam	10-18	higher H/C ratio, higher investment costs
Oxygen	12-28	lower hydrogen and higher carbon-based compounds content in product gas, higher investment costs

Table 2. Influence of particle size on the properties of biomass gasification [Luque and Speight, 2015].

Biomass particle size [mm]	0.6-0.9	0.45-0.6	0.3-0.45	0.2-0.3
Average size [mm]	0.75	0.53	0.38	0.25
Gas yield [Nm ³ /kg of biomass]	1.53	1.93	2.37	2.57
Lower heating value of gas [kJ/Nm ³]	6976	7937	8708	8737
Carbon conversion efficiency [%]	77.62	84.4	90.6	95.1

Most of the studies show that the concentration of component gases in syngas, its heating value and yield is highly dependent also on temperature. Referring to some results, high gas yield is achieved for gasification under temperatures higher than 900 °C [Lapuerta, et al., 2008; Skoulou et al., 2008; Sharma, 2008]. The concentration of carbon oxide and hydrogen increases with the temperature, while concentration of carbon dioxide, methane,

tar and light hydrocarbons decreases [Skoulou et al., 2008]. On the other hand, Zhao et al. (2010) reported that concentration of carbon oxide decreases with increase in reactor temperature, while concentration of carbon dioxide and hydrogen increases with temperature. Same study also concluded that the concentration of light hydrocarbons such as methane and ethylene, heating value, carbon conversion were found to be maximum for the temperature of reactor equal to 800 °C. This discrepancy of results is caused by the difference between type of reactors, their conditions and biomass characteristic, but one can be sure that temperature has high influence on product's properties.

Hydrothermal Liquefaction

Hydrothermal liquefaction (HTL) is a technology that directly converts biomass into liquid fuels (biocrude, bio-oil) under moderate temperature (200-400 °C) and high pressure (5-25 MPa) in presence of water or water-containing solvent and a catalyst [Cheng et al., 2014; Liu et al., 2017]. HTL's products are also solid residue and gaseous products, but liquid products are the most desirable. During hydrothermal liquefaction process, the biomass conversion degree, biocrude oil yield and its quality depend on many factors. A properly designed HTL process may reach a yield of biocrude oil at the level of 65% with high quality (lower oxygen content) [Cheng et al., 2014].

The biomass hydrothermal process includes following steps:

1. feedstock preparation,
2. mixing feedstock with liquefaction solvent,
3. optional addition of reducing/inert gas and/or catalyst,
4. reaction of mixture in proper conditions,
5. separation of products.

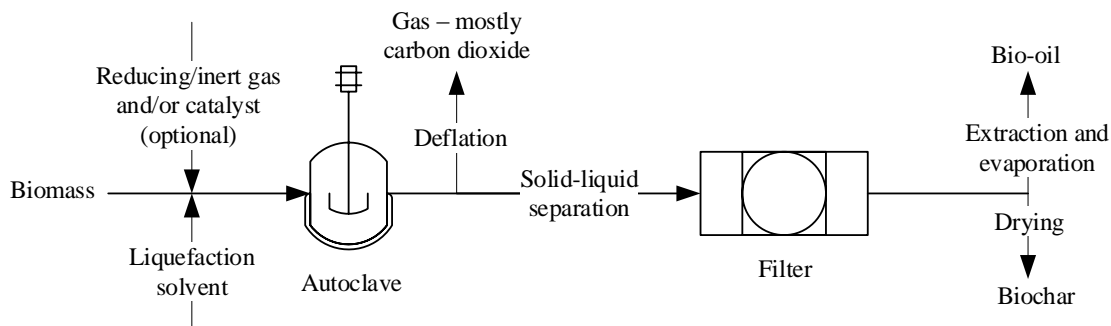


Figure 12. Biomass hydrothermal liquefaction [Huang et al., 2017].

Solvent type and composition has considerable effect of biomass decomposition process and intermediate/final products during hydrothermal liquefaction of biomass. There are two main categories of liquefaction solvents: water and organic solvents (e.g. methanol, ethanol, phenol, acetone). Generally, solvents should strongly react with biomass, one option is to use solvents which are derived from the liquefaction of biomass itself such as phenol, simple alcohol, and phenol and its derivatives [Huang et al., 2017]. Studies show that acetone, phenol and 1,4-dioxane are found to be more effective for liquefaction of lignocellulosic biomass, whereas in case of algal biomass ethanol is considered to be most suitable. Additionally, solvent with strong polarity results in higher conversion rate and polarity of solvent does not really affect the yield of bio-oil [Huang and Yuan, 2015].

The selection and use of catalyst is also critical for hydrothermal liquefaction of biomass aiming for maximizing the biomass conversion and producing of liquid products. The common catalysts include heterogeneous and homogeneous catalysts. Despite there is no obvious catalytic activity for heterogeneous catalysts towards the liquefaction of biomass research shows that homogeneous catalysts exhibit higher activity than heterogeneous catalysts. According to Huang et al. (2017):

- organic acids as catalysts yield lower solid residue content as compared with inorganic acids,
- salts such as chlorides, phosphates, carbonates, acetates, sulfates show lower catalytic activity than sodium hydroxide (at typical liquefaction temperatures),
- alkali salts enhance yield of bio-oil (at subcritical conditions),
- acids enhance yield of water-soluble products.

The biggest advantage of HTL is the fact that it can process wet feedstock without need of the energy which is used in the drying process. Also, the bio-oil obtained from HTL presents higher quality, higher yield, lower water and oxygen content as compared to the bio-oil produced in pyrolysis process. It has also higher HHV (25-35 MJ/kg) than pyrolysis bio-oil (14-20 MJ/kg) [Caprariis et al., 2017]. However, there are also few drawbacks such as use of high pressure which potentially lead to high cost in the equipment necessary for industrial scale biomass hydrothermal liquefaction applications.

Pretreatment techniques

Biomass pretreatment is a prerequisite for handling heterogeneous biomass and removal of unwanted species from the feed streams [Bomans et al., 2013]. Some of biomass resources like lignocellulosic materials (wood, stalks, straw, etc.) require pretreatment such as size reduction before they can be used for pyrolysis in order to obtain acceptable yield [Baskar et al., 2012]. The goal of pretreatment is to make some of compounds which are present in processed biomass more accessible to conversion processes. Pretreatment techniques are capable of changing both physical and chemical structure of biomass and results in improvement of reaction rates [Barros et al., 2014].

The selection of the appropriate pretreatment technique strongly depends on the proportion of constituents present in the processed feedstock. In order to carry out the treatment process efficiently, it should meet following requirements [Bajpai, 2016; Gogate and Joshi, 2017]:

- the pretreatment technology should be universal and capable of treating different feedstocks with same or at least congenial efficiency,
- it should be environmentally friendly and produce as less harmful by-products and waste chemicals as possible,
- it should result in high recovery desirable components in useable form in separate fractions,
- it should require low investment, operational costs, and energy demand.

Pretreatment methods are divided into different categories as follows:

- a) biological pretreatment,
- b) physical pretreatment:
 - a. milling,
 - b. extrusion,
 - c. ultrasound pretreatment,
 - d. hydrodynamic cavitation,
 - e. microwave pretreatment,
- c) chemical and physicochemical treatment:
 - a. steam explosion,
 - b. liquid hot water treatment,
 - c. acid hydrolysis,
 - d. alkaline hydrolysis,
 - e. ammonia fiber explosion (AFEX),
 - f. organosolv pretreatment,
 - g. wet oxidation,
 - h. CO₂ explosion,
 - i. ionic liquids pretreatment,
 - j. ozonolysis.

Biological pretreatment

Biological pretreatment generally involves lignin-degrading organisms and is used in treating cellulose-based biomass and algae biomass, preceded by physical or chemical treatment [Li and Wan, 2013; Wang and Yin, 2017]. It is a low carbon footprint technology and is an alternative to many other pretreatments techniques in many applications. The organism that are used to secrete multiple cell wall degrading enzymes are wood rot fungi (including white rot, brown rot, and soft rot), ruminant bacteria, and symbiotic bacteria present in invertebrate animals such as termites and earthworms. Wood rot fungi are the most attractive for biological pretreatment due to their ability of degrading or modifying

lignin through ligninolytic enzymes [Li and Wan, 2013]. Generally, brown and soft rots attack cellulose and partially modify lignin, while white rot fungi more actively degrade the lignin component [Bajpai, 2016].

Biological pretreatment is conducted via solid-state fermentation (SSF) process and is mainly focused on delignification. It requires mild reaction conditions (15-40 °C; pH 4-5), low energy demand, and no strict reactor parameters such as pressure and/or corrosion resistivity [Moreno and Olsson, 2017]. However, using microorganisms is time consuming, hence it requires even up to several weeks. The overall process time can be reduced to 4-24 hours if the external enzymes are added, but this requires additional investments. Despite few disadvantages, it has great potential to reduce environmental impacts and energy expenditure as compared to prevailing pretreatment technologies [Bajpai, 2016].

Physical pretreatment

Milling

Milling is generally conducted in order to reduce polymerization and increase the available surface area of biomass based on the reduction size. The particle size affects extraction, hydrolysis, and digestion rates [Aden et al., 2017]. There are many different types of milling, including [Barros et al., 2014; Gogate and Joshi, 2017]:

- hammer milling,
- ball milling,
- two-roll milling,
- vibro energy milling,
- colloid milling.

Selection of proper type of milling depends on the moisture content of treated material. Typically, materials with lower moisture content (10-15%) are usually treated with two-roll, hammer, attrition, and knife mills, whereas for higher moisture content, colloid mills and extruders are preferred [Gogate and Joshi, 2017].

Extrusion

Extrusion is a thermo-mechanical pretreatment process. An extruder consists of single or twin screws with rotating barrels and subjects material to mixing, heating, and cutting. This process is based on the effect exerted by tight rotation of a screw at certain temperature, which leads to physical and chemical modifications. The level of degradation of treated material depends on the rotation speed and barrel temperature [Moreno and Olsson, 2017]. The physical properties of material are changed when it is forced through narrow clearance between screw and barrel. The surface area in extrusion process can be increased by up to 75% [Khanal and Takara, 2012]. In case of e.g. lignocellulosic biomass, it is beneficial to apply some catalysts (acid, alkali and/or hydrolytic enzyme) during extrusion in order to obtain more efficient fractionation, leading to higher sugar yield in subsequent steps [Aden et al., 2017; Gogate and Joshi, 2017].

Ultrasound pretreatment

Ultrasound pretreatment also called as ultrasonication is a technology that uses rapid compression and decompression cycles of sonic waves to generate cavitation. This leads to formation, growth and subsequent collapse of bubbles, which is characterized by high temperature (500-15000 K) and pressure (100-5000 atm) attained locally [Gogate and Joshi, 2017]. Collapsing bubbles generate hydrodynamic shear force which leads to disruption of the lignocellulosic materials' structure, increasing the specific surface area and reducing polymerization, leading to increased biodegradability [Sivakumar and Tang, 2015]. The efficiency of cavitation effect is maximized between 30 °C and 70 °C, because this range allows integration of ultrasonication and enzymatic hydrolysis. Combination of ultrasound pretreatment with other techniques such as alkali- and acid-based pretreatments can increase delignification up to 90% [Moreno and Olsson, 2017].

Hydrodynamic cavitation

Unlike acoustic cavitation, where cavitation is generated by ultrasonic equipment, hydrodynamic cavitation is caused by use of alternations in the liquid flow in the hydraulic system [Dębowski et al., 2017]. Hydrodynamic cavitation occurs when a moving fluid suddenly changes its velocity resulting in localized pressure drop. For instance, it can occur with the help of Venturi or orifice plates [Coward-Kelly et al., 2017; Gogate and Joshi, 2017]. Besides some minor differences like temperature and pressure of the collapsing cavities, the principles which govern the acoustic cavitation bubbles and hydrodynamic cavitation bubbles are basically the same [Almeida et al., 2017; Dębowski et al., 2017]

Microwave pretreatment

Microwave pretreatment technique uses electromagnetic waves with frequencies in range of 0.3-300 GHz to irradiate lignocellulosic materials. The interaction between treated feedstock and electromagnetic field results in rapid heating, leading to faster reaction rate and better yields. This encourages both thermal and non-thermal effects for enhancing the accessibility of cellulose present in lignocellulosic materials to hydrolytic enzymes [Gogate and Joshi, 2017].

There are various advantages of microwave pretreatment as compared to conventional methods of heating. First of all, this process is more efficient, because microwave irradiation is capable of heating whole sample at the same time. Unlike conventional heating, it does not require time spent for waiting till sample heats up or cools down. Also, controllability is very high and allows easy control over temperature and pressure [Bajpai, 2016]. Microwave technique is often combined with other pretreatment methods such as ultrasound, ionic liquids, alkali and acid solutions to obtain better performance [Moreno and Olsson, 2017]. Studies report that the effectiveness of microwave irradiation strongly depends on treating temperature and electromagnetic field power. To some extent, the increase of temperature and/or electromagnetic power enhances effectiveness [Wang and Yin, 2017]. However, the process' energy and time demand is very

high, hence limitations in large-scale application and lack of economic feasibility, especially as an individual operation [Bajpai, 2016; Gogate and Joshi, 2017].

Chemical and physicochemical pretreatment

Torrefaction

Torrefaction is a thermochemical treatment of biomass that can be described as a mild form of pyrolysis at temperature ranging between 200 °C and 320 °C. Torrefaction changes the properties of biomass in order to obtain fuel with better quality for combustion and gasification applications. It is carried out under atmospheric conditions and in the absence of oxygen. During the process, water and redundant volatiles are removed, leaving as a product solid, dry, blackened material which is also called “torrefied biomass” or “bio-coal”. The combination of torrefaction and densification leads to a very energy dense fuel carrier of 20-25 GJ/ton [Baskar et al., 2012; Kurchania, 2012]. It was estimated that about 70 wt% of treated material is retained as a solid which contains 90% of initial energy content. On the other hand, the remaining 30 wt% that is converted into gas contains 10% of the energy of biomass [Mohee et al., 2018].

Steam explosion

Steam explosion process releases individual biomass components through steam impregnation under high pressure for a short contact time. This is the one of the most studied methods for pretreatment of lignocellulosic biomass. It is usually used for treating grinded biomass with saturated steam at temperatures 160-270 °C and pressures 0.69-4.83 MPa. The contact time varies from few seconds to 30 min and after that the pressure is suddenly released, which causes an explosion [Woiciechowski et al., 2013]. Due to material's expansion and high temperature the biomass' structure is disrupted and hemicellulose, cellulose, and lignin are degraded.

Study shows, that the optimal parameters for best performance is either high temperature and short residence time (270 °C; 1 min) or lower temperature and long residence time (190 °C; 10 min) [Li and Wan, 2013]. Although harsher conditions lead to

higher depolymerization of the biomass, these cause formation of toxic and fermentation-inhibiting molecules. Steam explosion can be effectively improved by addition of acid catalyst, preferably H_2SO_4 [Gogate and Joshi, 2017]. The use of catalyst results in increasing recovery of hemicellulose sugars, improving enzymatic hydrolysis on the solid residue, and decreasing production of inhibitory compounds [Bajpai, 2016]. However, the formation of inhibitory compounds (furan derivatives, weak acids, and phenolic compounds) in harsh conditions is high hence the process still needs to be optimized. Obviously, some advanced detoxification methods were supplied with success, but this represents additional costs in overall process [Barros et al., 2014].

Liquid hot water treatment

Liquid hot water (LHW) process treats biomass with water only and none of chemicals are added, even catalysts. For this reason, it is more economically profitable as compared to other methods. This process is similar to steam explosion, but uses water in the liquid state at high temperature instead of steam [Bajpai, 2016]. The temperature of water varies in the range of 150-230 °C and is maintained under pressure to keep it in liquid form. Hot water makes cellulose more accessible by solubilizing mainly hemicellulose also with a significant formation of inhibitors. In order to prevent this, the pH should be kept at relatively low level between 4 and 7 during the pretreatment. In this way, production of oligosaccharides is favored instead of monosaccharides, which can subsequently degrade into inhibitors. The main disadvantage of this technique is the fact that the concentration of solubilized product is much lower as compared to steam explosion [Barros et al., 2014; Khanal and Takara, 2012]

Acid hydrolysis

Dilute acid pretreatment enhances the degradation of hemicellulose, increasing porosity of the pretreated biomass and improving reaction rates for the enzymatic saccharification. This technique is widely reported pretreatment for rice straw, wheat straw, and corn stover [Huang et al., 2017]. The most commonly acid that is used for this process is the sulfuric, but there also other reagents such as hydrochloric, nitric, and phosphoric acids which are found to be effective as well. However, using dilute sulfuric is considered

as one of the most cost-effective methods [Woiciechowski et al., 2013]. Generally, the concentration of acid varies between 0.5% and 5%. Use of concentrated acids (even higher than 30%) is also possible, but due to problems with equipment corrosion, difficulties in acid recovery, and considerable degradation products formation, diluted acids are more popular [Moreno and Olsson, 2017].

The process is carried out at temperatures ranging from 140 °C to 215 °C. The residence time highly depends on the temperature and feedstock and varies from few seconds to even 24 hours [Bajpai, 2016; Wang and Yin, 2017]. From the economic point of view, it is believed that concentrated acid accompanied with lower temperature is reasonable however use of diluted acids with higher temperature occurs more often for its better performance [Woiciechowski et al., 2013; Wang and Yin, 2017]. Despite that, few studies reports that unusual process conditions can also lead to high efficient outcome, e.g. 81.6% of recovered sugar from bamboo by treating with 90.5% acid or 99% yield and 0.07% acid in case of poplar wood [Woiciechowski et al., 2013]

Alkaline hydrolysis

In this technique the alkaline chemicals interacts directly on lignin, thus sugar components are unaffected which is huge advantage when it comes to production of biofuels [Khanal and Takara, 2012]. The lignin structure is disrupted due to swelling of lignocellulosic material leading to increase of its internal surface, decrease in the degree of polymerization and cellulose crystallinity, and separation of linkages between carbohydrates and lignin [Woiciechowski et al., 2013]. Production of degradation compounds, which can later transform into inhibitors, is lower as compared to acid treatment [Gogate and Joshi, 2017].

Since use of alkali results mainly in solubilization of lignin and to certain, but low degree of hemicellulose and cellulose, the effectiveness of alkaline treatment is dependent mostly on lignin content in feedstock. Processing may take from minutes to days depending on characteristics of treated material and can be performed at room temperature. The most common treatment agents are NaOH, KOH, Ca(OH)₂, NH₃ and NH₄OH, however due to lower safety concerns and costs lime and ammonia are more commonly used [Gogate and

Joshi, 2017; Moreno and Olsson, 2017]. Alkaline pretreatment as well as acid pretreatment have one major drawback, which is pH adjustment required after treatment process, which is both expensive and harmful for the environment. The performance of alkaline treatment can also be enhanced by addition of some chemical reagents such as perhydrol or oxygen, however this creates more work for the subsequent processing [Gogate and Joshi, 2017; Wang and Yin, 2017].

Wet oxidation

In wet oxidation pretreatment, the material is treated with air or oxygen, which acts as an oxidizing agent in process. The key parameters are the temperature, oxygen pressure, and reaction time which are 170-200°C, 10-12 bar, and 5-15 minutes, respectively [Gogate and Joshi, 2017; Li et al., 2017]. As phenolic compounds are degraded into carboxylic acids during wet oxidation pretreatment, end products consists of less inhibitors as compared to steam explosion and liquid hot water pretreatment. The other advantage is the fact that wet oxidation is an exothermic process, thus the energy demand is reduced. Addition of catalyst such as Na_2CO_3 also helps with reduction of inhibitory products formation and maintaining pH at appropriate range. However, addition of catalysts involves higher costs [Gaur et al., 2018]. Wet oxidation is considered to be effective for many biomass sources such as corn stover and spruce giving high yields of monomeric sugars. The main disadvantage of this method is that the produced lignin cannot be used as fuels as it is oxidized during process. The other drawback is the risk of uncontrolled combustion that can occur at the oxygen injection points. Therefore, this pretreatment method will most likely not find practical applications in large-scale biomass processing [Bajpai, 2016; Gogate and Joshi, 2017].

CO₂ explosion

Carbon dioxide explosion process enhances the digestibility of lignocellulosic biomass by involving the use of supercritical CO₂ under pressure. The mechanism of this method is similar to AFEX and steam explosion, however it is conducted at lower temperatures than steam explosion and has a reduced expense as compared to AFEX. The efficiency of CO₂ explosion is also higher than both AFEX and steam explosion due to

smaller size of carbon dioxide molecule as compared to ammonia or water. The size of molecules matters, because with its decrease the effectiveness of penetration process is enhanced, thus hydrolysis is improved [Bajpai, 2016].

The relatively low temperature of the process prevents any significant decomposition of monosaccharides by the carbonic acid formed when dissolved in water. This acid also tends to increase the hydrolysis rate. CO₂ explosion method is environmentally friendly, since it does not discharge harmful chemicals. Another advantage from environmental point of view is the use of CO₂ which is abundantly available and co-produced during many industrial processes. The processing costs are low, but the high cost of equipment suitable for high pressure conditions of CO₂ explosion pretreatment is a strong limitation to the application for a large scale. Furthermore, it is not effective on feedstock with no moisture content [Gogate and Joshi, 2017].

Pyrolysis reactor and configurations

The type of reactor and its configuration depend on the objective of the pyrolysis process. Various types of reactors have been designed and they are divided into:

- fixed bed reactors,
- fluidized bed reactors:
 - bubbling fluidized bed reactors,
 - circulating fluidized bed reactors,
- ablative pyrolysis reactors,
- auger/screw reactors,
- rotating cone reactors,
- ultra-rapid reactors,
- vacuum pyrolysis reactors.

Fixed bed reactors

Fixed bed reactors, operating in batch mode, are the oldest pyrolysis reactor type. Batch mode means that feedstock, catalyst, filter media, carrier system and other substances remain stationary. The heat for the thermal decomposition of feedstock in this reactor type is supplied either from an external or internal source by allowing limited combustion of gaseous products. In some designs, an inert and oxygen free gas is used as a sweep gas for effective removal of produced gases from the reactor often combined with a cold trap that is used to collect condensable vapors to condense them into bio-oil [Adhikari and Thangalazhy-Gopakumar, 2016; Basu, 2013].

The technology used in these reactors is simple, suitable, reliable, and is independent of particle size. Fixed bed reactors can be made of firebricks, steel, or concrete and their design includes feeding unit, an ash removal unit, a gas exit a gas cooling and cleaning system that can be facilitated by addition of cyclone, and wet and dry scrubbers [Bhuyan et al., 2018].

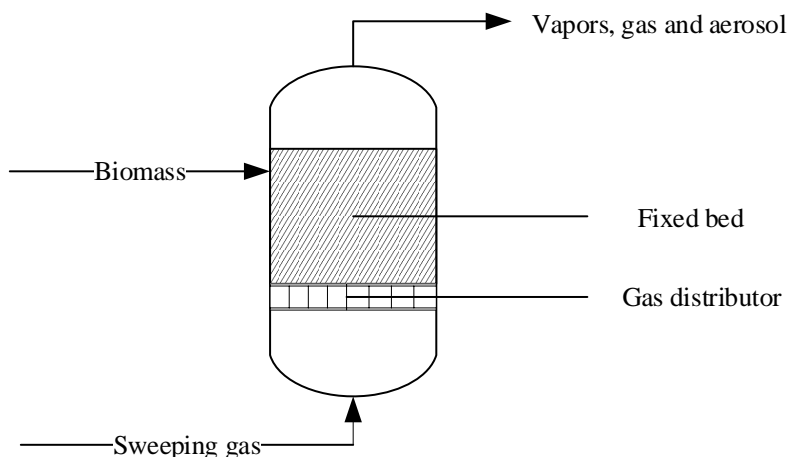


Figure 13. Fixed bed reactor [Bhuyan et al., 2018].

Fluidized bed reactors – BFB and CFB

Fluidized bed is a well-developed technology that is attractive and popular for biomass fast pyrolysis. They provide following features [Pizarro de Oro and Thormann, 2018]:

- rapid heat transfer,
- uniform heat distribution,
- short residence time,
- high surface area contact,
- ease of control,
- ease of scale.

In fluidized conditions, processed feedstock and heat carrier solids (bed material, e.g. sand) are in fluid-like state generally achieved by introducing pressurized gas through distributor plate which is located in the bottom of the furnace. The pyrolysis is carried out by the contact of feedstock with hot bed particles. A fluidized state is obtained only when a drag force of upwards moving gas is equal to weight of the particles [Stępień, 2015]. Hence, the size distribution of particles and gas velocity need to be determined precisely. This distributor plate includes plenty of vessels or orifices, etc. and ensures even distribution of injected inert gas such as nitrogen or helium [Adhikari and Thangalazhy-Gopakumar, 2016]. They come in different design, depending on the size of particles and flow regimes. Typical gas distributors are perforated and multiorifices plates, tuyers, caps, pipe grids, and spargers [Kunii and Levenspiel, 1991]. As for pyrolysis, there are two types of fluidized bed reactors which mainly differ in the residence times of vapors: bubbling fluidized bed and circulating fluidized bed [Pizarro de Oro and Thormann, 2018].

Bubbling fluidized bed reactors have a simpler design. The particles in BFB reactors have sizes of less than 2-3 mm and are bigger than those processed in CFB. Both BFB and CFB have relatively high yield of bio-oil which is in range of 70-75% on dry wood feed. In CFB the gas flow rate is higher so that the vapor residence times are shorter. Additionally, both bed material and char particles are taken out of the CFB together with carrier gas and pyrolysis vapors, hence CFB requires more heat carrier solids as compared to BFB. High

velocity combined with excellent mixing allows a CFB to have larger throughputs of feedstock [Basu, 2013; Bhattacharyya et al., 2018].

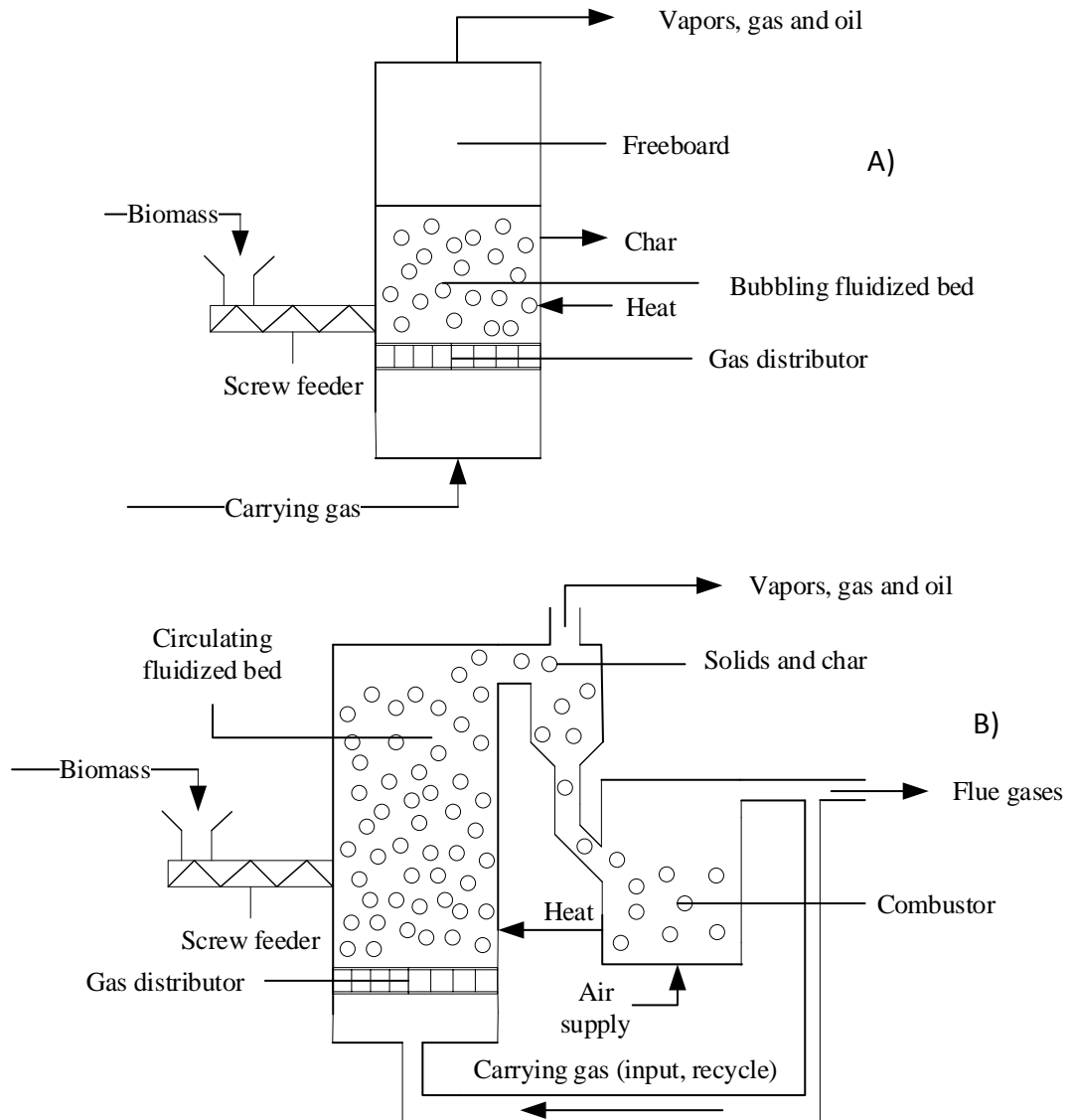


Figure 14. A) Bubbling and B) circulating fluidized bed pyrolyzers [Pizarro de Oro and Thormann, 2018].

Ablative pyrolysis reactors

Ablative pyrolysis is different in concept as compared with other methods of fast pyrolysis. It is characterized by having the biomass pressed against a hot surface. This somehow causes the “melting” effect forms an oil residue film on that surface. Its temperature is approximately 600 °C and can be significantly enhanced by adjusting the pressure force [Nachenius et al., 2013].

The evaporation of the decomposed biomass takes place when the feed is mechanically moved away from the hot surface. At the same time, a char is deposited and later removed through abrasion by subsequent feed. This leads to obtaining a bio-oil product with a relatively high content of fine char particles that need to be removed. Typically, the vapors that are produced during ablative pyrolysis have a lower molecular weight due to vapor cracking occurring on the metal surface [Meier, 2017; Pizarro de Oro and Thormann, 2018].

As the reaction rate in ablative pyrolysis does not depend on heat transfer through the feed, this method can not only process larger particles, but what is more, there is no upper limit for the size and that is the major advantage [Bridgwater, 2017]. Also, in this case no transport gas is necessary to remove the volatile pyrolysis products. Nevertheless, the mechanical nature of the process is complex and costly and the throughput of this process is limited by the amount of heat that can be transferred to the hot surface. Due to that, this method is technologically challenging and is difficult to scale up [Pizarro de Oro and Thormann, 2018; Nachenius et al., 2013]

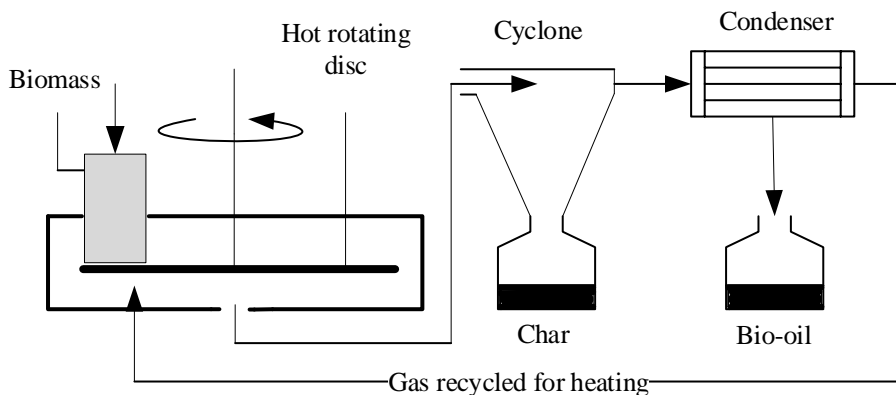


Figure 15. Ablative pyrolysis reactor [Bhuyan et al., 2018; Pizarro de Oro and Thormann, 2018].

Auger/screw reactors

This type of reactors used rotating screw of auger to displace the biomass feedstock through an inert cylindrical heated tube. The function of the screw is also mixing the feed, hence controlling the residence time of the biomass in the reactor [Adhikari and Thangalazhy-Gopakumar, 2016]. The temperature of the feedstock passing through the tube is lifted up to the temperature in range of 400-800 °C. The vapors residence time can be easily manipulated by changing length of the heating zone. This method does not require carrier gas, is very compact, energy efficient, and even portable in some cases, thus allowing on-site conversion of biomass. However, auger/screw reactors are suitable only for small scale production [Bhuyan et al., 2018; Nachenius et al., 2013].

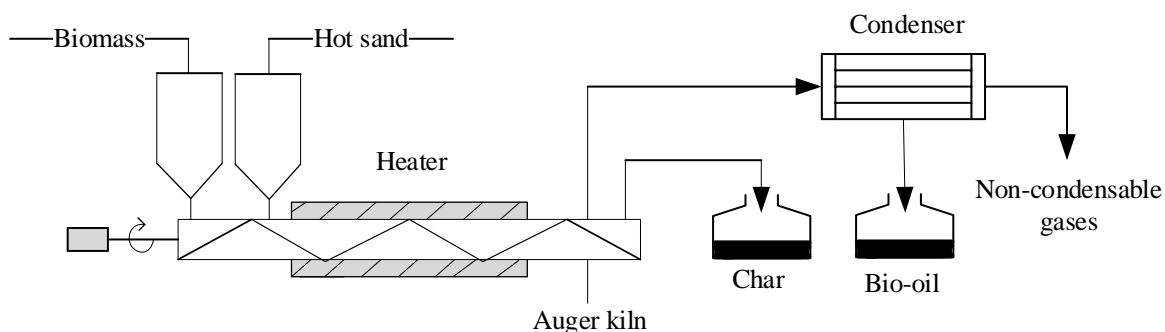


Figure 16. Auger pyrolysis reactor [Bhuyan et al., 2018].

Rotating cone reactors

In these reactors, the mixture of feed and hot sand as heat carrier solids is fed into the bottom of rotating cone. The use of intense mixing of feed and hot inert particles is the most efficient approach as for heat transfer [Pizarro de Oro and Thormann, 2018]. In this case, the excellent mixing allows rapid heating up to 5000 K/s. This method is similar to the one used in fluidized bed reactors, however it does not require vast amounts of inert gas. The rotation (up to 600 rpm) creates a centrifugal force that pushes the heat carrier solids and char formed during pyrolysis against hot wall and finally out of the reactor [Basu, 2013]. Upon exiting the cone, the char is combusted to supply heat for pyrolysis, while sand is returned to the pyrolysis reactor. The produced gas vapors leave through another tube. The absence of carrier gas simplifies bio-oil condensation and bio-oil yields are approximately 70 wt% when using wood as a feed material [Nachenius et al., 2013]. Rotating cone method is characterized by very fast heating and short residence time. Unfortunately, it is relatively difficult to control an scale up [Bhuyan et al., 2018; Pizarro de Oro and Thormann, 2018].

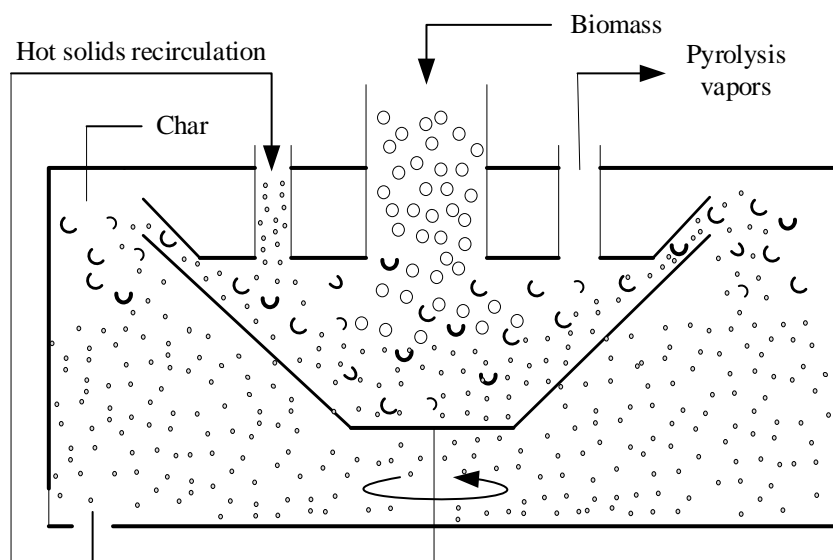


Figure 17. Rotating cone pyrolysis reactor [Anatunović et al., 2017].

Ultra-rapid reactors

Ultra-rapid pyrolyzer is characterized by extremely short mixing time (10-20 ms), reactor residence time (70-200 ms), and quench time (ca. 20 ms). Due to low processing temperature that varies around 650 °C, it is possible to achieve a very high liquid yield, which is around 90%. The feed is treated by inert gas heated to ca. 100 °C that is injected into reactor via multiple jets at very high velocities in order to bombard the stream of biomass. That type of pyrolyzer can also use heat carrier solids that might be introduced to the reactor in the same way as inert gas [Basu, 2013].

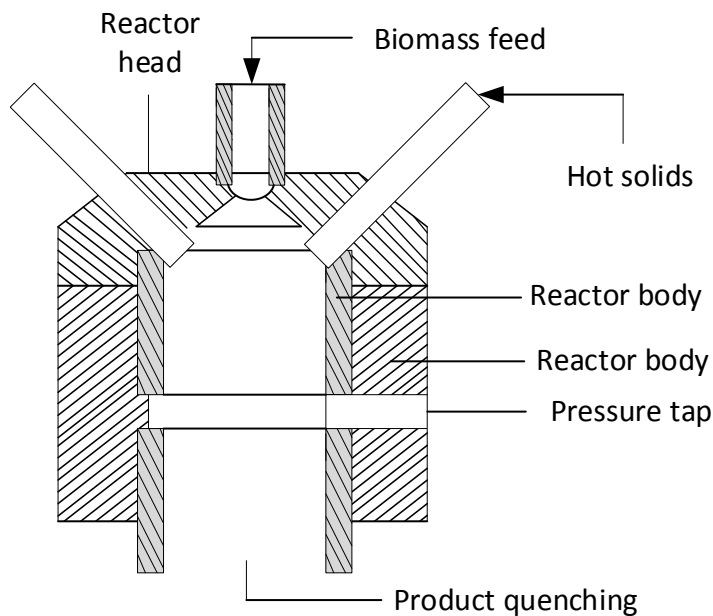


Figure 18. Ultra-rapid pyrolysis reactor [Basu, 2013].

Vacuum pyrolysis reactor

In this system, a vacuum pyrolyzer comprises a number of stacked heated circular plates. The temperature of these plates rises down the reactor from about 200 °C to 400 °C. Biomass is fed from the top of the reactor and drops to successive lower plate as it undergoes thermal decomposition. The produced vapors during pyrolysis are taken away

from the reactor by a vacuum produced by pump. Hence, this type of reactor does not require carrier gas. The typical liquid yield reaches about 35-50% on dry feed, whereas char yield is very high [Adhikari and Thangalazhy-Gopakumar, 2016; Basu, 2013]. The advantage of this system is that it is able to process larger biomass particles (2-5 cm) and a short residence time which reduces secondary reactions. On the other hand, it represents poor heating rate, high investment and maintenance costs, and high risk of pump fouling [Bhuyan et al., 2018]

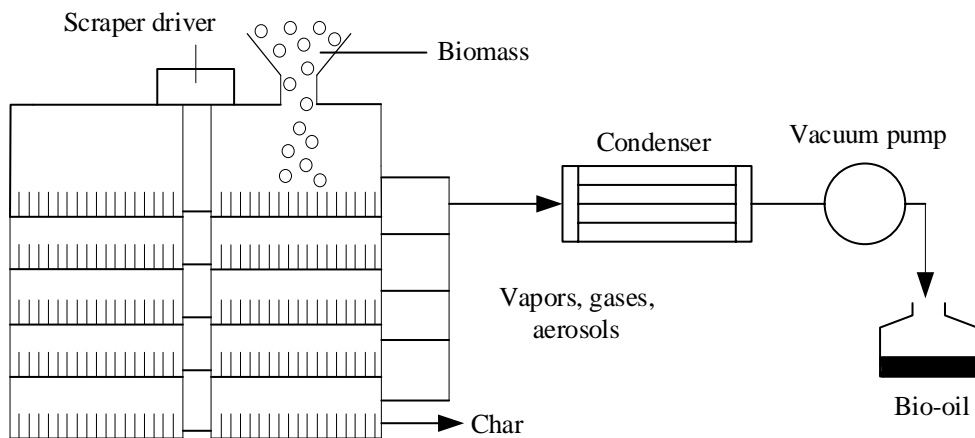


Figure 19. Vacuum pyrolysis reactor [Basu, 2013; Bhuyan et al., 2018].

Analytical techniques for organic matter devolatilization investigations

One of the most common techniques that are used to determine the nature and amount of volatile products formed during thermal decomposition of material is called evolved gas analysis (EGA). During thermal conversion of the biomass, a series of chemical reactions occur as a function of temperature resulting in formation of various gaseous species that can be analyzed using different analytical methods. By determining the composition of these products, EGA evaluates the chemical pathway of degradation reactions.

Generally, two analytical techniques are widely employed to investigate decomposition of biomass including TG/FTIR and TG/MS. The weight loss of one biomass

sample and decomposition gas and liquid products can be monitored simultaneously [Brown, 1988; TA instruments, 2012].

The sampled gas and liquid products from biomass decomposition process can be analyzed with continuous or intermittent mode. In continuous mode the gaseous and liquid products are introduced to the detector system directly, whereas intermittent mode refers to trapping evolved species at a low temperature or in absorption chamber before introducing them for the identification. Intermittent mode is used mostly in TG/GC-MS or Pyrolysis/GC-MS and it allows the investigator to optimize the detector parameters to make the best choice for different samples [Pan and Xie, 2001].

Thermogravimetric analysis (TG/TGA)

Thermogravimetric analysis is one of the most widely used methods for studying biomass decomposition behaviours under different conditions. During the thermogravimetric analysis, loss of biomass sample weight is recorded as a function of conversion parameters including temperature, atmosphere, heating rate, etc. The change in weight measured by TGA is quantitative and no information on the chemistry of evolved gases is obtained. For chemical analysis of vapor products, TGA can be coupled to mass spectrometer (MS) or Fourier transform infrared (FTIR) [Thomas and Schmidt, 2010]. at each series for increasing temperature.

Thermal analyzers that are used for studying thermal decomposition include a high-sensitivity balance, a temperature controlled furnace, a unit for evacuation and control of the atmosphere in the furnace, and a control and data recording system.

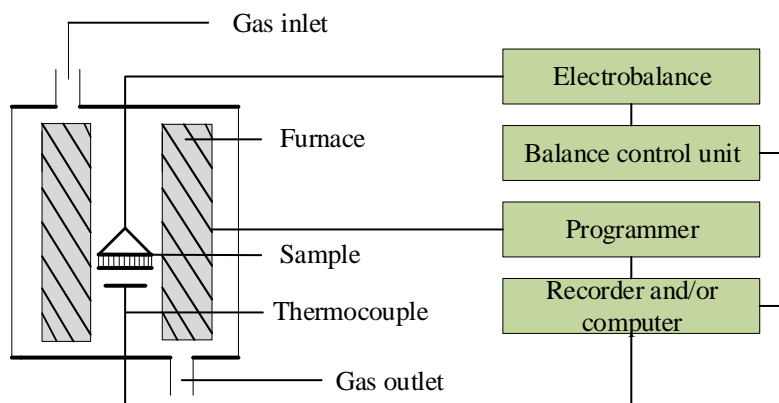


Figure 20. Schematic diagram of thermobalance system [Haines, 1995].

Depending on a specific model, the maximum load varies around 1 g, whereas sensitivity around $0.1 \mu\text{g}$ [TA instruments, 2012]. As it comes to sample placement, there are three main variations of positioning the sample relative to the furnace (**figure 21.**). The first one is that the sample may be suspended from the balance beam and hang down into a controlled-temperature environment. Alternatively, the sample may be placed above the balance beam. This method has an important advantage over the first one, because unlike suspended type, it does not require any protection system to prevent rising hot gases from affecting the balance mechanism. The last and most commonly used is the horizontal arrangement, where the sample support is an extension of the balance beam [Brown, 1988].

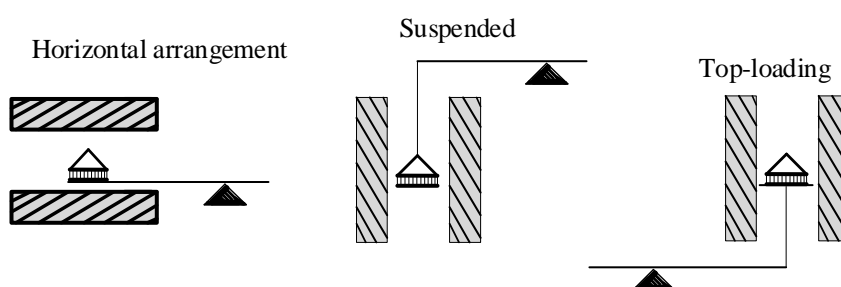


Figure 21. Ways of positioning the sample relative to the furnace in TG unit [Brown, 1988].

The furnace normally is an electrical resistive heater and as it is shown in (**figure 22.**) it may be within the balance housing, part of the housing, or out of the housing. These rely mainly on heating of the sample by conduction through solid or gas. Large temperature

gradients, especially when sample is characterized by low thermal conductivity (e.g. polymers, inorganic glasses) is inevitable. The most important features needed from the furnace are as follows [Brown, 1988; Haines, 1995]:

- the furnace should have a zone of uniform temperature that is larger than the sample including holder,
- balance mechanism should not be affected by heat from the furnace,
- the temperature range should include values well above those of interest,
- it should be capable of rapid response and be able to work in many different heating and/or cooling rates,
- the furnace lining should be inert at all temperatures.

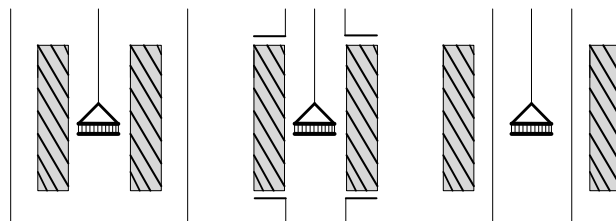


Figure 22. Furnace positioning within the balance housing [Brown, 1988].

Normally, there are two kinds of temperature program used for TGA analysis of biomass materials, including [Nirav, 2017]:

- Isothermal (static)-the temperature keeps at a certain value for desired time,
- Dynamic-the temperature increase at a certain heating rate),

Mass spectrometry (MS)

MS technique is to identifying composition and determine amount of gas products released from decomposition of biomass at elevated temperatures. based on determining masses of free ions in high vacuum and [Popp and Reichenbacher, 2012]. The gas products are first ionized in high vacuum to produce free ions. Its sensitivity makes it useful for the detection and analysis of traces of macromolecules down to less than 1 pg [Nolting, 2009]. The general design of a mass spectrometer includes:

- sample injector,
- sample ionizer,

- mass analyzer,
- ion detector.

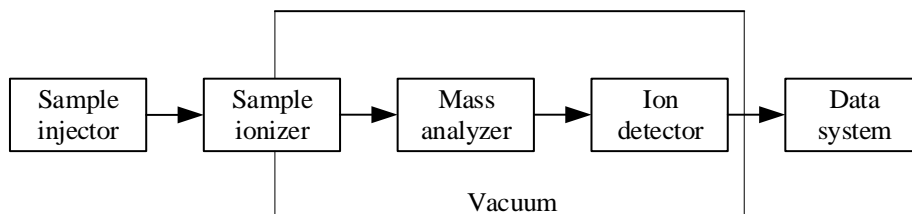


Figure 23. Basic components of a mass spectrometer [Chu and Lebrilla, 2010; Nolting, 2009].

There is variety of methods for ion generation. Volatile molecules are best ionized in the gas phase by bombarding them with electrons. The optimal methods for this purpose are electron-impact ionization (EI) and its derivative-chemical ionization (CI). The ionization of thermally labile or large volatile compounds is conducted by desorbing them directly from solid or liquid samples. For solid samples, matrix-assisted laser desorption/ionization (MALDI) is used, whereas electrospray ionization (ESI) for liquid samples [Chu and Lebrilla, 2010]. In EI ionization, ions are generated by directing an electron beam of energetic electrons into the molecule of interest. The electron beam is produced by heating a filament (often tungsten) to emit electrons which are accelerated towards a positively charged anode. The molecular vapor is passed through the ion source and individual molecules collide with high-energy electrons which results in formation of a molecular ion [Malainey, 2011]. CI technique is essentially EI with a reagent gas resulting in ionization of the much more abundant reagent gas that reacts through ion-molecule reactions with the analyte. Common reagent gases are methane, ammonia, and iso-butane [Chu and Lebrilla, 2010; Popp and Reichenbacher, 2012]. In MALDI, the sample is dissolved in a matrix and ionized using an UV laser. The matrix itself absorbs the laser energy which leads to vaporization of the sample and matrix material, and as a proton donor and acceptor initiates charge transfer to the analyte [Bobst and Kaltashov, 2013]. Electrospray ionization as the most popular liquid chromatography-mass spectrometry (LC-MS) is highly sensitive technique [Smith, 2017]. In ESI, the separated sample component and solvent mobile phase is sprayed from a small tube into a strong electric field in the presence of a flow of warm

nitrogen to assist desolvation. The spray droplets evaporate in a region maintained at a vacuum causing the charge increase on the droplets. The charged ions then enter the analyzer [Malainey, 2011; Smith, 2010]. Once the ions are formed in the ionizing source, they are accelerated towards the mass analyzer and separated according to m/z ratios.

Mass analyzers separate the charged molecules or their fragments based on their m/z ratio, which are further detected by ion detector. There are normally three kinds of mass analyzer including quadrupole, magnetic sector, and an ion trap [Christian et al., 2012]. In quadrupole mass analyzer a combination of DC and AC potentials are applied to a set of four rods (quadrupole). When the ion beam is accelerated to a high velocity by an electric field and passes through the quadrupole, only ions with one mass-to-charge ratio can pass at a time [Nolting, 2009]. Ions that have unstable trajectory through the quadrupole are filtered by colliding with rods and never reach the detector [Christian et al., 2012]. For this reason, quadrupole MS should be called mass filter, rather than mass analyzer, because this device allows ions within a narrow m/z range to be transmitted [Bobst and Kaltashov, 2013].

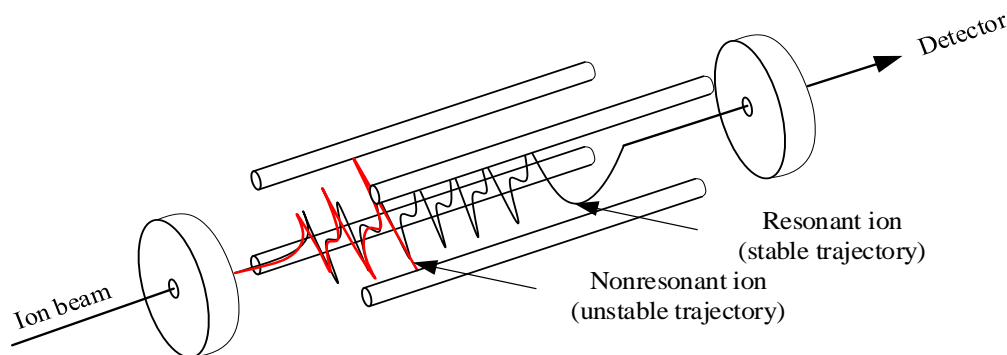


Figure 24. Quadrupole mass spectrometer [Malainey, 2011; Nolting, 2009].

The simplest means of mass separation is achieved through use of magnetic fields alone. Ions leaving the ion source are accelerated and pass through the sector in which the magnetic (or electric) field is applied perpendicular to the direction of the ions trajectory. Ions with the same charge, mass, and energy will follow the identical circular path if the strength of magnetic field is constant [Malainey, 2011; Nolting, 2009]. Ion traps are basically multidimensional quadrupole mass analyzers that store (trap) ions and eject them according to their m/z ratios [Smith, 2017]. The ion trap consists of two end cap electrodes

and a doughnut-shaped ring electrode to which variable radio frequency (RF) voltage is applied. Ions enter the trap through a hole in one-end cap electrode and circulate within the electric field in three-dimensional orbits. The destabilization of the orbits by increasing a voltage is used to eject ions through the other end cap to the detector [Malainey, 2011].

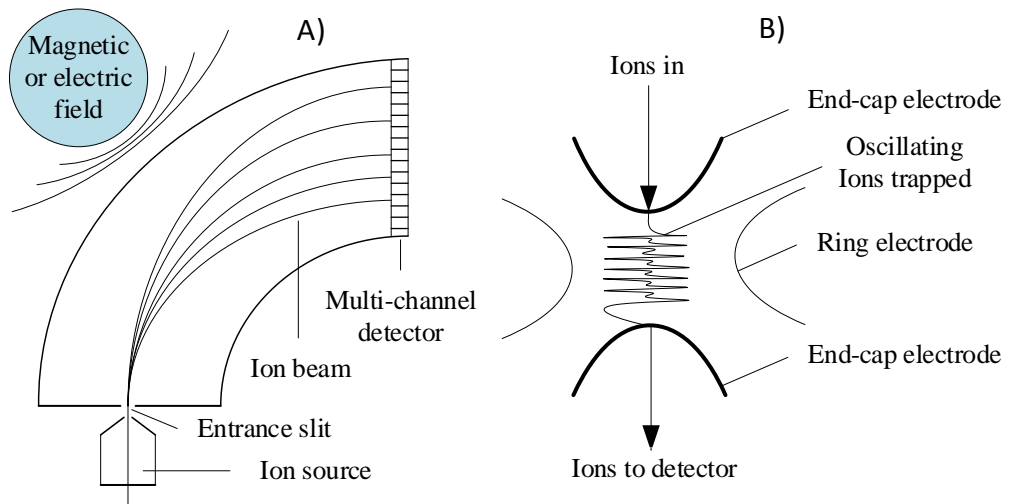


Figure 25. a) Magnetic mass spectrometer and b) Ion trap mass spectrometer [Nolting, 2009; Smith, 2017].

The detection of ions generally involves either converting them into negative charges and multiplying the number of electron to amplify the signal (electron multiplier) or counting the positive charges (Faraday cup). Faraday cup records impacts of positive ions emerging from mass analyzer on a collector surface or collector electrode. The collector is connected to the ground potential through a resistor and whenever a positive ion hits the collector, a voltage drop occurs across the resistor and the resulting signal is amplified and recorded. Electron multipliers use a process that is called secondary electron emission. When the ions hit the inner surface of electron multiplier, secondary electrons are emitted and then accelerated through an electric field which is generated by applying proper voltage to that surface. The electric field forces emitted electrons to make impacts like ions, which cause more electrons to be emitted. This process continues until there are enough electrons to create a measureable current [Malainey, 2011; Nolting, 2009].

Fourier Transform Infrared Spectroscopy (FTIR)

The main goal of using FTIR is to determine chemical functional groups present in the sample. Each functional group absorbs characteristic frequencies of IR radiation. The intensity of the absorption is related to the concentration of a compound. As the result, the two-dimensional plot (spectrum) consisting of intensity and frequency of sample absorption is obtained [Dhoble et al., 2012]. The IR spectra is acquired using special instrument known as spectrometer. One of the modern types of spectrometer is the single-beam FTIR spectrometer that uses modulator (interferometer). In this device, the energy that passes through the sample is examined using a Fourier transform instrument [Madejova and Petit, 2013].

The main element of FTIR spectrometer is an amplitude division interferometer, most commonly Michelson interferometer. It consists of a beamsplitter, a compensating plate, and a pair of mirrors [Stuart, 2004]. The beamsplitter divides radiation in two directions. One beam goes to a stationary mirror and then back to the beamsplitter. The other one goes to a second mirror which is moving. The sinusoidally moving mirror with constant velocity makes the total path length variable versus that taken by the stationary-mirror beam. These two beams meet again at the beamsplitter where they recombine, but the difference in path lengths creates destructive and constructive interference that is called interferogram [Doyle, 1992]. The interferogram is a plot of intensity of absorbed energy versus time, but using a Fourier transform it is possible to obtain intensity versus frequency spectrum [Christian et al., 2012].

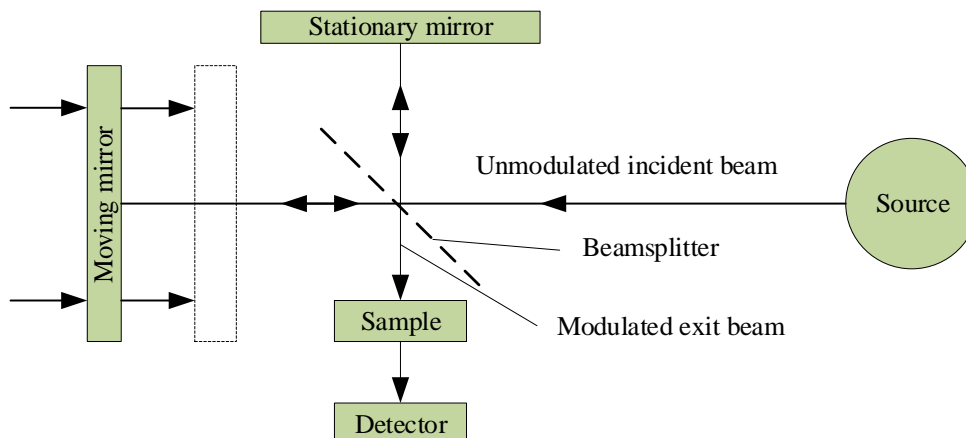


Figure 26. Scheme of a simple interferometer [Christian et al., 2012; Stuart, 2004].

Gas chromatography (GC)

Chromatography is a general term applied to a variety of separation methods based on the partitioning or distribution of a sample within moving or mobile phase and a fixed or stationary phase. GC is the type of chromatography in which gas is a mobile phase, whereas stationary phase may be an immobilized liquid or an inert solid in either a packed or capillary-type column. The gaseous sample, under a controlled temperature gradient is injected onto the head of the column and entrained by the flow of an inert mobile phase that is usually driven by pressure or gravity. The separation of volatiles is based on several properties such as molecular size, boiling point, and polarity. Each compound interacts with the column matrix, resulting in different mobilities down the column [Baraem, 2017]. The modern chromatographic systems consist of:

- carrier gas,
- flow control,
- sample inlet and sample devices,
- columns,
- controlled temperature zones,
- detectors,
- data system.

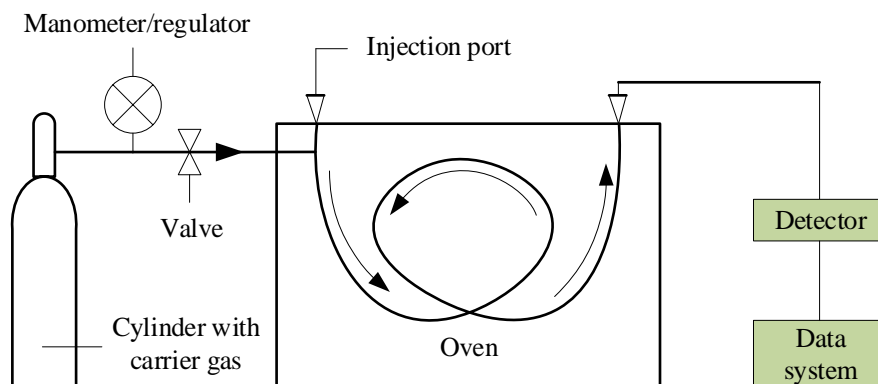


Figure 27. Scheme of a typical gas chromatograph [Mcnair and Miller, 2009].

The gas chromatograph functions as follows. An inert carrier gas flows continuously from a gas cylinder through the injection port, the column, and the detector. Apart from just carrying the sample, a secondary purpose of an inert gas is to provide a suitable matrix for the detector to measure the sample components. Inert gas selected according to standards should minimize detector drift and noise, and ensure reproducible retention times. Retention time is the amount of time needed for a compound to pass through the column. It is considered to be a time from injection to detection and it is different for each compound (there might be some exceptions). The sample is introduced via heated injection port from and carried into the column where it is separated into individual components. After the column, sample together with carrier gas pass through the detector that measures the quantity of the sample and generates an electrical signal. In the end, signals are processed in a data system and a chromatogram is generated [Mcnair and Miller, 2009; Vitha, 2017].

Chemistry of lignocellulosic biomass decomposition

Reactions occurring during devolatilization and potential products

During devolatilization of biomass, large number of reactions take place in series or in parallel, including depolymerization, dehydration, aromatization, isomerization, decarboxylation, charring and etc. Generally, devolatilization of biomass consists of three

main stages: free drying at early stage, primary decomposition , and secondary decomposition, including repolymerization and cracking of tarry vapors. These stages are more or less intermingled and their transitional behaviors can be observed through thermal analysis [Anca-Couce, 2016; Evans et al., 2016].

As it was mentioned before, lignocellulosic biomass consists of three main components which are cellulose, hemicellulose and lignin. Mechanisms of thermal decomposition of these constituents differ from each other, which need to be considered and investigated separately. The first thorough analyzes regarding pyrolysis of cellulose were reviewed in 1982 by Shafizadeh and since then some schemes were proposed, developed and later simplified. On the other hand, information about pyrolysis of hemicellulose in literature is much more limited than for cellulose. As a substitute for hemicellulose, a commercially available straight-chain polymer of xylose known as xylan is often used, because of the fact that it is hard to extract native hemicellulose [Garcia-Perez and Pecha, 2015]. The first studies on thermal decomposition of cellulose were also conducted by Shafizadeh et al and there were found a lot of similarities as well as differences between pyrolysis of cellulose and hemicellulose [Anca-Couce, 2016; Cai et al., 2017]. Lignin's structure is more complex than the polysaccharides cellulose and hemicellulose therefore the scheme of its decomposition completely differs and covers much wider temperature range [Evans et al., 2016; D. Rana and V. Rana, 2017].

Cellulose breaks down into smaller sugar units through various degradation reactions.. It is considered that primary reactions of cellulose lead to the production of sugars cellobiosan and most desired levoglucosan (LGA). After that, secondary reactions degrade primary products into smaller compounds and convert them into char and larger products [Anca-Couce, 2016; Broadbelt et al., 2016; Pareek et al., 2013].

Identifying and verifying cellulose pyrolysis scheme experimentally is difficult and complicated, but they are essential for fitting data and estimating product yields. Thus, there is a continuous debate about the real cellulose pyrolysis mechanism among many researchers. Striving for the right model is additionally complicated by inconclusive kinetic data that are collected with each reactor setup due to differences in fluid mechanics and heat

transfers [Bhaskar and Dhyani, 2017]. However, there are few common models that were considered as accurate and reliable and contributed to development of present model.

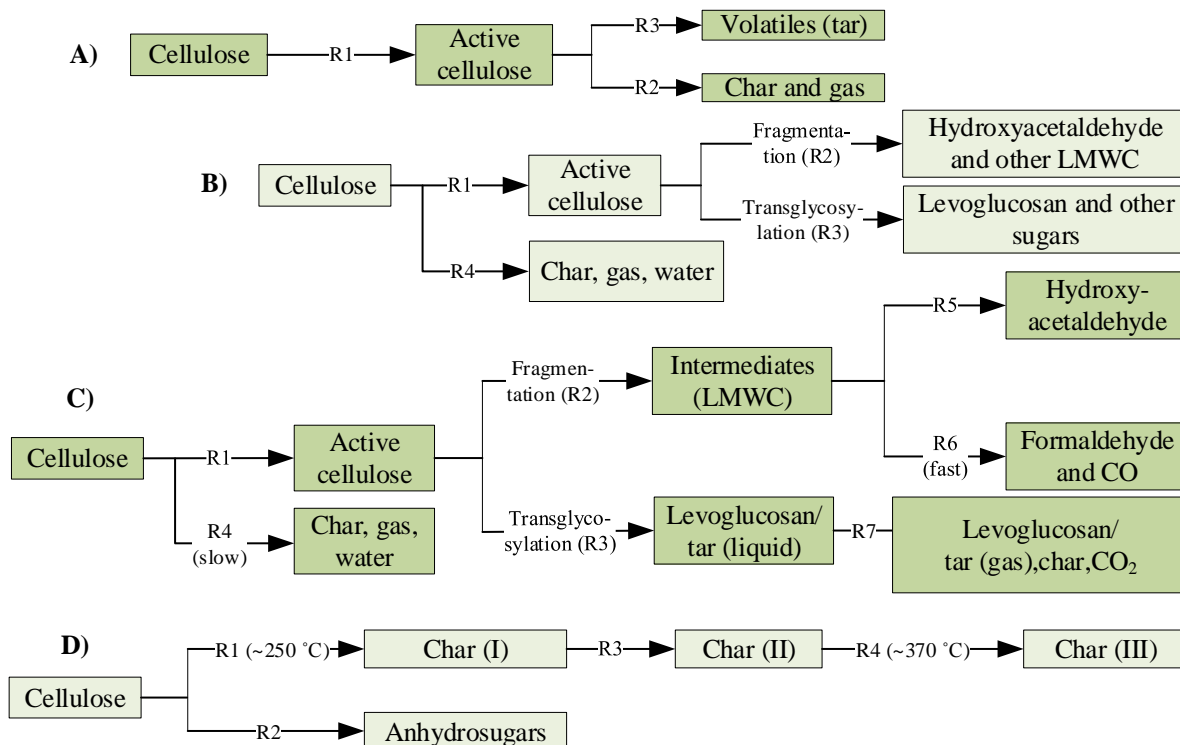


Figure 28. First models of lignocellulosic biomass pyrolysis. A) Broido- Shafizadeh scheme; B) Piskorz scheme; C) Banyasz scheme; D) Varhegyi-Antal scheme [Anca-Couce, 2016; Garcia-Perez and Pecha, 2015].

According to Broido-Shafizadeh, Piskorz, and Banyasz pyrolysis model, the reaction R1 leads to formation of active cellulose by depolymerization of cellulose, reducing the degree of polymerization, but without any volatiles as a product. The following decomposing reactions involving active cellulose with low degree of polymerization are either slower reaction (R2), producing char and permanent gases or main reaction (R3) producing tarry pyrolyzate containing levoglucosan, cellobiosan (dimer), cellotriosan (trimer) and other larger sugars [Anca-Couce, 2016; Dai et al., 2017]. Both crystalline and amorphous cellulose first melt into liquid phase formed by oligo-anhydrosugars and levoglucosan, then the products can evaporate or can be thermally ejected. The products

that evaporate are mostly smaller sugars (like levoglucosan), whereas larger sugars are less likely to evaporate at pyrolysis conditions and are removed by thermal ejection [Blasiak et al., 2012; Garcia-Perez and Pecha, 2015].

Under fast heating rate conditions, the depolymerization of cellulose into LGA takes place above 300 °C, when reaction R2 dominates over reaction R3. Below that temperature, the crystalline cellulose remains as solid due to presence of cross-linking reactions and because of the fact that reaction R2 has lower activation energy than reaction R3, charring is favored at lower temperatures. It is generally considered that the amorphous cellulose is the first to pyrolyze, followed by crystalline cellulose which requires more energy to break interchain bonds. The boiling point of levoglucosan is in the range of 290 and 300 °C, whereas cellobiosan and cellotriosan around 581 and 792 °C, respectively [Anca-Couce, 2016; Blamey et al., 2016; Garcia-Perez and Pecha, 2015]. For this reason, larger sugars remain in the liquid phase and turn into char or smaller undesired products and are not observed under atmospheric pressure pyrolysis conditions.

During slow pyrolysis of cellulose, instead of depolymerization, the dehydration reactions dominate, thus formation of levoglucosan is much more limited. LGA is typically observed in fast pyrolysis or at slow pyrolysis under vacuum. Additionally, high yields of LGA mostly consist of small particle sizes and with rapid cooling of the vapors [Anca-Couce, 2016; Dong et al., 2013].

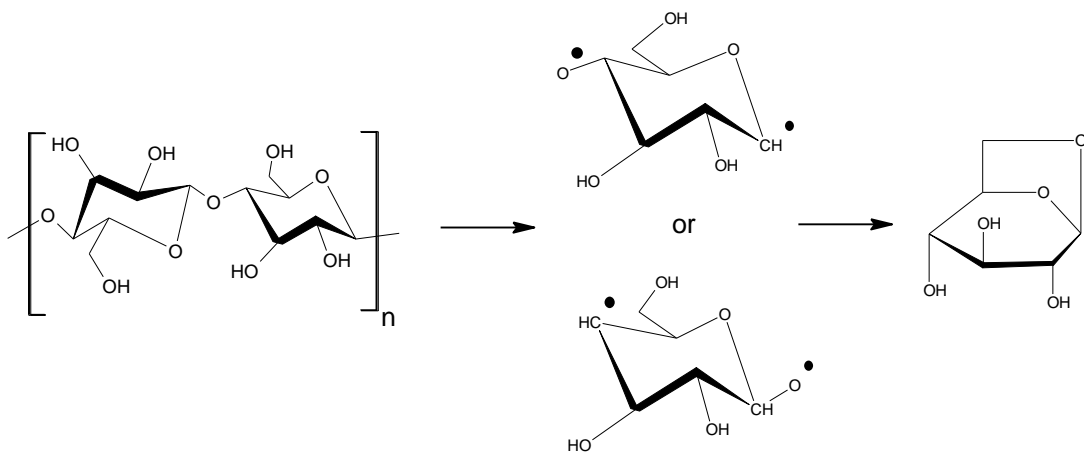


Figure 29. One of few proposed mechanisms of LGA formation – free radical mechanism [Dong et al., 2013]

In the free-radical mechanism, the formation of levoglucosan during cellulose pyrolysis is preceded by the decomposition of cellulose chain into anhydroglucose radical units. After that, anhydroglucose radicals can be transferred into levoglucosan. The formation of free-radical is considered to be caused by cleavage of a cellulose chain by breaking β -(1,4)-glycosidic bonds into two equal molecules [Bai and Brown, 2013; Dong et al., 2013].

The Piskorz model involves a competition between low temperature char formation reaction (R4) and a rapid depolymerization of cellulose to active cellulose (R1) in the initial stage. At the later stage, the competitions exists between formation of intermediates like hydroxyacetaldehyde due to ring fragmentation (R2) and depolymerization by transglycosylation to obtain mainly levoglucosan and other sugars (R3) [Garcia-Perez and Pecha, 2015].

Banyasz et al. later modified and completed the Piskorz model, including additionally char and permanent gases. In this scheme, intermediate products are generated in reaction R2 and liquid LGA is produced in reaction R3. The intermediated decompose rapidly hydroxyacetaldehy in competition with the production of formaldehyde and CO. Liquid LGA from R3 evaporates and undergoes char-forming reactions leading to production of CO₂ and obviously char [Dong et al., 2013; Saka et al., 2016]. The interesting fact is that CO and CO₂ in this model come from two different pathways. Furthermore, the activation energies of reactions R2 and R3 are known and calculations estimated that activation energy of ring fragmentation (R2) is higher so transglycosylation is favored in lower temperatures [Anca-Couce, 2016].

As opposed to other models, Varhegyi and Antal reported that anhydrosugars are not secondary products, but primary products [Garcia-Perez and Pecha, 2015]. According to Varhegyi-Antal model, during decomposition of cellulose, primary together with secondary reactions of pyrolytic vapors are the source of produced char. Therefore, char is both primary and secondary product like it was also presented in Banyasz model. The formation of char depends mostly on residence time of tar in char-forming environment, because as it was mentioned before, after LGA vaporizes, it undergoes charring if it cannot diffuse out of the sample matrix [Anca-Couce, 2016; Broadbelt et al., 2016]. Fast removal of primary char is a general requirement as it acts as a catalyst for crack primary organic vapors to for

secondary char, water, and gas, leading to lower bio-oil yields. Thereat, increase of mass transfer prevents char production [Broadbelt et al., 2016; Pareek et al., 2013].

Despite the fact that above models were created quite long time ago, most of their fundamental are believed to be valid and are often referred in the literatures. However, there are still few controversies about some details of these schemes, such as the role of active cellulose, the importance of secondary reactions, the optimal method to determine kinetics, and the activation energies for production of volatiles and tar [Anca-Couce, 2016].

Although a broad knowledge has been acquired about cellulose pyrolysis, the exact mechanism is still unknown. In recent years, several papers concerning same survey have been published, which have brought more insights. The current understanding of pyrolysis of cellulose is presented in **figure 30**.

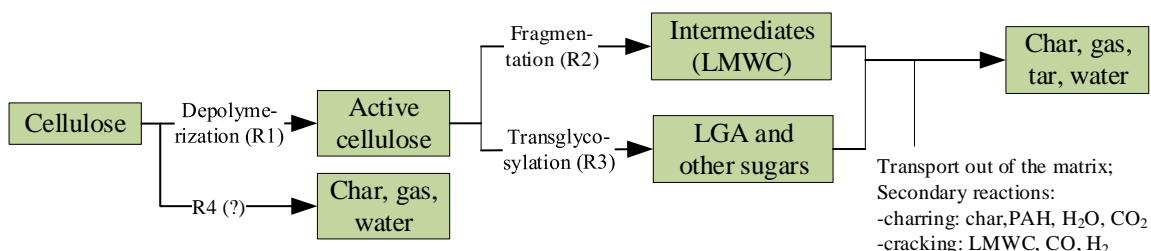


Figure 30. Cellulose pyrolysis scheme summarizing information available in the literature [Anca-Couce, 2016].

According to that scheme, after depolymerization (reaction R1) and formation of active cellulose as an intermediate liquid compound, there is a competition between fragmentation (R2) and transglycosylation (R3). The main products of fragmentation and transglycosylation are low molecular weight compounds (LMWC) and LGA, respectively. It is assumed that transglycosylation leads to formation of some cavities in the cellulose matrix, which are filled up mainly by LGA forming liquid tar with high boiling point. This disrupted macromolecule partially consists of LGA-end and non-reducing chain end. These moieties take a part in converted reactions and form LGA. Heterolytic reactions leading LMWC formation are favored in higher temperatures and can be favored by the catalytic effect of inorganic compounds [Anca-Couce, 2016; Evans et al., 2016].

Primary pyrolysis products further undergo secondary reactions outside the cellulosic matrix or in the condensed phase. According to **figure 30**, char is both primary and secondary product however its production through reaction R4 is still highly questionable. The reaction pathways of char-forming reaction R5 are yet to be discovered. For now, charring is associated with the production of H₂O, CO₂ and polyaromatic hydrocarbons (PAH) [Anca-Couce, 2016]. As in previous models, secondary reactions are more likely to occur at lower temperatures and with increasing residence times of volatiles, pressure and amount of inorganic impurities. The reaction R6 which is cracking of the volatiles can occur both inside and outside of the cellulosic matrix. The main products of cracking are LMWC, hydrogen and CO, wherein production of carbon oxide is more substantial in higher temperatures, above 500 °C [Broadbelt et al., 2016; Dai et al., 2017]

Most of the fundamentals regarding cellulose pyrolysis are also valid for hemicellulose. The exception is that the competition occurs between the formation of fragmentation products and sugars (but for example xyloses for xylan, instead of levoglucosan) [Anca-Couce, 2016]. Hemicellulose is understood to convert to different activated forms of hemicellulose according to fixed stoichiometry. The first activated hemicellulose species is either converted to light hydrocarbons, gases, and char or to xylose. The second form is converted to vapors, gases, and char [Nachenius et al., 2013; Peng and Wu, 2010].

Hemicellulose undergoes degradation reactions at similar temperatures as amorphous cellulose does (250-300 °C). It was found products from decomposition of hemicellulose includes acetic acid, formic acid, acetol, furfural, 1-hydroxy-2-propanone, CO, CO₂, and H₂O [Peng and Wu, 2010]. As it was pointed out before, hemicellulose is similar to cellulose in that it is made up of sugars. Pentoses and hexoses in hemicellulose have different pyrolytic behaviors. It is considered that unlike pentoses (main component of hardwoods), hexoses (main component of softwood) tend to produce hydroxymethylfurfural [Anca-Couce, 2016].

Pyrolysis of lignin occurs over a broad temperature range and is often classified into several stages that in general are divided into low-temperature reactions range (160-300 °C) and high-temperature reactions range (300-600 °C). After lignin softening at 160-190 °C,

dehydration occurs at around 200 °C and from 150 to 300 °C there is a cleavage of α - and β -aryl-alkylether linkages. With the start of high-temperature stage at around 300 °C, cleavage of aliphatic side chains occurs and cleavage of C – C linkages at 370-400 °C. The cleavage methoxy groups that are present in soft- and hardwood takes place at different temperatures which are 340 and 310 °C, respectively [Babler et al., 2015; Garcia-Perez and Pecha, 2015; Hu et al., 2017].

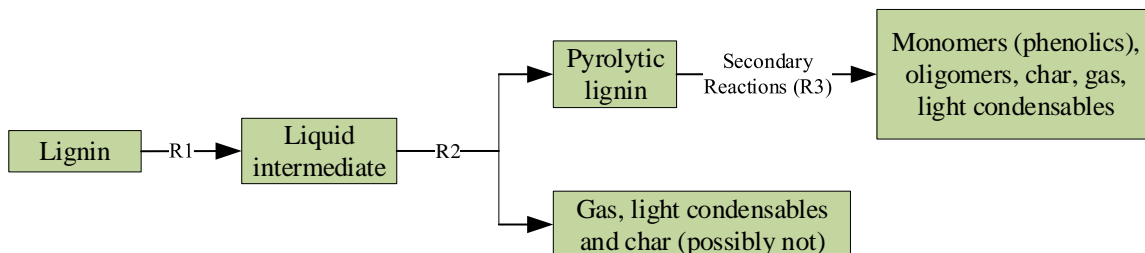


Figure 31. Mechanism of pyrolysis of lignin [Garcia-Perez et al., 2014].

Like in case of cellulose and hemicellulose pyrolysis, when large molecules are not able to evaporate under temperature and pressure conditions, a liquid intermediate forms during pyrolysis of lignin and persists. It thermally ejects lignin oligomers which can further crack to form lignin monomers during secondary reactions taking place at vapor phase. A liquid lignin remains heated at a wide temperature range, which eventually cross-links and forms char. At higher temperatures, due to cross-linking and polycondensing of lignin in liquid intermediate phase, a polyaromatic carbonaceous solid is formed. The side reactions of this process release methanol and formaldehyde [Broadbelt et al., 2016; Dai et al., 2017].

Generally, lignin pyrolysis produces phenolics, water vapor, carbonyls, alcohols, and permanent gases like CO, CO₂, and methane. Phenolics are the most characteristic group of volatiles that are produced from lignin pyrolysis. Methanol and methane are also distinctive of this process, and their formation is the result of methoxy group cleavage [Garcia-Perez and Pecha, 2015]. In hardwoods, there is an extra methoxy group in syringyl units that lead to less charring than in softwoods [Ding et al., 2016]. Methoxy groups decompose into small molecular radicals, which further stabilize the large-molecule fragments produced during lignin pyrolysis and prevent their polymerization to char. For this reason, lignin with higher methoxy group contents produces less char during pyrolysis

process. Furthermore, the catalyzing effect of presence of inorganic species is similar to that of cellulose and hemicellulose [Anca-Couce, 2016; Evans et al., 2016].

During primary pyrolysis mainly pyrolytic lignin is produced. It comes along with permanent gases and light condensable species, such as water, alcohols, and carbonyls. Char is also included as primary product. However it is believed that as for cellulose, char is mainly or exclusively a secondary product. Secondary reactions may take place inside the matrix or in the gas phase when volatiles leave it. Pyrolytic lignin as the major reactant produces phenolic oligomers, phenolic monomers, char, gases, and light condensable species at this stage. Generally, during these secondary reactions the molecular weight is reduced, but oligomers can also arise from re-oligomerisation. Typically, the degree of oligomerisation increases with the decrease of residence time [Anca-Couce, 2016; Bhaskar and Dhyani, 2017; Garcia-Perez and Pecha, 2015].

Biomass devolatilization kinetic modeling and evaluation

Typically, there are two main mathematical approaches that are used for the analysis of biomass devolatilization/pyrolysis in order to obtain the kinetics data: model-fitting (model-based) and isoconversional (model-free) methods. Model-fitting methods can be classified as one-component or multi-component according to how the initial biomass is considered (e.g., specific type of biomass or by its components) and if the reaction mechanism is lumped or detailed depending on how the products are defined (by lumped products like gas, char and tar or by species in each lumped product) [Babler et al., 2015; Cai et al., 2017].

Kinetic models are generalizable to a wider range of biomass in which the overall decomposition is the weighted sum of the individual decomposition of cellulose, hemicellulose, and lignin. Hence, a combination of the individual mechanism of these components is used. The multi-component mechanism is suitable for a wide range of biomasses long as the biomass is properly characterized. Determination and quantification of each of main biomass component is crucial for multi-component mechanism to study decomposition behavior of biomass [Li et al., 2016].

Criado et al. (2013) concluded that model-fitting methods should be employed cautiously, because it might be possible they cannot exactly describe a real biomass decomposition process. However, this uncertainty in estimation caused by model-fitting methods is less likely to happen in the use of isoconversional methods.

In the first step, model-based methods require assumption of a reaction model. The appropriate reaction model is selected on the basis of the quality of the regression fit. In case of biomass, the most commonly employed method to fit experimental data (from TGA) and evaluate the Arrhenius parameters is the nonlinear least squares fitting. Typically, first and n-th order reaction model are selected [Biernacki et al., 2016; Li et al., 2016].

On the other hand, isoconversional methods can be used to calculate kinetic parameters during conversion without model-based assumptions. In these methods the activation energies are calculated at fixed conversions, taking advantage of the fact that the reaction rate depends exclusively on the reaction temperature. There are many isoconversional kinetic evaluation methods including [Anca-Couce, 2016; Cai et al., 2017]:

- Friedman differential method (FR),
- Ozawa-Flynn-Wall linear integral method (OFW),
- Kissinger-Akahira-Sunose linear integral method (KAS),
- The Vyazovkin nonlinear integral method (NL),
- The advanced Vyazovkin nonlinear integral method (ANL),
- Cai-Chen iterative linear integral method.

Each method has both advantages and disadvantages. For instance, FR method can give accurate results, but it is limited to the use of TGA data obtained from experiments by using linear heating rate. Additionally, the use of FR method requires derivative conversion data, which are typically numerically unstable and noise sensitive. The advantage of OFW method is also linearity like in case of FR and additionally the fact that an oversimplified temperature integral approximation is used in the derivation. On the other hand, OFW method was derived with the assumption of constant activation energy from the beginning of the reaction to the conversion degree of interest and may lead to significant errors. The pros and cons of KAS method are same as for OFW. Unlike FR method, the NL method is not limited to the use of the linear variation of the heating rate and is free of temperature

integral approximations. NL method has same drawbacks as KAS and OFW and additionally it is nonlinear. ANL method does not lead to obtaining errors of activation energies like in case of OFW, KAS, and NL however it is also nonlinear like NL. The main advantage of ANL is the fact that the results obtained from this method are very close to the true values. It is also free of integral temperature approximations. The advantages Cai-Chen method are its linearity and accuracy of results as for ANL method [Anca-Couce, 2016; Criado et al., 2013; Li et al., 2016; Li et al., 2017].

In general, the rate of thermally stimulated processes can be parameterized in term of temperature (T) and conversion degree (α) as follows [Fan et al., 2017; Mishra and Mohanty, 2018]:

$$\frac{d\alpha}{dt} = f(\alpha)k(T) \quad (1)$$

where $f(\alpha)$ is the reaction model which depends of the reaction mechanism and $k(T)$ is the rate constant which depends on the temperature.

The conversion degree defined by masses of sample at specific time is expressed by:

$$\alpha = \frac{m_0 - m_t}{m_0 - m_f} \quad (2)$$

Where m_0 , m_t , and m_f are the sample masses at the beginning, at a given time t , and at the end of TG analysis.

For sample decomposition, the rate constant $k(T)$ is usually expressed with the Arrhenius dependence:

$$k(T) = Ae^{-E/RT} \quad (3)$$

where A is the pre-exponential factor, E is the activation energy and R is the gas constant.

Including the Arrhenius expression in the Eq (1), the general expression for a single step kinetic equation can be defined by the following Eq. (4):

$$\frac{d\alpha}{dt} = Af(\alpha)e^{-E/RT} \quad (4)$$

Friedman method is based on the equation obtained by taking the logarithm in Eq. (1) and assuming that the term of $Af(\alpha)$ as a function of α , as shown as [Font and Garrido, 2018; Jong et al., 2009]:

$$\ln\left(\frac{d\alpha}{dt}\right) = \ln(Af(\alpha)) - \frac{E}{RT} \quad (5)$$

Hence $Af(\alpha)$ will be constant at a fixed conversion degree for runs performed at different heating rates. By measuring the temperature and the reaction rate ($d\alpha/dt$) at fixed conversion degree for all experiments performed at different heating rates, the activation energy can be calculated from the slope of $\ln(d\alpha/dt)$ vs $1/T$ whereas pre-exponential factor is obtained from the intercept of $\ln(Af(\alpha))$.

FR method does not employ any mathematical approximation as in the case of integral methods and it can be considered as much accurate as the integral ones. On the other hand, these methods are sensitive to calibration of the thermal analysis equipment leading to significant inaccuracy in the reaction rate. However, Friedman method can be applied to data from TG experiments under different conditions, including isothermal heating, dynamic heating, and stepwise linear heating, etc., with the only requirement – values of $\ln(d\alpha/dt)_{\alpha,1}$ must be correctly determined [Anca-Couce, 2016; Font and Garrido, 2018].

Ozawa-Flynn-Wall method uses Doyle's approximation for temperature integration [Cai et al., 2017; Çepelioğullar et al., 2016]:

$$g(\alpha) = \frac{A}{\beta} 0.00484 \exp\left(-1.052 \frac{E}{RT}\right) \quad (6)$$

where β is the heating rate.

By taking the natural logarithm and rearrangement of Eq. (6), following Eq. (7) is obtained:

$$\ln(\beta) = \ln\left(\frac{AE}{Rg(\alpha)}\right) - 5.331 - 1.052 \frac{E}{RT} \quad (7)$$

The plot between $\ln(\beta)$ vs $1/T$ at different heating rates provides parallel line for conversion value of 0 to 1, and each and every conversion yield corresponds to E from slope $-\frac{0.457E}{R}$.

KAS method does not require the knowledge of the exact thermal degradation mechanism. It is based on the approximation of Coats-Redfern method as displayed in Eq. (8) [Lai Fui Chin et al., 2016]; Reshmi et al., 2016]:

$$p(\alpha) = \frac{A}{\beta} \cdot \frac{RT^2}{E} \exp\left(-\frac{E}{RT}\right) \quad (8)$$

The KAS equation (9) can be defined by taking the natural logarithm and rearrangement of Eq. (8):

$$\ln\left(\frac{\beta}{T^2}\right) = \ln\left(\frac{AE}{Rp(\alpha)}\right) - \frac{E}{RT} \quad (9)$$

As for OFW method, the regression line of $\ln(\beta/T^2)$ vs $1/T$ based on the same conversion at different temperature heating rates, provide the activation energy obtained from the slope.

Vyazovkin method, which is also an integral isoconversional method, is based on minimization of the function shown in Eq. (10) by using approximation of Senum-Yang [Khayati and Shahcheraghi, 2014; Vyazovkin, 2006].

$$\Phi(E) = \sum_{i=1}^n \sum_{j=1}^n \frac{I(E,T)\beta_j}{I(E,T)\beta_i} \quad (10)$$

$$I(E, T) = \int_{T_{\alpha-\Delta\alpha}}^{T_{\alpha}} \exp\left(-\frac{E}{RT}\right) dT \quad (11)$$

Where β_i and β_j represent different heating rates; T_{α} and $T_{\alpha-\Delta\alpha}$ are the reaction temperatures corresponding to α and $\alpha-\Delta\alpha$, respectively. Due to great calculation accuracy and comprehensive applicability for different heating programs, the advanced isoconversional method developed by Vyazovkin is adopted to analyze the non-isothermal reactions. Specifically, it is applicable to a non-isothermal kinetic process with a series of linear heating. The advanced Vyazovkin method allows for the activation energy to be accurately calculated, however its computational complexity is high, because it involves nonlinear optimization calculations [Ozsin and Putun, 2017].

The Cai-Chen method offers two major advantages and allows for avoidance of some problems occurring in above popular methods. Firstly, the integrations in Cai-Chen method are performed over small conversion and temperature segments. It allows for eliminating the systematic errors occurring in the conventional linear integral isoconversional methods when the activation energy varies significantly with the conversion. Secondly, as other linear methods it allows for faster determination as compared to Vyazovkin nonlinear method [Cai et al., 2014].

This method is based on the integration of the basic kinetic equation:

$$g(\alpha, \alpha - \Delta\alpha) = \int_{\alpha-\Delta\alpha}^{\alpha} \frac{d\alpha}{f(\alpha)} = \frac{A_{\alpha-\Delta\alpha/2}}{\beta} \int_{T_{\alpha-\Delta\alpha}}^{T_{\alpha}} \exp\left(-\frac{E_{\alpha-\Delta\alpha/2}}{RT}\right) dT \quad (12)$$

where the subscript $\alpha - \Delta\alpha/2$ denotes the values related to constant extent of conversion. Rearranging Eq. (12) yields:

$$\ln \left(\frac{\beta}{T_{\alpha}^2 \left(h(x_{\alpha}) - \frac{x_{\alpha}^2 e^{x_{\alpha}}}{x_{\alpha-\Delta\alpha}^2 e^{x_{\alpha-\Delta\alpha}}} h(x_{\alpha-\Delta\alpha}) \right)} \right) = \ln \left(\frac{A_{\alpha-\frac{\Delta\alpha}{2}}}{E_{\alpha-\frac{\Delta\alpha}{2}} g(\alpha, \alpha-\Delta\alpha)} \right) - \frac{E_{\alpha-\frac{\Delta\alpha}{2}}}{RT_{\alpha}} \quad (13)$$

where

$$x_{\alpha} = \frac{E_{\alpha-\frac{\Delta\alpha}{2}}}{RT_{\alpha}} \quad (14)$$

$$x_{\alpha-\Delta\alpha} = \frac{E_{\alpha-\frac{\Delta\alpha}{2}}}{RT_{\alpha-\Delta\alpha}} \quad (15)$$

$$h(x) = x^2 e^x \int_x^{\infty} \frac{e^{-x}}{x^2} dx \quad (16)$$

For series of non-isothermal experiments, $i=1, 2, 3, n$, Eq. (13) transforms into:

$$\ln \left(\frac{\beta}{T_{\alpha,i}^2 \left(h(x_{\alpha,i}) - \frac{x_{\alpha,i}^2 e^{x_{\alpha,i}}}{x_{\alpha-\Delta\alpha,i}^2 e^{x_{\alpha-\Delta\alpha,i}}} h(x_{\alpha-\Delta\alpha,i}) \right)} \right) = \ln \left(\frac{A_{\alpha-\frac{\Delta\alpha}{2}}}{E_{\alpha-\frac{\Delta\alpha}{2}} g(\alpha, \alpha-\Delta\alpha)} \right) - \frac{E_{\alpha-\frac{\Delta\alpha}{2}}}{RT_{\alpha,i}} \quad (17)$$

The activation energy in this method is obtained from the slope of the plot of the left hand side Eq. (17) vs $-(RT_{\alpha,i})^{-1}$. The left hand side of the equation is calculated from the last iterative calculation value of $E_{\alpha-\Delta\alpha/2}$.

Isoconversional methods are not commonly employed for biomass pyrolysis however their popularity has recently increased. Differential isoconversional methods are very sensitive to noises, thus integral methods are generally applied more often.

The complexity of biomass pyrolysis has led to development of more complex models than the previously mentioned ones, with one reaction and single activation energy for cellulose, hemicellulose and lignin separately. One of these models is the distributed activation energy model (DAEM). DAEM was firstly applied for coal and later adapted for

biomass. Their principle is based on the assumption that during the decomposition of biomass, the first order of reaction and several irreversible parallel reactions are associated with different activation energy varying with different bond strength species [Anca-Couce, 2016; Li et al., 2016]. DAEM is a powerful tool for understanding and expanding pyrolysis kinetics of several materials. Moreover, it is in good agreement with experimental data, especially at low heating rates [Blanco-Cano et al., 2014; Ceylan and Kazan, 2015].

According to Vand (the creator of DAEM), at a given temperature, change in total volatiles can be written as:

$$1 - \frac{V}{V_t} = \int_0^\infty \exp\left(-A \int_0^t e^{-\frac{E}{RT}} dt\right) f E dE \quad (18)$$

where V represents effective volatile content and V_t represents the amount of volatile content at time t , A is a pre-exponential factor, and $\int E$ represents distribution curve of activation energy. Simplified method of DAEM model regarding Arrhenius equation is given as [Garcia-Hernando et al., 2018]:

$$\ln\left(\frac{\beta}{T^2}\right) = \ln\left(\frac{AR}{E}\right) + 0.6075 - \frac{E}{RT} \quad (19)$$

From Eq. (19), the plot between $\ln\left(\frac{\beta}{T^2}\right)$ vs $1/T$ gives straight line equation. E/R provides slope of the equation. However, $\ln\left(\frac{AR}{E}\right)$ provides intercept value while value of 0.6075 is kept constant for simplicity.

Effect of pyrolysis parameters on the process performance

The thermo-chemical decomposition of biomass is dependent on various process parameters such as feedstock type and share of their constituents, operating conditions and

physic-chemical properties of biomass, which affect the conversion time and pyrolysis rate with product distribution and quality.

Effect of biomass constituents

The proportions of cellulose, hemicellulose and lignin with other components such as minerals and extractives (generally polymers and smaller organic molecules) are different depending on the biomass type. These proportions influence mainly the product distribution in pyrolysis. Pyrolysis of each constituent features unique reaction pathways and thermochemical characteristics, and produces different products [Abnisa et al, 2018; Ganesan et al., 2016].

In the pyrolysis process, the main biomass components contribute to product yields as follows: cellulose and hemicellulose form volatile pyrolysis products, while lignin generally produces charred residues. It has been found that the yield of gaseous products is larger for the biomass with higher cellulose content,. More biochar forms from the biomass with higher content of cellulose and lignin. Lignin content of the biomass has more dominant role than other two compounds in terms of char formation from the biomass pyrolysis. Generation of the char from lignin is the result of fracturing of relatively weak bonds and the consequent formation of more condensed solid structure [Ganesan et al., 2016; Pareek et al., 2015]. Different contents of lignin associated with various species of biomass result in different rates of degradation. Additionally, it was found that deciduous lignin is less stable than coniferous lignin and the latter produces larger char [Brebú and Vasile, 2010].

Minerals, particularly the alkali metals (especially potassium, calcium and sodium) generally contribute to char production and have catalytic effect on pyrolysis reactions leading to increased char yields depending on other conditions. Extractives which refer to non-structural materials that can be extracted by solvents behave more like cellulose and hemicellulose, forming liquid and gas products either through simple devolatilization and decomposition [Abnisa et al, 2018; Evans et al., 2015].

Biomass always contains some amount of water or moisture content, which can exist either as free liquid water, water vapor or as chemically bound water (adsorbed within the

pores of biomass). Generally, it is well known fact that water content reduces the heating value of processed biomass. It was also observed that the higher moisture biomass leads to less amount of char residue. This was proved by conducting the pyrolysis of wood with 5 and 20 % moisture content and the result was respective with different heating rates [Biswas et al., 2014]. Xiong et al. (2013) conducted the pyrolysis of sewage sludge and observed that increase in water content decreases the char yield. Low moisture content is advisable for char production using pyrolysis making the overall process more economically viable by saving time and increasing the heating value of final product. Biomass can have up to 60 % of water content, while biomass with more than 30 % moisture is not suitable for pyrolysis. For this reason, is it recommended to reduce the water content by, e.g. air drying, sun drying or mechanical drying.

Effect of temperature and heating rate

To certain extent, heating rate can change the nature and composition of the final products. Low heating rate reduces the possibility of secondary pyrolysis reactions and ensure that no thermal cracking of biomass takes place resulting in more biochar yield. On the other hand, high heating rates backs the fragmentation of biomass and favors production of gases and liquid, thus limiting the possibility of formation of the biochar. Evans et al. (2016) observed a rapid increase in liquid yield for pyrolysis of cottonseed cake when elevating the heating rate from 5 °C/min to 300 °C/min, but with no significant changes with further increase to 700 °C/min. The similar results were also obtained for sawdust by increasing heating rate from 500 °C/min to 700 °C/min however no obvious change in bio-oil yields was detected when further increasing the heating rate to 1000 °C/min [Abedi et al., 2009]. Aysu and Kucuk, and Angin and Sensoz observed the decrease of biochar yield on the pyrolysis of ferula and safflower, respectively on increasing the heating rate from 30 °C/min to 50 °C/min.

The temperature also has significant impact on products yield and their properties. Generally, higher temperatures result into lower char yield in pyrolysis reactions. The reason for that is the fact that at temperatures, more volatile material is stripped from the char as this condition allows the thermal cracking of heavy hydrocarbon materials. Atreya et

al. (2009) reported the decrease of char yield from 31 % to 17 % on increase of the temperature from 365 °C to 603 °C. The temperature also affects the biochar composition. Generally, chars produced at higher temperatures have higher carbon contents. Liquid yields tend to increase with the increase of pyrolysis temperature up to a maximum value, which for biomass is usually 400-550 °C, depending on other operating conditions. Typically, above these temperatures liquid yields are reduced, because of secondary reactions that cause vapor decomposition becoming more dominant. Although there are many literatures available with the study of effect of temperature on biochar yield, it is difficult to find the suitable temperature for biochar production, because the optimized temperature for its high yield strongly depends on nature, composition, type of biomass, and other conditions.

Effect of particle size

Particle size is the factor that controls heat and mass transfer during conversion biomass. The larger the particle's size the longer the distance between the surface of the one biomass particle and its core, which decreases the heat and mass transfer from the hot surface to colder inner region of the particle. Additionally, with the increase of the particle size, the vapor formed during the thermal cracking of biomass covers more distance through the char layer which causes more secondary reactions resulting in higher char yield. Garcia-Perez et al. (2009) investigating the effect of particle size of Australian oil mallee woody biomass from 0.81 to 5.6 mm at 500 °C observed that increase from 0.3 to 1.5 mm has considerably decreased the bio-oil quantity. Many researchers stated that particles of size bigger than 2 mm may be responsible for increasing the probability of secondary pyrolysis reactions. Abedi et al. (2010) showed an increase in biochar yield from 11.85 % to 23.28 % on increasing the particle size from 0.25 to 0.475 mm by pyrolysing the wheat straw and interestingly with no significant increase of the biochar yield was noticed within the particle size range between 0.475 and 1.35 mm. On the other hand, Angin et al. (2000) observed the effect of biomass particle size of 0.224-0.425, 0.425-0.6, 0.6-0.85, and 0.85-1.8 mm and the result showed that the highest liquid yield was obtained for the latter. According to Hisham

et al. (2012), particle size of approximately 2 mm is necessary to produce significantly higher liquid yield.

Effect of residence time

The residence time of volatiles depends on gas flow rate through the reactor, which affects the contact time between primary vapors and hot char, and thus affects the severity of secondary reactions and also volatile product properties. Increase of the vapor residence time facilitates the repolymerization of the biomass constituents by giving them sufficient time to react. Hence the yield of biochar is reduced when the residence time of volatiles in the reactor and char matrix is shorter [Abnisa et al, 2018; Pareek et al., 2015]. The residence time does not only affect the biochar yield, but the quality and characteristics of biochar by promoting the development of macro- and micro- pores. Typically, the longer residence time favors formation of char with larger pores and surface area. Additionally the increase of biochar yield affected by prolonged residence time is observed for pyrolysis at high temperature, whereas at low temperature the increase in residence time reduces the biochar yield. It is considered that the effect of residence time is often dominated by other parameters like temperature, heating rate, etc., which makes the role of residence time on the production of biochar a little uncertain [Aysu and Kuzuk, 2014; Angin and Sensoz]. Choi et al. (2011) reported only slight increase in the char yield on increasing the residence time during the fast pyrolysis of poplar wood.

Effect of pressure

Generally, yield of biochar has been found to be increased when the pyrolysis is completed under the influence of pressure higher than ambient pressure. Due to pressure increase, specific volume of volatiles decreases causing higher intra-particle residence time which favors their decomposition while escaping the biomass particle. This also leads to higher partial pressure (concentration) of volatiles, thus increasing the decomposition reaction rate of secondary reactions. High pressure also influences the carbon content in the biochar. Typically, the content of carbon in biochar rises when the biomass is pyrolyzed under the high pressure. This leads to formation of biochar with higher energy density. This

effect is useful in maximizing the carbon sequestration potential of biochars [Aysu and Kuzuk, 2014; Evans et al., 2015; Ganesan et al., 2016].

Experimental procedure

Materials

The samples that were used in this study were representatives of softwoods and hardwoods: spruce and birch. The spruce and birch were harvested in South Norway from a spruce forest (Latitude 59°38'N, Longitude 09°09'E) and a birch forest (Latitude 59°55'N, Longitude 10°89'E). The harvested spruce and birch trees were first debarked and the stem wood parts were chipped. Both spruce and birch wood chips were dried at 105 °C for 24 hours and then milled into particles with size smaller than 1 mm.

The powder samples produced after milling were sieved by a vibrating sieving machine (Fritsch Analysette 3 Pro) with the following mesh sizes: 1 mm, 0.5 mm, 0.3 mm, 0.2 mm, 0.1 mm and 0.063 mm and divided into two groups of particle sizes 0.063-0.1 mm and 0.2-0.3 mm.

The proximate analysis of the chosen samples was studied by using a thermogravimetric analyzer Mettler Toledo TGA 851e. The general fuel properties of two wood samples are listed in the Table 4.

Table 3. The results of proximate analysis of tested samples.

Sample	Moisture [%]	Volatile (ar) [%]	Volatile (d) [%]	Ash (ar) [%]	Ash (d) [%]
Spruce	1.55	85.81	85.58	0.74	0.76
Birch	1.27	88.35	88.20	0.71	0.72

TGA procedure

The devolatilization behaviours of two wood samples were studied by using a thermogravimetric analyzer Mettler Toledo TGA 851e. Before each experiment, 5 mg sample was loaded in a TGA crucible and spread on the bottom. Then the crucible was

loaded into the TGA and purged with high purity nitrogen (99.999%) for flushing away the residual air in the furnace. The volume flow of nitrogen was 60 ml/min for performed experiments.

Thermogravimetric analysis was performed in the temperature range from 30 to 600 °C and consisted of four steps:

1. sample stabilization at 30 °C for 30 minutes,
2. heating from 30 to 105 °C with heating rate 5 K/min,
3. drying at 105 °C for 30 minutes,
4. devolatilization from 105 to 600 °C with three different heating rates: 5, 20 and 50 K/min.

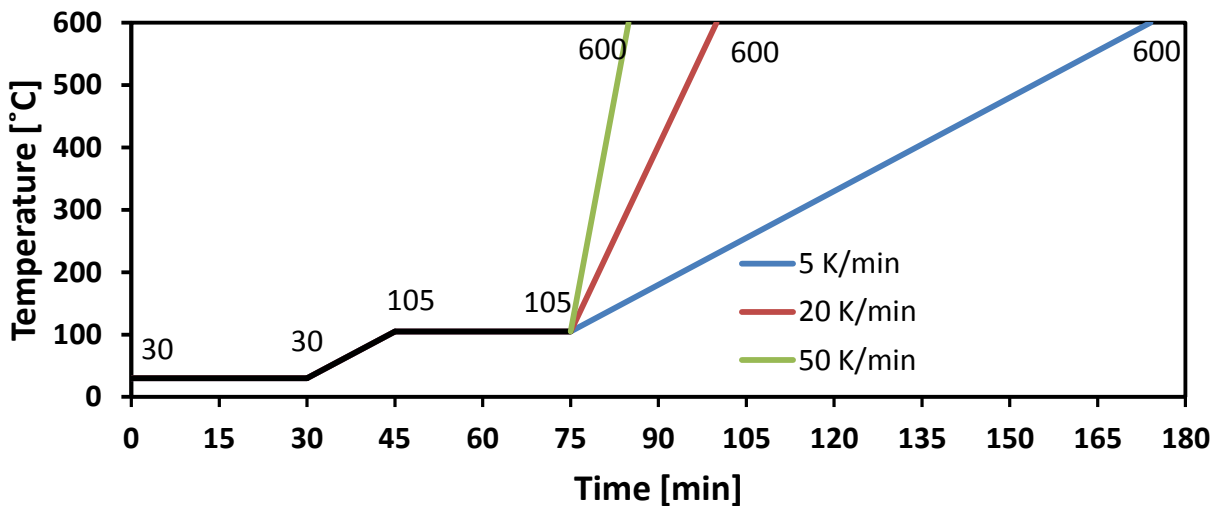


Figure 32. Experimental methodology of performed TGA.

Results and discussion

TGA

Blank tests

During TGA experiments, heating and other parameters affects not only sample itself, but also the properties of purging gas and crucible. even with an empty crucible, weight changes will be recorded due to for example buoyancy effect of purging gas as a result of temperature increase. Hence, before an experiment with sample loaded, it is

necessary to run one experiment with an empty crucible and obtain blank curve. The blank curve with further subtracted from runs with sample loaded. After subtraction of blank curve, the recorded mass loss from one experiment are those associated to decomposition of one sample at elevated temperature. **Figure 33.** shows TGA curves obtained from blank curve runs under different temperature programs.

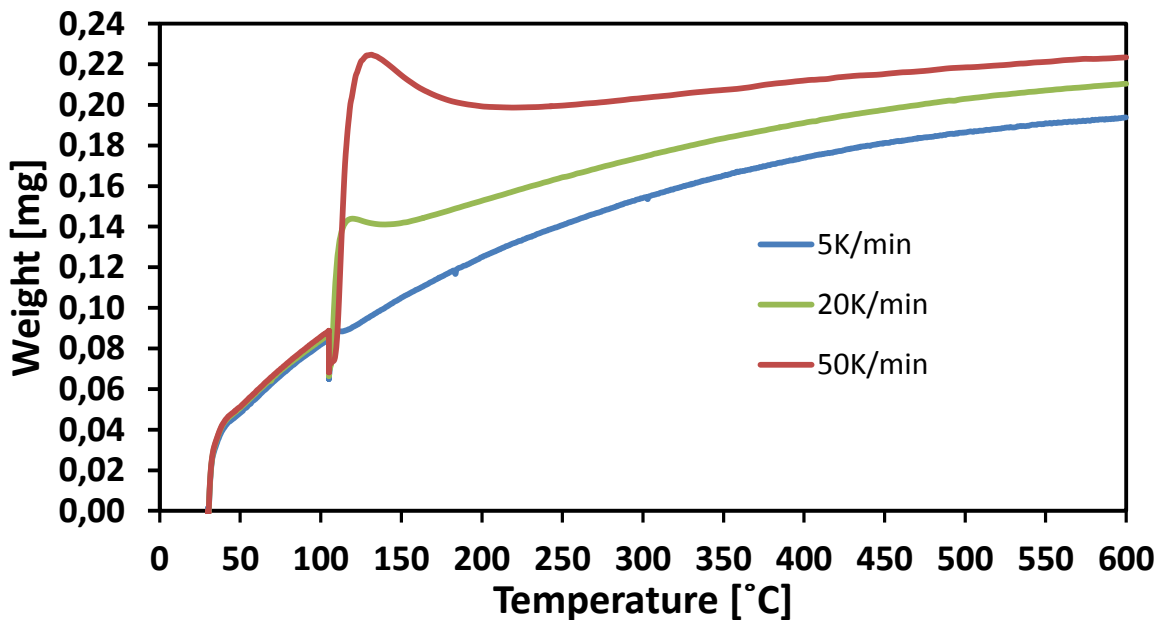


Figure 33. Blank curves obtained from experiments with different heating rate 5 K/min, 20 K/min and 50 K/min

The increase of weight is mainly due to decrease of the density of surrounding gas with increase of the temperature. The buoyancy effect from the gas is the upward force on the crucible. Once the density of gas decreases this upward force decreases. Due to that, the crucible appears to gain weight.

Apart from that, there are also other factors affecting the measurement curve and that are not directly caused by the sample, such as fluctuation of the purge gas flow rate, sudden mass deviations arising from intensive release of volatile part of the sample, etc. These effects may negatively affect the results of experiments and it can be minimized by running a blank test. This allows to record buoyancy effect and other deviations that are present during the experiment and to subtract them from the final data obtained from the

experiments ran with sample. Majority of modern instruments do this automatically however in some cases it needs to be done manually.

As it is shown in the **figure 33.**, more significant weight deviation was recorded from the higher heating rates experiments at the temperature increases from 105 to 600 °C. During an experiment, the TGA furnace is heated up and the heat transfer to purging gas through conduction and radiation . As the temperature increases from the initial low temperature (105 °C as shown in Figure 34) to a higher temperature (155 °C as shown in Figure 34), the higher heating rate will cause more intensive heat transfer and change of gas density as well. For this reason, the recorded weight deviating become more evident. On the other hand, as the temperature in the furnace is over than a certain value, the the radiation becomes the primary route for heat transfer and gas properties change slightly. Thus only smaller mass changes observed at higher temperatures.

In order to check the repeatability of experiments, three blank tests were conducted using the same crucible. The results are shown in the **figure 34.**

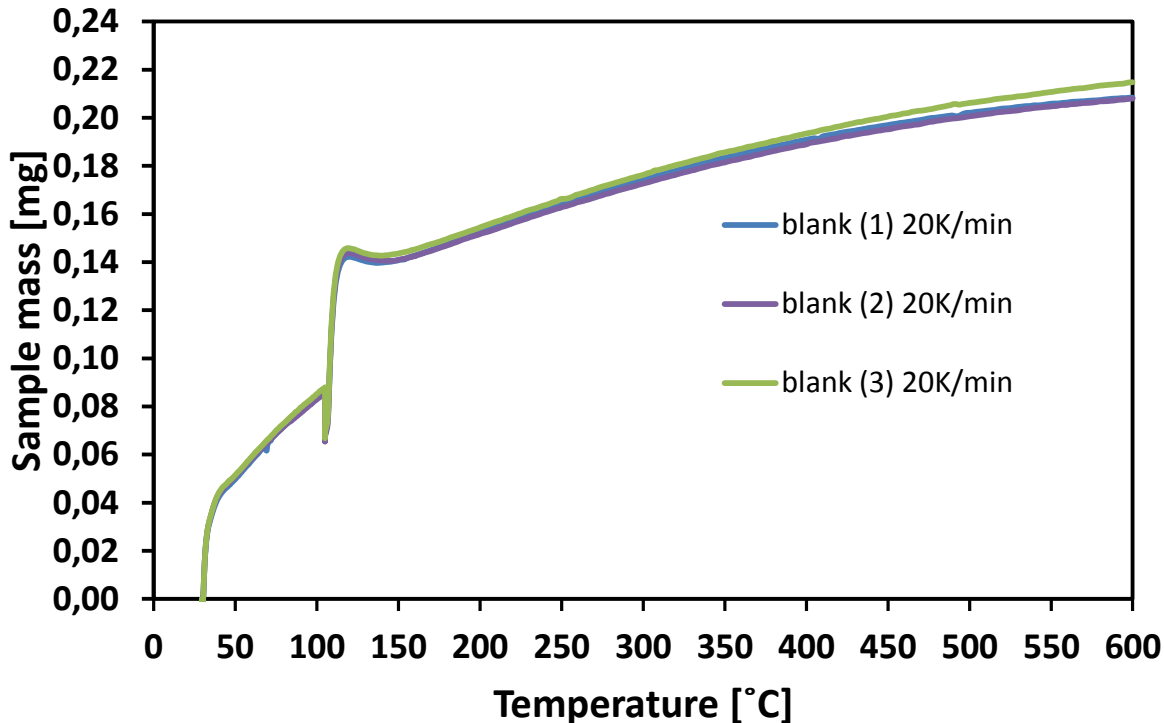


Figure 34. Comparison of blank curves from three repeating experiments

The difference between these tests are quite small and is about 0.01 μg .

For the current work, the crucibles made from alumina with same size and dimension were used. There is slight difference of them in terms of weight. Figure 36 shows two blank curves obtained from two new and clean crucibles under same heating program. It can be see the two curves overlap well and only very small differences of measured weight can be observed as the temperature over 500 $^{\circ}\text{C}$. **figure 35.**

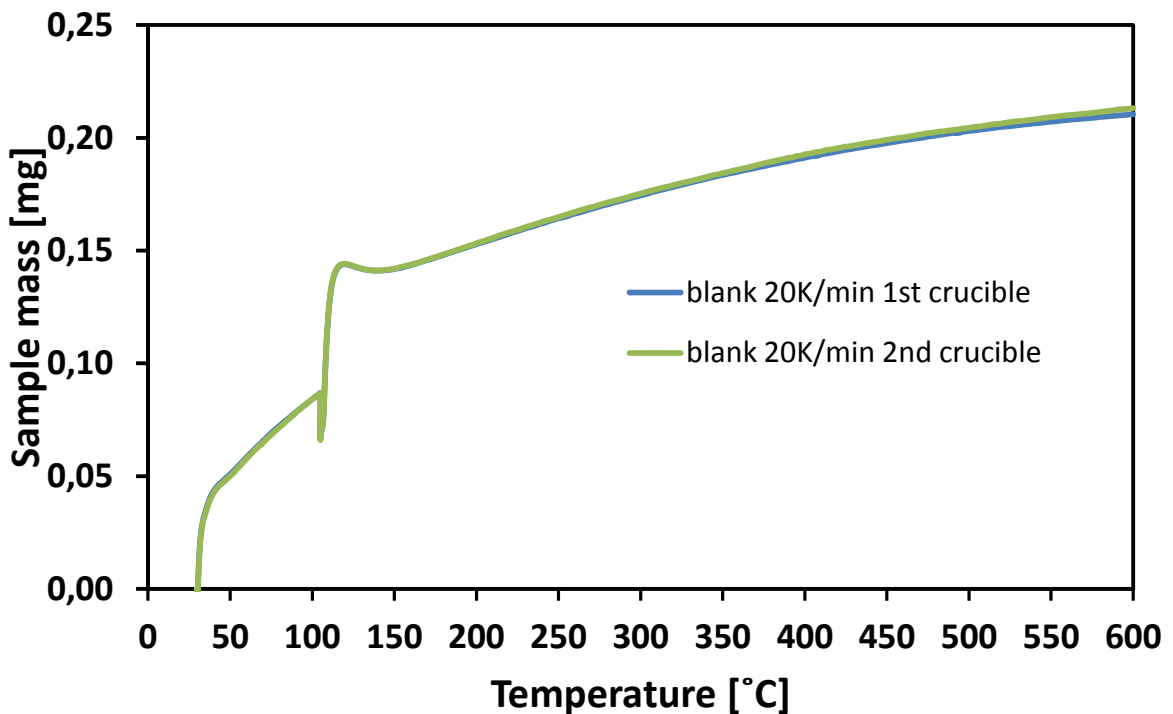


Figure 35. The result of blank tests for the same heating rate using same two different crucibles.

The thermobalance is very sensitive and even the smallest disturbances that occur near TGA instrument can affect the result. However, it would be more reasonable to say that deviations that can be observed in **figure 34.** and **figure 35.** are the result of the instrument's accuracy rather than disturbances or slight dissimilarity of characteristics of two crucibles.

General decomposition behaviours of spruce and birch wood sample

In figures below, it can be seen that three regions are evident which correspond to water evaporation, active and passive pyrolysis. The first region from ambient temperature to 105 °C is related to extraction of moisture and adsorbed water in the sample. For comparison purpose, the sample weight recorded at the end of drying stage at 105 °C is considered as initial value for calculating weight loss and further data processing and kinetic evaluation.

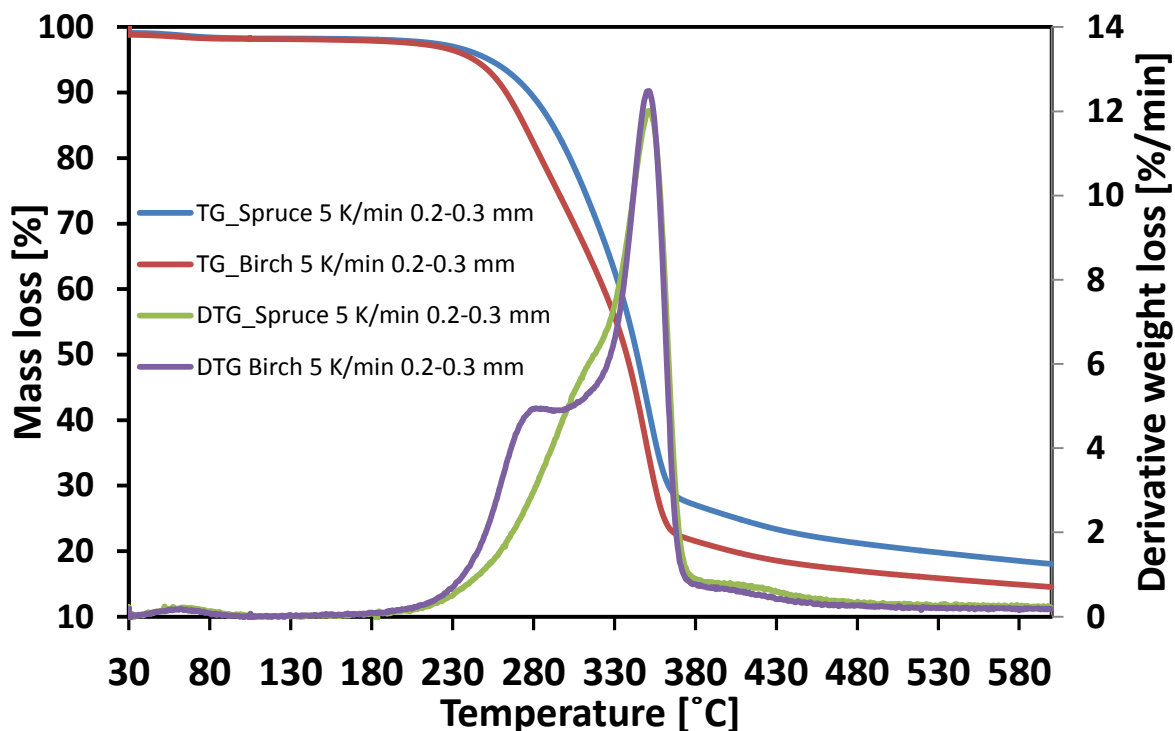


Figure 36. TG and DTG curves of both samples within temperature range 30 - 600 °C.

The passive pyrolysis region occurs from the end temperature of passive pyrolysis region to 600 °C where continuous slight devolatilization takes place. It is considered that reactions associated with lignin decomposition are the most prominent in this region [Bhaskar et al., 2015].

In the active pyrolysis region, one peak and one shoulder can be observed from each DTG curve. In general, the main peak of DTG profile corresponds to cellulose degradation

and the shoulder at lower temperature corresponds to the decomposition and hemicelluloses and lignin, which covers a wider temperature range.

Effect of particle size

The effect of particle size on decomposition behavior of spruce and birch was investigated. The sample particles in the size range of 0.2-0.3 mm and 0.063-0.1 mm were pyrolyzed at different heating rates: 5 K/min; 20 K/min and 50 K/min. The TG and DTG curves obtained from these experiments are shown in **figure 38** and **figure 39**.

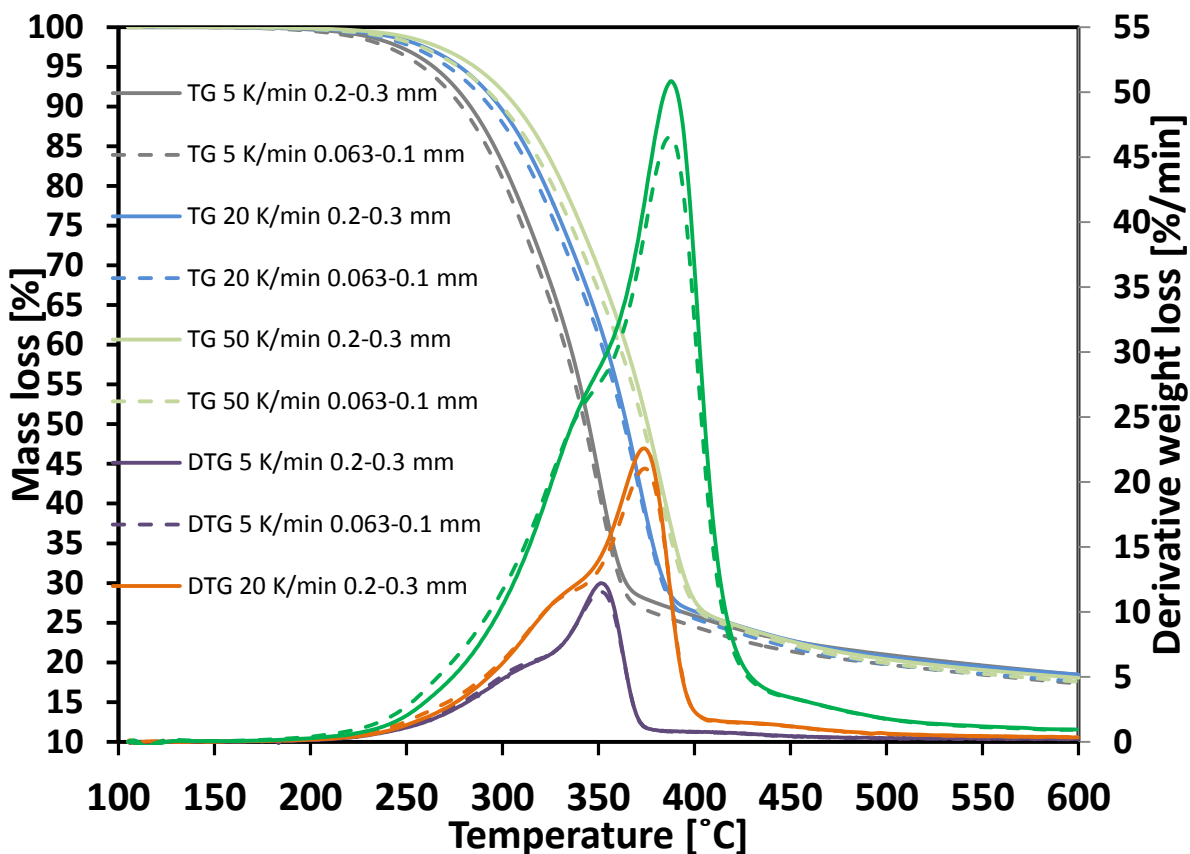


Figure 37. TG and DTG curves of devolatilization of spruce wood samples at 5 K/min, 20 K/min and 50 K/min

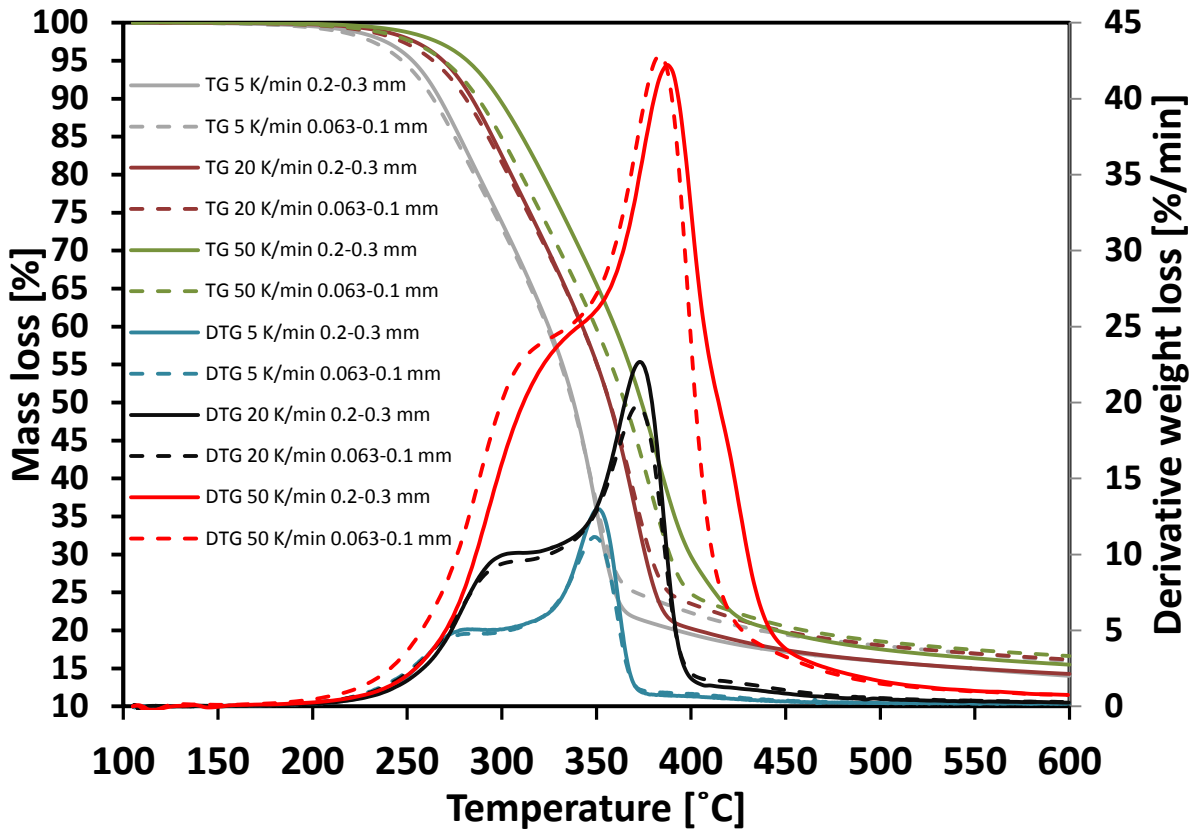


Figure 38. The comparison of TG and DTG curves of pyrolysis of birch wood samples at three different heating rates.

Figure 37. shows devolatilization of spruce wood sample under different heating rates. Decomposition of sample with the smaller particles is faster compared to sample with large particle. In addition, char yield of small particle samples are lower than those obtained from larger particle samples. It is partially caused by better heat and mass transfer of small particle samples. Also, it is observed that DTG peaks are higher for bigger particles which mean that the decomposition is more rapid in this case.

Figure 38. shows devolatilization behavior of studied birch wood sample Although the beginning of devolatilization proceeds similarly as for spruce, it can be observed that in case of birch the smaller particles lead to lower biochar yield. This phenomenon can be more easily seen on figure 39.

In figure 38., for the heating rate 50 K/min, the DTG curve follow different pattern, as the mass loss rate in the cellulose decomposition stage is slightly higher for smaller particles. For the same heating rate value, it can be seen that devolatilization of smaller

particles occurs much earlier as compared to 5 and 20 K/min, which may lead to the statement that the higher the heating rate, the bigger the impact of particle size on the pyrolysis process. Similar effect can be observed in **figure 38**. in case of spruce.

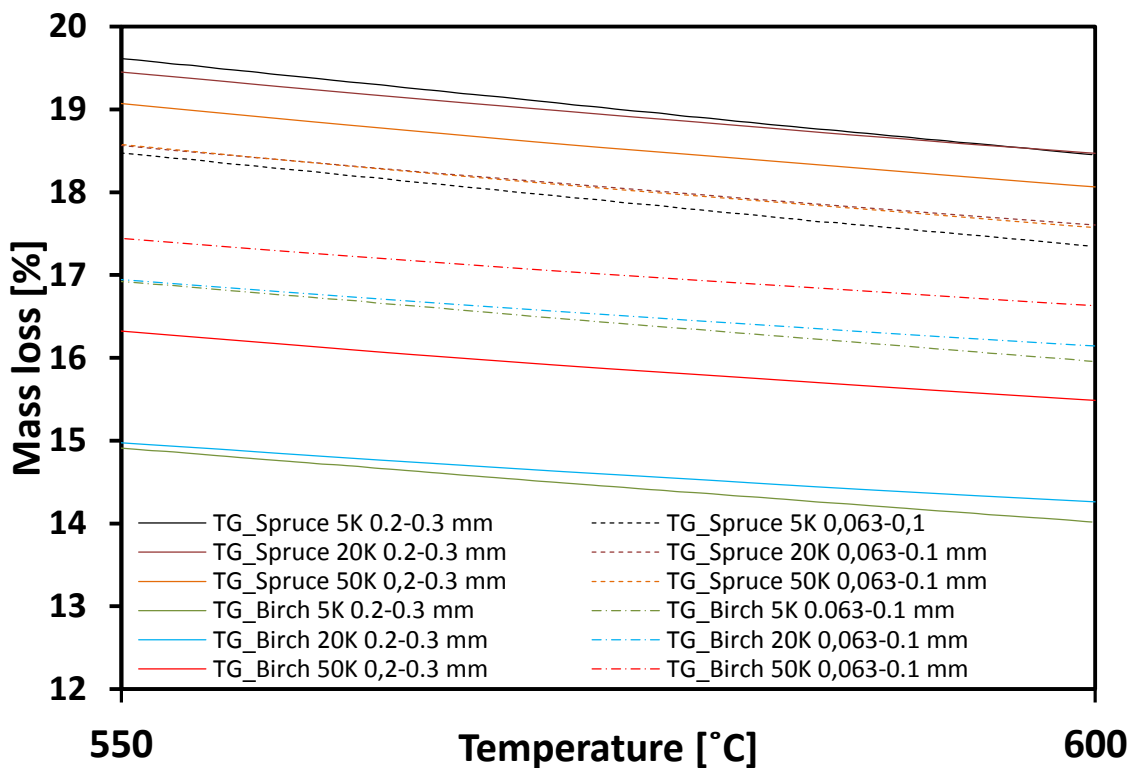


Figure 39. The comparison of zoomed TG curves of pyrolysis of spruce and birch samples at three different heating rates.

Effect of biomass type

One can clearly notice in **figure 39**. that hardwood (birch) tend to yield less char residue as it was expected. This might be due to presence of additional methoxy group in syringyl units as compared to softwoods which limits charring reactions [Ding et al., 2016]. **Figures 40., 41. and 42.** present comparison of TG and DTG curves of spruce and birch at certain heating rates. For DTG curves obtained from birch samples the three heating rates, shoulder corresponding to decomposition of hemicellulose is more evident as compared to

those from spruce sample. For the spruce sample, there might be overlap of DTG peaks related to decomposition of cellulose and hemicellulose [Anca-Couce, 2016].

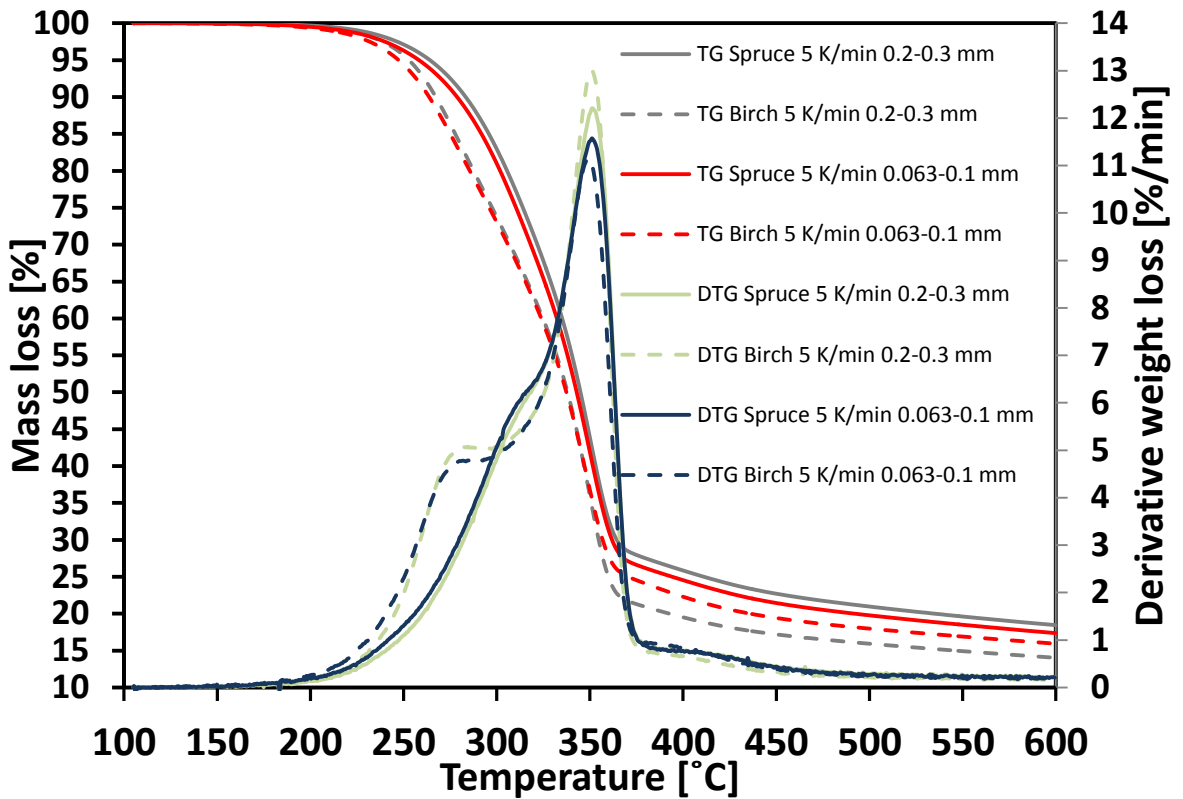


Figure 40. The comparison of TG and DTG curves of pyrolysis of spruce and birch samples at heating rate 5 K/min.

From TG, it can be seen that samples of hardwood tend to start the decomposition process at lower temperatures. The reason for that might be the difference in content and ratio of main constituents between spruce and birch.

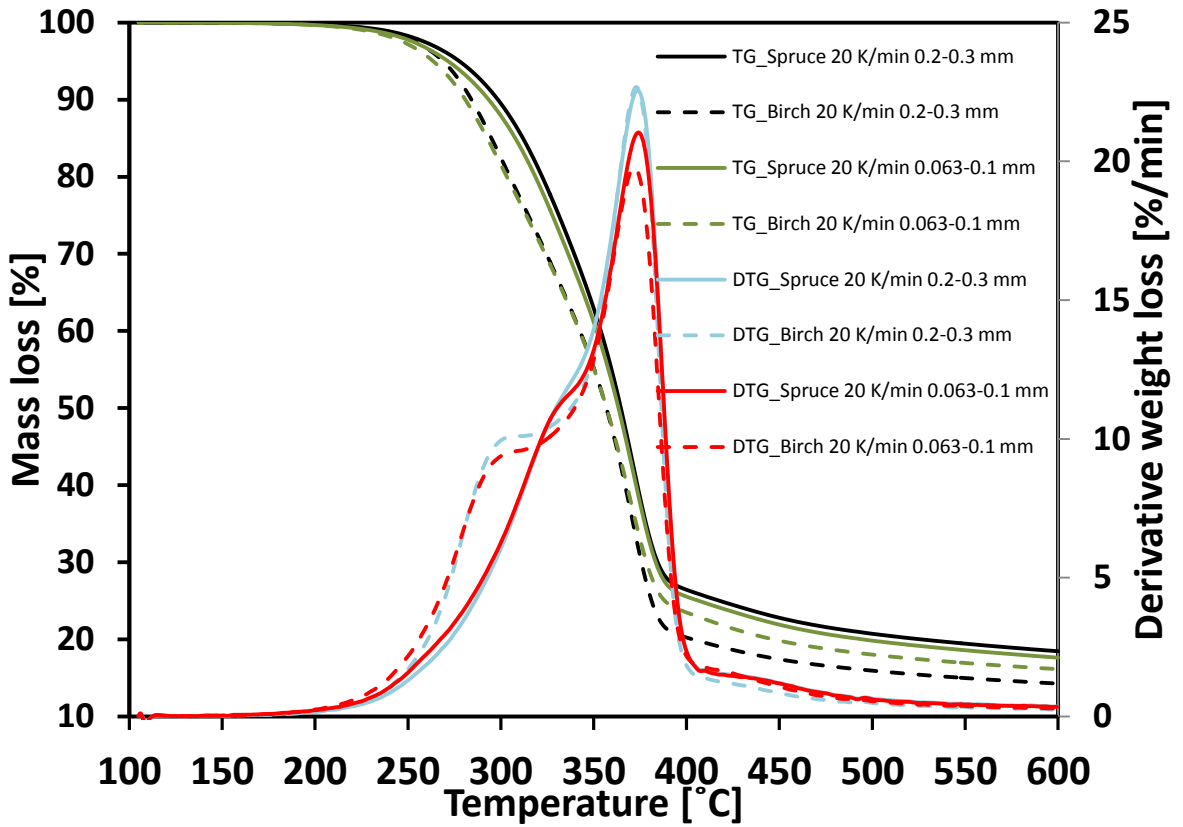


Figure 41. The comparison of TG and DTG curves of pyrolysis of spruce and birch samples at heating rate 20 K/min.

DTG curves show that the growth of maximum speed of devolatilization with the growth of heating rate is greater for spruce than for birch. As the heating rate rises, the difference seems to be more pronounced.

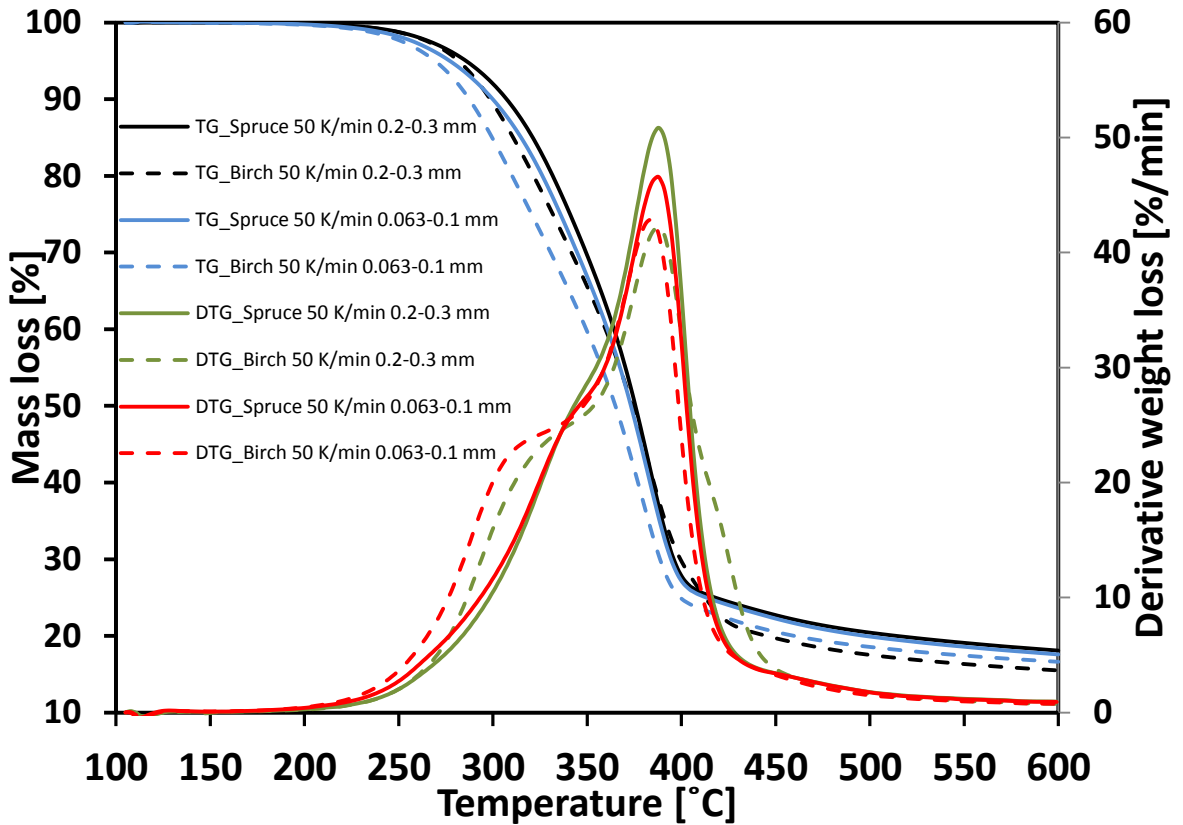


Figure 42. The comparison of TG and DTG curves of pyrolysis of spruce and birch samples at heating rate 50 K/min.

Effect of heating rate

The main pyrolysis process proceeds in different ranges depending on type of the sample and on heating rate:

Spruce:

- 105-360 °C for heating rate 5 K/min,
- 105-385 °C for heating rate 20 K/min,
- 105-400 °C for heating rate 50 K/min.

Birch:

- 105-360 °C for heating rate 5 K/min,
- 105-390 °C for heating rate 20 K/min,
- 105-420 °C for heating rate 50 K/min.

Figures 43-46. present the effect of heating rate separately for spruce and birch. The heating rate is one of the most critical factors affecting devolatilization behavior of biomass sample. All four figures show more or less the same pattern. From the DTG curves it can be noticed that as the heating rate was increased, the rate of decomposition shifted to a higher magnitude. Also with the increase of heating rate, the DTG peak tends to relocate towards higher temperatures and it can be observed that at higher heating rates the overlapping of hemicellulose and cellulose peaks is favored. TG curves show that higher heating rates delays the start of devolatilization. The reason for above phenomena is that the minimum heat required for the cracking of particles is reached later at higher temperature since the heat transfer at rapid heating is less effective as compared to slow heating rates. Additionally, at low rate of heating, a high instantaneous thermal energy is ensure in the system and the purging gas can take an extra time to reach equilibrium with the furnace temperature. In this case, an increased heating rate corresponds to a shortened reaction time and, hence, to a higher temperature of sample decomposition [Islamova and Khamatgalimoc, 2017].

Except for birch sample of particle size between 0.2 and 0.3, other samples do not comply with the rule that with the increase of heating rate the yield of residue (ash) also has to increase. Typically, pyrolysis of such material should be more moderate with slower heating rate. The intensity of the pyrolysis reaction and the volatiles production rate should increase with the increase of heating rate. Probably for such small particles the difference in heating rates is too small in this case. Nonetheless, a different effect was expected.

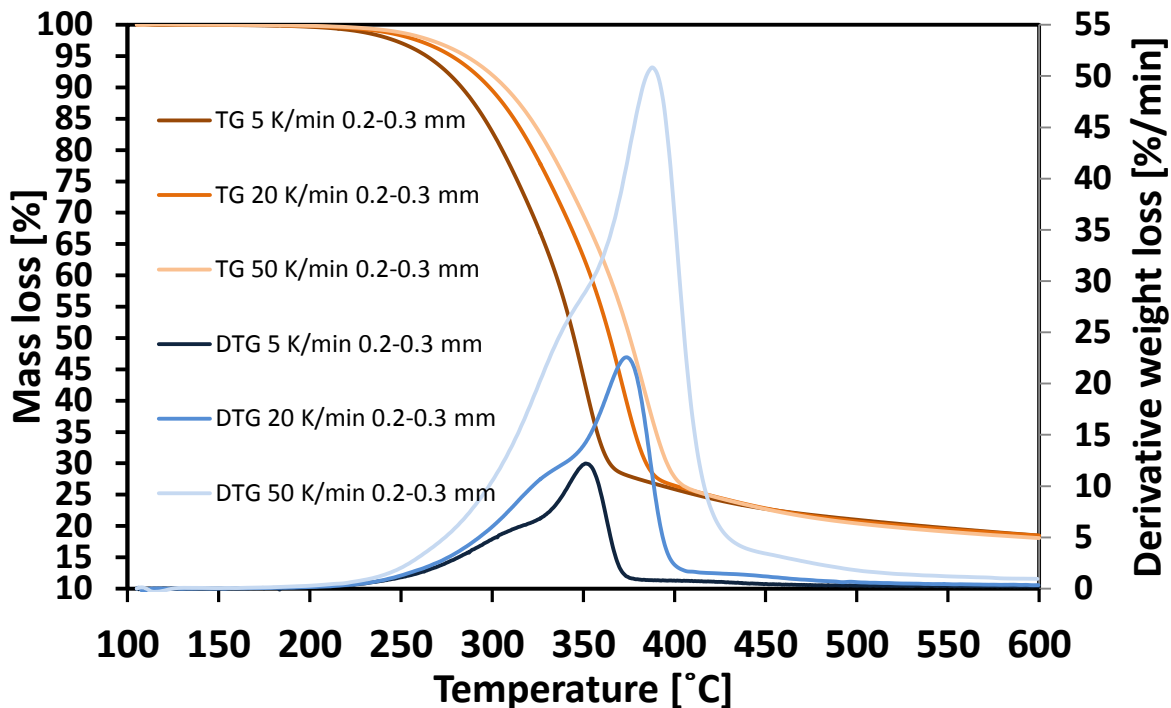


Figure 43. The TG and DTG curves of spruce samples of size 0.2 - 0.3 mm obtained from three different heating rates.

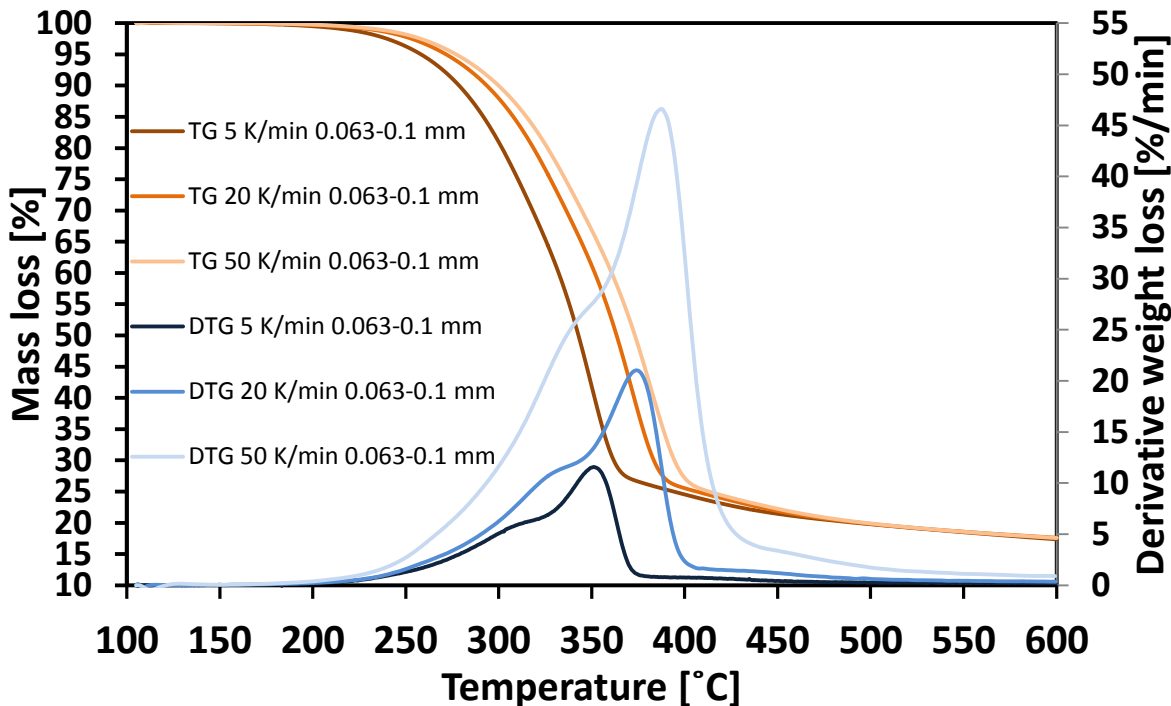


Figure 44. The TG and DTG curves of spruce samples of size 0.063 - 0.1 mm obtained from three different heating rates.

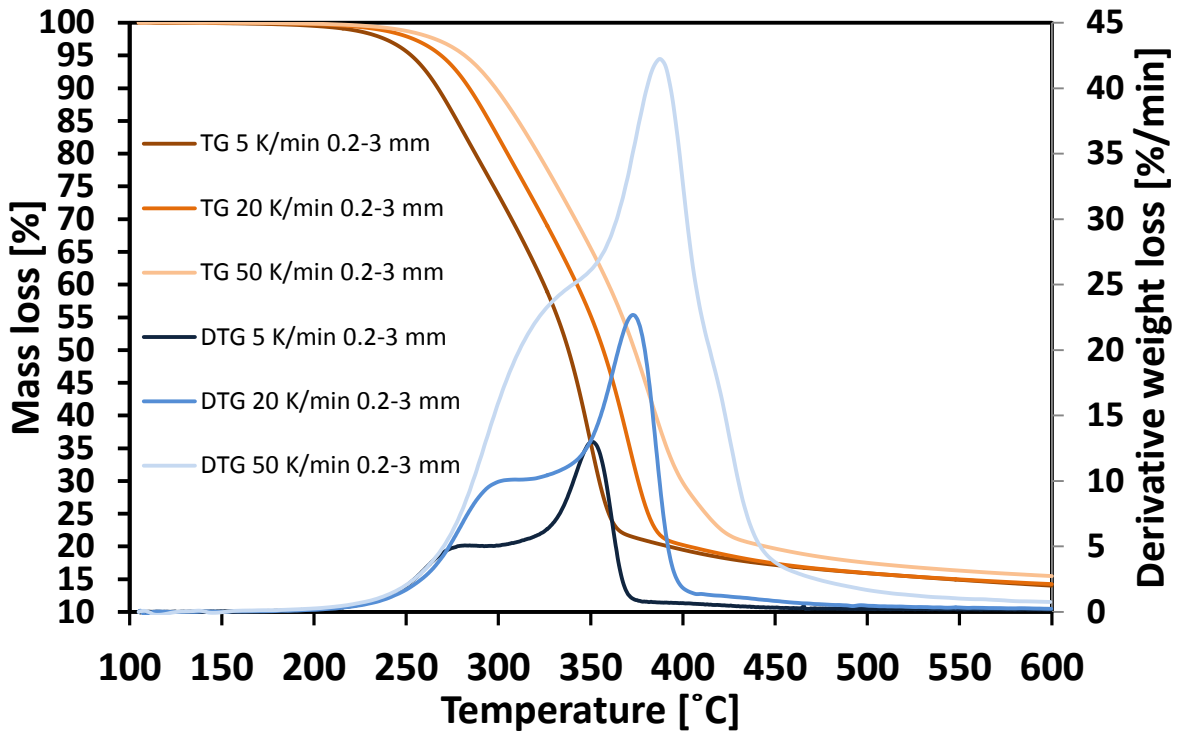


Figure 45. The TG and DTG curves of birch samples of size 0.2 - 0.3 mm obtained from three different heating rates.

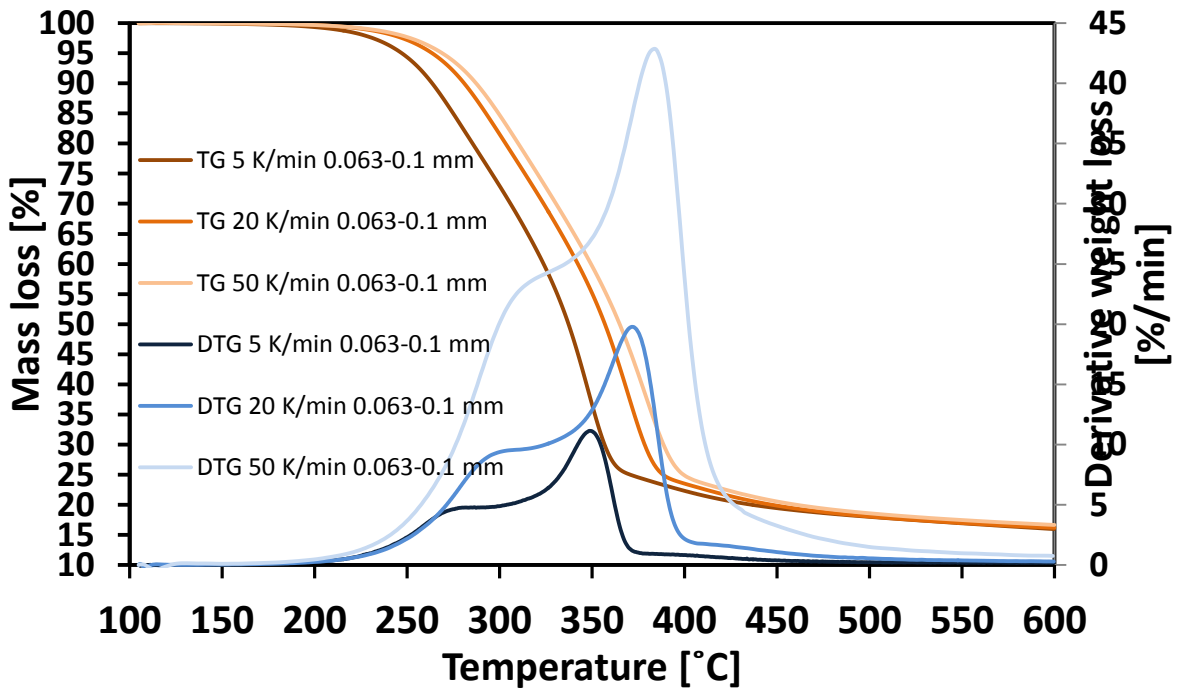


Figure 46. The TG and DTG curves of birch samples of size 0.063 - 0.1 mm obtained from three different heating rates.

Kinetic evaluation

The results obtained during the TGA measurements allow to estimate the kinetic parameters using the Coats-Redfern method. In this method (for $n = 1$), the following equation is used:

$$\ln\left(\frac{-\ln(1-\alpha)}{T^2}\right) = \ln\left(\frac{AR}{\beta E}\left(1 - \frac{2RT}{E}\right)\right) - \frac{E}{RT} \quad (20)$$

Since the term $\frac{2RT}{E} \ll 1$, then it can be omitted. After simplification, equation 20. can be givec in the form:

$$\ln\left(\frac{-\ln(1-\alpha)}{T^2}\right) = \ln\left(\frac{AR}{\beta E}\right) - \frac{E}{RT} \quad (21)$$

The activation energy E and the pre-exponential factor A were determined from the curve $\ln\left(\frac{-\ln(1-\alpha)}{T^2}\right) = f\left(\frac{1}{T}\right)$ in the range of temperatures from 150 to 600 °C. Experimental data were fitted by a linear least square refinement as the slope and the exponential of the y-axis intercept are proportional to E and A , respectively. The reaction order was assumed to be equal to 1. The results were tabulated and are as follows:

Table 4. Kinetic parameters of spruce pyrolysis calculated using Coats-Redfern method.

Spruce				
Heating rate [K/min]	E [kJ/mol]	A [1/s]	lnA	particle size [mm]
5	57.07	36.45	3.60	0.2-0.3
	53.48	18.97	2.94	0.063-0.1
20	63.08	380.90	5.94	0.2-0.3
	58.93	182.25	5.21	0.063-0.1
50	66.76	1688.94	7.43	0.2-0.3
	60.44	567.31	6.34	0.063-0.1

Table 5. Kinetic parameters of birch pyrolysis calculated using Coats-Redfern method.

Birch				
Heating rate [K/min]	E [kJ/mol]	A [1/s]	lnA	particle size [mm]
5	53.31	20.77	3.03	0.2-0.3
	50.03	10.80	2.38	0.063-0.1
20	62.58	412.52	6.02	0.2-0.3
	58.31	189.17	5.24	0.063-0.1
50	65.04	1431.47	7.27	0.2-0.3
	58.08	412.33	6.02	0.063-0.1

The obtained values are within the range that has been reported for similar biomass samples (**table 6.**). The difference in activation energies and pre-exponential factors between spruce and birch are not so significant. It can be noticed, that in this case, there two major factors that affect the values. which are particle size and heating rate. With the increase of heating rate and/or particle size, the activation energies also increase. This is associated with less effective heat transfer as it was mentioned before. The values of activation energies as well as pre-exponential factors seem to be higher in case of spruce as compared to birch. The reason for this phenomenon could be the presence more developed network of bonds (for example hydrogen bonds) in spruce samples than in birch samples that requires more energy to be broken. Also, spruce wood and birch wood represent two different types of wood that differ in ratios and types of cellulose, hemicellulose and lignin, and each of them require different amount of energy to react. So the fluctuation of the activation energies can be attributed to the different reactions, namely the reactions of these three major components in the sample. The other reason however least likely, could be the difference in water content as it can be seen in **table 3.**

Table 6. Survey of TGA study on devolatilization of woody biomass

		model	Ea [kJ/mol]	ln (A) [1/s]	Reference
hardwood	Beech wood	FOW	165.18	31.74	Ding et al.. 2016
		KAS	163.25	11.54	
	Poplar wood	OFW	158.58	32.01	Bartocci et al.. 2012
		K	153.92	28.39	
		KAS	157.27	30.46	
	Balsa wood	K	104.20	17.53	Jacquemin et al.. 2014
softwood	Spruce trunk	EIPR	131.83	19.09	Brillard et al.. 2016
	Pine trunk		98.00	11.16	
	Spruce bark		79.33	8.37	
	Pine bark		84.83	9.70	
	Pine	NL	145.70	-	Alves et al.. 2018
		KAS	145.24		
		FR	155.46		
		FOW	147.84		
	Pine wood sawdust	DAEM	170.04	30.54	Chen et al.. 2015

Conclusions

The following conclusions can be drawn from this study:

- Thermal decomposition of biomass samples occurred within temperature range of 170-510 °C of which a significant mass loss occurred in the temperature range of 230-420 °C. Beyond 510 °C, there was only a slight change in mass loss.
- Mass loss rate increased with increase in heating rate with the highest mass loss rate occurring at temperature range of 345-385 °C.
- With the increase of heating rate, the difference of DTG curves of same species differing in particle size seems to become more visible, so the impact of particle size increases with the increase of heating rate.
- Efficiency of heat transportation and values of kinetic parameters strongly depend on particle size and heating rate.

List of tables and figures

Table 1. Heating values of product gas and characteristics of gasification processes basing on gasifying medium.....	30
Table 2. Influence of particle size on the properties of biomass gasification	30
Table 3. The results of proximate analysis of tested samples.	79
Table 4. Kinetic parameters of spruce pyrolysis calculated using Coats-Redfern method.....	94
Table 5. Kinetic parameters of birch pyrolysis calculated using Coats-Redfern method.	95
Table 6. Survey of TGA study on devolatilization of woody biomass	96
Figure 1. The change of electricity consumption and access to electricity of population over the years	9
Figure 2. GDP and GHG emissions change over the years	10
Figure 3. GHG emissions by sector	11
Figure 4. Amount of electricity produced from renewables over the years.....	12
Figure 5. The glucopyranoside residues and the inter-, intra-, and glycosidic bonding of cellulose.	14
Figure 6. Molecular structure of typical hemicellulose composed of xylose, mannose, glucose and galactose linked together via 1,4-glycosidic bonds.....	15
Figure 7. Monomeric lignin building unit.....	16
Figure 8. Biomass conversion routes diagram.	20
Figure 9. Simplified layout of a pyrolysis plant.....	21
Figure 10. Combustion of biomass for heat and power generation.	28
Figure 11. Biomass Integrated Gasification Combined Cycle (BIGCC).....	29
Figure 12. Biomass hydrothermal liquefaction.....	32
Figure 13. Fixed bed reactor [Bhuyan et al., 2018].	43
Figure 14. A) Bubbling and B) circulating fluidized bed pyrolyzers.....	45
Figure 15. Ablative pyrolysis reactor.....	47
Figure 16. Auger pyrolysis reactor.	47
Figure 17. Rotating cone pyrolysis reactor	48
Figure 18. Ultra-rapid pyrolysis reactor.....	49
Figure 19. Vacuum pyrolysis reactor	50
Figure 20. Schematic diagram of thermobalance system.....	52
Figure 21. Ways of positioning the sample relative to the furnace in TG unit	52
Figure 22. Furnace positioning within the balance housing.....	53
Figure 23. Basic components of a mass spectrometer	54
Figure 24. Quadrupole mass spectrometer.....	55
Figure 25. a) Magnetic mass spectrometer and b) Ion trap mass spectrometer	56
Figure 26. Scheme of a simple interferometer	58
Figure 27. Scheme of a typical gas chromatograph	59
Figure 28. First models of lignocellulosic biomass pyrolysis.....	61
Figure 29. Free radical mechanism of LGA formation.....	62
Figure 30. Cellulose pyrolysis scheme summarizing information available in the literature	64
Figure 31. Mechanism of pyrolysis of lignin.....	66

Figure 32. Experimental methodology of performed TGA.....	80
Figure 33. Blank curves obtained from experiments with different heating rate 5 K/min, 20 K/min and 50 K/min.....	81
Figure 34. Comparison of blank curves from three repeating experiments	82
Figure 35. The result of blank tests for the same heating rate using same two different crucibles....	83
Figure 36. TG and DTG curves of both samples within temperature range 30 - 600 °C.....	84
Figure 37. TG and DTG curves of devolatilization of spruce wood samples at 5 K/min, 20 K/min and 50 K/min	85
Figure 38. The comparison of TG and DTG curves of pyrolysis of birch wood samples at three different heating rates.....	86
Figure 39. The comparison of zoomed TG curves of pyrolysis of spruce and birch samples at three different heating rates.....	87
Figure 40. The comparison of TG and DTG curves of pyrolysis of spruce and birch samples at heating rate 5 K/min.....	88
Figure 41. The comparison of TG and DTG curves of pyrolysis of spruce and birch samples at heating rate 20 K/min.....	89
Figure 42. The comparison of TG and DTG curves of pyrolysis of spruce and birch samples at heating rate 50 K/min.....	90
Figure 43. The TG and DTG curves of spruce samples of size 0.2 - 0.3 mm obtained from three different heating rates.....	92
Figure 44. The TG and DTG curves of spruce samples of size 0.063 - 0.1 mm obtained from three different heating rates.....	92
Figure 45. The TG and DTG curves of birch samples of size 0.2 - 0.3 mm obtained from three different heating rates.....	93
Figure 46. The TG and DTG curves of birch samples of size 0.063 - 0.1 mm obtained from three different heating rates.....	93

References

Faik Bilgili, Emrah Koçak, Ümit Bulut, Sevda Kuşkaya, Can biomass energy be an efficient policy tool for sustainable development?, *Renewable and Sustainable Energy Reviews*, Volume 71, 2017, Pages 830-845, ISSN 1364-0321, <https://doi.org/10.1016/j.rser.2016.12.109>.

Yanming Ding, Ofodike A. Ezekoye, Shouxiang Lu, Changjian Wang, Thermal degradation of beech wood with thermogravimetry/Fourier transform infrared analysis, *Energy Conversion and Management*, Volume 120, 2016, Pages 370-377, ISSN 0196-8904, <https://doi.org/10.1016/j.enconman.2016.05.007>.

Katarzyna Słopiecka, Pietro Bartocci, Francesco Fantozzi, Thermogravimetric analysis and kinetic study of poplar wood pyrolysis, *Applied Energy*, Volume 97, 2012, Pages 491-497, ISSN 0306-2619, <https://doi.org/10.1016/j.apenergy.2011.12.056>.

Jean Constantino Gomes da Silva, José Luiz Francisco Alves, Wendell Venicio de Araujo Galdino, Silvia Layara Floriani Andersen, RENNIO Felix de Sena, Pyrolysis kinetic evaluation by single-step for waste wood from reforestation, *Waste Management*, Volume 72, 2018, Pages 265-273, ISSN 0956-053X, <https://doi.org/10.1016/j.wasman.2017.11.034>.

Luan TranVan, Vincent Legrand, Frédéric Jacquemin, Thermal decomposition kinetics of balsa wood: Kinetics and degradation mechanisms comparison between dry and moisturized materials, *Polymer Degradation and Stability*, Volume 110, 2014, Pages 208-215, ISSN 0141-3910, <https://doi.org/10.1016/j.polymdegradstab.2014.09.004>.

Evgeniya Popova, Aleksandr Chernov, Pavel Maryandyshev, Alain Brillard, Damaris Kehrlí, Gwenaëlle Trouvé, Viktor Lyubov, Jean-François Brillhac, Thermal degradations of wood biofuels, coals and hydrolysis lignin from the Russian Federation: Experiments and modeling, *Bioresource Technology*, Volume 218, 2016, Pages 1046-1054, ISSN 0960-8524, <https://doi.org/10.1016/j.biortech.2016.07.033>.

Zhíhua Chen, Mian Hu, Xiaolei Zhu, Dabin Guo, Shimíng Liu, Zhíquan Hu, Bo Xiao, Jíngbo Wang, Mahmood Laghari, Characteristics and kinetic study on pyrolysis of five lignocellulosic biomass via thermogravimetric analysis, *Bioresource Technology*, Volume 192, 2015, Pages 441-450, ISSN 0960-8524, <https://doi.org/10.1016/j.biortech.2015.05.062>.

Vaibhav Dhyani, Thallada Bhaskar, A comprehensive review on the pyrolysis of lignocellulosic biomass, *Renewable Energy*, 2017, ISSN 0960-148, <https://doi.org/10.1016/j.renene.2017.04.035>.

G. Pahla, T.A. Mamvura, F. Ntuli, E. Muzenda, Energy densification of animal waste lignocellulose biomass and raw biomass, *South African Journal of Chemical Engineering*, Volume 24, 2017, Pages 168-175, ISSN 1026-9185, <https://doi.org/10.1016/j.sajce.2017.10.004>.

Shurong Wang, Gongxin Dai, Haiping Yang, Zhongyang Luo, Lignocellulosic biomass pyrolysis mechanism: A state-of-the-art review, *Progress in Energy and Combustion Science*, Volume 62, 2017, Pages 33-86, ISSN 0360-1285, <https://doi.org/10.1016/j.peccs.2017.05.004>.

Huilíng Long, Xiaobíng Lí, Hóng Wáng, Jíngdùn Jíá, Biomass resources and their bioenergy potential estimation: A review, *Renewable and Sustainable Energy Reviews*, Volume 26, 2013, Pages 344-352, ISSN 1364-0321, <https://doi.org/10.1016/j.rser.2013.05.035>.

Kurchania A.K. (2012) Biomass Energy. In: Baskar C., Baskar S., Dhillon R. (eds) Biomass Conversion. Springer, Berlin, Heidelberg.

Shang-Lien Lo, Yu-Fong Huang, Pei-Te Chiueh, Wen-Hui Kuan, Microwave Pyrolysis of Lignocellulosic Biomass, *Energy Procedia*, Volume 105, 2017, Pages 41-46, ISSN 1876-6102, <https://doi.org/10.1016/j.egypro.2017.03.277>.

Sedjo, Roger A., Carbon Neutrality and Bioenergy: A Zero-Sum Game? (April 7, 2011). Resources for the Future Discussion Paper No. 11-15; PERC Research Paper No. 12/14. Available at SSRN: <https://ssrn.com/abstract=1808080> or <http://dx.doi.org/10.2139/ssrn.1808080>.

Maurya R.K., Patel A.R., Sarkar P., Singh H., Tyagi H. (2018) Biomass, Its Potential and Applications. In: Kumar S., Sani R. (eds) Biorefining of Biomass to Biofuels. Biofuel and Biorefinery Technologies, vol 4. Springer, Cham.

Rödl, Anne. (2018). Lignocellulosic Biomass. *Biokerosene: Status and Prospects*. 189-220. 10.1007/978-3-662-53065-8_9.

Roth, Arne & Riegel, Florian & Batteiger, Valentin. (2018). Potentials of Biomass and Renewable Energy: The Question of Sustainable Availability. *Biokerosene: Status and Prospects*. 95-122. 10.1007/978-3-662-53065-8_6.

Ayhan Demirbas (2006) Sustainable Biomass Production, Energy Sources, Part A, 28:10, 955-964, DOI: 10.1080/00908310600718866

AYHAN DEMIRBAS (2004) The Importance of Biomass, Energy Sources, 26:4, 361-366, DOI: 10.1080/0090831049077406

Hisham Alidrisi & Ayhan Demirbas (2016) Enhanced electricity generation using biomass materials, *Energy Sources, Part A: Recovery, Utilization, and Environmental Effects*, 38:10, 1419-1427, DOI: 10.1080/15567036.2014.948647.

Ridzuan N.H.A.M., Marwan N.F. (2016) Energy Consumption, Carbon Dioxide Emission, and Economic Growth in Malaysia. In: Mohd Sidek N., Ali S., Ismail M. (eds) *Proceedings of the ASEAN Entrepreneurship Conference 2014*. Springer, Singapore.

Le Quére, Corinne. "The Implications of COP21 for Our Future Climate." *Public Health Reviews* 37 (2016): 29. PMC. Web. 11 May 2018.

IPCC, 2014: Summary for Policymakers, In: *Climate Change 2014, Mitigation of Climate Change. Contribution of Working Group III to the Fifth Assessment Report of the Intergovernmental Panel on Climate Change* [Edenhofer, O., R. Pichs-Madruga, Y. Sokona, E. Farahani, S. Kadner, K. Seyboth, A. Adler, I. Baum, S. Brunner, P. Eickemeier, B. Kriemann, J. Savolainen, S. Schlömer, C. von Stechow, T. Zwickel and J.C. Minx (eds.)]. Cambridge University Press, Cambridge, United Kingdom and New York, NY, USA.

United Nations, The Paris Agreement, FCCC/CP/2015/L.9/Rev.1, 12 December 2015.

Greenhouse Gas Protocol, <https://ghgprotocol.org/>, 27 February 2018, 14:50.

United States Environmental Protection Agency, <https://www.epa.gov/>, 01 March 2018, 08:30.

Diego Moya, Clay Aldás, Germánico López, Prasad Kaparaju, Municipal solid waste as a valuable renewable energy resource: a worldwide opportunity of energy recovery by using Waste-To-Energy Technologies, *Energy Procedia*, Volume 134, 2017, Pages 286-295, ISSN 1876-6102, <https://doi.org/10.1016/j.egypro.2017.09.618>.

World Energy Council, *World Energy Resources – Waste to Energy*, 2016.

Branchini, Lisa. *Waste-to-energy: Advanced Cycles and New Design Concepts for Efficient Power Plants.*, 2015. Internet resource.

J. Malinauskaite, H. Jouhara, D. Czajczyńska, P. Stanchev, E. Katsou, P. Rostkowski, R.J. Thorne, J. Colón, S. Ponsá, F. Al-Mansour, L. Anguilano, R. Krzyżyńska, I.C. López, A. Vlasopoulos, N. Spencer, Municipal solid waste management and waste-to-energy in the context of a circular economy and energy recycling in Europe, *Energy*, Volume 141, 2017, Pages 2013-2044, ISSN 0360-5442, <https://doi.org/10.1016/j.energy.2017.11.128>.

Chinnappan, Baskar & Shikha Baskar, Dr & Ranjit S. Dhillon, Prof & , Editors. (2012). *Biomass Conversion: The interface of biotechnology, chemistry and materials science*.

Atnaw, Samson & Sulaiman, Shaharin & Suzana, Yusup. (2017). *Biomass Gasification* http://link.springer.com/chapter/10.1007/978-3-319-49595-8_8. 159-185. 10.1007/978-3-319-49595-8_8.

Decker S.R. et al. (2017) *Biomass Conversion*. In: Kent J., Bommaraju T., Barnicki S. (eds) *Handbook of Industrial Chemistry and Biotechnology*. Springer, Cham.

Erakhrumen, A.A.. (2007). Overview of various biomass energy conversion routes. *Am Eurasian J Agric Environ Sci*. 2. 662-671.

Ahmed Osama Abdulrahman, Donald Huisingh, The role of biomass as a cleaner energy source in Egypt's energy mix, *Journal of Cleaner Production*, Volume 172, 2018, Pages 3918-3930, ISSN 0959-6526, <https://doi.org/10.1016/j.jclepro.2017.05.049>.

Rago Y.P., Mohee R., Surroop D. (2018) A Review of Thermochemical Technologies for the Conversion of Waste Biomass to Biofuel and Energy in Developing Countries. In: Leal Filho W., Surroop D. (eds) *The Nexus: Energy, Environment and Climate Change*. Green Energy and Technology. Springer, Cham.

Farré, Gemma & Gómez-Galera, Sonia & Naqvi, Shaista & Bai, Chao & Sanahuja, Georgina & Yuan, Dawei & Zorrilla-López, Uxue & Tutusaus Codony, Laura & Rojas, Eduard & Fibla, Marc & Twyman, Richard & Capell, Teresa & Christou, Paul & Zhu, Changfu. (2012). *Encyclopedia of Sustainability Science and Technology*.

Jones, J.M. & Lea-Langton, A & Ma, Lin & Pourkashanian, M & Williams, Alan. (2014). Pollutants Generated by the Combustion of Solid Biomass Fuels. 10.1007/978-1-4471-6437-1.

Oochit, Dooshyantsingh & Selvarajoo, Anurita & Arumugasamy, Senthil Kumar. (2017). Pyrolysis of Biomass. *Waste Biomass Management - A Holistic Approach*. 10.1007/978-3-319-49595-8_10.

Prabir Basu, Chapter 5 - Pyrolysis, In *Biomass Gasification, Pyrolysis and Torrefaction (Second Edition)*, Academic Press, Boston, 2013, Pages 147-176, ISBN 9780123964885, <https://doi.org/10.1016/B978-0-12-396488-5.00005-8>.

Vaz Jr, Silvio. (2018). Biomass and the Green Chemistry Principles. *Biomass and Green Chemistry: Building a Renewable Pathway*. 1-9. 10.1007/978-3-319-66736-2_1.

Ayhan Demirbas, Biorefineries: Current activities and future developments, *Energy Conversion and Management*, Volume 50, Issue 11, 2009, Pages 2782-2801, ISSN 0196-8904, <https://doi.org/10.1016/j.enconman.2009.06.035>.

R. Luque and J.G. Speight, 1 - Gasification and synthetic liquid fuel production: an overview, In *Woodhead Publishing Series in Energy*, edited by Rafael Luque and James G. Speight, Woodhead Publishing, 2015, Pages 3-27, *Gasification for Synthetic Fuel Production*, ISBN 9780857098023, <https://doi.org/10.1016/B978-0-85709-802-3.00001-1>.

Prabir Basu, Chapter 7 - Gasification Theory, In *Biomass Gasification, Pyrolysis and Torrefaction (Second Edition)*, Academic Press, Boston, 2013, Pages 199-248, ISBN 9780123964885, <https://doi.org/10.1016/B978-0-12-396488-5.00007-1>.

Jenkins, Robert. (2015). *Thermal Gasification of Biomass - A Primer*. 261-286. 10.1016/B978-0-12-407909-0.00016-X.

Avdhes Kr. Sharma, Equilibrium and kinetic modeling of char reduction reactions in a downdraft biomass gasifier: A comparison, *Solar Energy*, Volume 82, Issue 10, 2008, Pages 918-928, ISSN 0038-092X, <https://doi.org/10.1016/j.solener.2008.03.004>.

V. Skoulou, A. Zabaniotou, G. Stavropoulos, G. Sakelaropoulos, Syngas production from olive tree cuttings and olive kernels in a downdraft fixed-bed gasifier, *International Journal of Hydrogen Energy*, Volume 33, Issue 4, 2008, Pages 1185-1194, ISSN 0360-3199, <https://doi.org/10.1016/j.ijhydene.2007.12.051>.

Magin Lapuerta, Juan J. Hernández, Amparo Pazo, Julio López, Gasification and co-gasification of biomass wastes: Effect of the biomass origin and the gasifier operating conditions, *Fuel Processing Technology*, Volume 89, Issue 9, 2008, Pages 828-837, ISSN 0378-3820, <https://doi.org/10.1016/j.fuproc.2008.02.001>.

Yijun Zhao, Shaozeng Sun, Hao Zhou, Rui Sun, Hongming Tian, Jiye Luan, Juan Qian, Experimental study on sawdust air gasification in an entrained-flow reactor, *Fuel Processing Technology*, Volume 91, Issue 8, 2010, Pages 910-914, ISSN 0378-3820, <https://doi.org/10.1016/j.fuproc.2010.01.012>.

Huang, Huajun & Yuan, Xing-Zhong & Wu, Guo-qiang. (2017). Liquefaction of Biomass for Bio-oil Products. *Waste Biomass Management - A Holistic Approach*. 231-250. 10.1007/978-3-319-49595-8_11.

Xu C.C. et al. (2014) Hydrothermal Liquefaction of Biomass in Hot-Compressed Water, Alcohols, and Alcohol-Water Co-solvents for Biocrude Production. In: Jin F. (eds) *Application of Hydrothermal Reactions to Biomass Conversion*. Green Chemistry and Sustainable Technology. Springer, Berlin, Heidelberg.

Tian C., Liu Z., Zhang Y. (2017) Hydrothermal Liquefaction (HTL): A Promising Pathway for Biorefinery of Algae. In: Gupta S., Malik A., Bux F. (eds) *Algal Biofuels*. Springer, Cham.

Benedetta de Caprariis, Paolo De Filippis, Antonietta Petruccio, Marco Scarsella, Hydrothermal liquefaction of biomass: Influence of temperature and biomass composition on the bio-oil production, *Fuel*, Volume 208, 2017, Pages 618-625, ISSN 0016-2361, <https://doi.org/10.1016/j.fuel.2017.07.054>.

Hua-jun Huang, Xing-zhong Yuan, Recent progress in the direct liquefaction of typical biomass, *Progress in Energy and Combustion Science*, Volume 49, 2015, Pages 59-80, ISSN 0360-1285, <https://doi.org/10.1016/j.pecs.2015.01.003>.

Gouveia L., Passarinho P.C. (2017) Biomass Conversion Technologies: Biological/Biochemical Conversion of Biomass. In: Rabaçal M., Ferreira A., Silva C., Costa M. (eds) *Biorefineries. Lecture Notes in Energy*, vol 57. Springer, Cham.

Aydin, Sevcan. (2016). Anaerobic Digestion. *Waste Biomass Management - A Holistic Approach*. XV, 345. 10.1007/978-3-319-49595-8_1.

Faaij, A. Mitig Adapt Strat Glob Change (2006) 11: 343. <https://doi.org/10.1007/s11027-005-9004-7>

Mei, Ran & Narihiro, Takashi & Nobu, Masaru & Kuroda, Kyohei & Liu, Wen-Tso. (2016). Evaluating digestion efficiency in full-scale anaerobic digesters by identifying active microbial populations through the lens of microbial activity. *Scientific Reports*. 6. 34090. 10.1038/srep34090.

Charles Gould, M. (2015). Chapter 18. Bioenergy and Anaerobic Digestion. 297-317. 10.1016/B978-0-12-407909-0.00018-3.

Teixeira, R. S., Silva, A. S., Moutta, R. O., Ferreira-Leitão, V. S., Barros, R. R., Ferrara, M. A., & Bon, E. P. (2014). Biomass pretreatment: a critical choice for biomass utilization via biotechnological routes. *BMC Proceedings*, 8(Suppl 4), O34. <http://doi.org/10.1186/1753-6561-8-S4-O34>.

P. Bajpai, Pretreatment of Lignocellulosic Biomass for Biofuel Production, *SpringerBriefs in Green Chemistry for Sustainability*, DOI 10.1007/978-981-10-0687-6_4.

Joshi S.M., Gogate P.R. (2017) Intensified Synthesis of Bioethanol from Sustainable Biomass. In: Singh L., Kalia V. (eds) *Waste Biomass Management – A Holistic Approach*. Springer, Cham.

Wan C., Li Y. (2013) Solid-State Biological Pretreatment of Lignocellulosic Biomass. In: Gu T. (eds) *Green Biomass Pretreatment for Biofuels Production*. SpringerBriefs in Molecular Science. Springer, Dordrecht.

Wang J., Yin Y. (2017) Pretreatment of Organic Wastes for Hydrogen Production. In: *Biohydrogen Production from Organic Wastes*. Green Energy and Technology. Springer, Singapore.

Moreno A.D., Olsson L. (2017) Pretreatment of Lignocellulosic Feedstocks. In: Sani R., Krishnaraj R. (eds) *Extremophilic Enzymatic Processing of Lignocellulosic Feedstocks to Bioenergy*. Springer, Cham.

Takara D., Khanal S.K. (2012) Biomass Pretreatment for Biofuel Production. In: Gopalakrishnan K., van Leeuwen J., Brown R. (eds) *Sustainable Bioenergy and Bioproducts*. Green Energy and Technology. Springer, London.

Tang S.Y., Sivakumar M. (2015) Ultrasound as a Green Processing Technology for Pretreatment and Conversion of Biomass into Biofuels. In: Fang Z., Smith, Jr. R., Qi X. (eds) *Production of Biofuels and Chemicals with Ultrasound*. Biofuels and Biorefineries, vol 4. Springer, Dordrecht.

Wojciechowski A.L. et al. (2013) The Pretreatment Step in Lignocellulosic Biomass Conversion: Current Systems and New Biological Systems. In: Faraco V. (eds) *Lignocellulose Conversion*. Springer, Berlin, Heidelberg.

Huang C., Jeuck B., Yong Q. (2017) Using Pretreatment and Enzymatic Saccharification Technologies to Produce Fermentable Sugars from Agricultural Wastes. In: Singh L., Kalia V. (eds) *Waste Biomass Management – A Holistic Approach*. Springer, Cham.

Zieliński, M., Dębowski, M., Kisiełowska, M. et al. *Waste Biomass Valor* (2017). <https://doi.org/10.1007/s12649-017-9977-y>

Jones Madison, Maxine & Coward-Kelly, Guillermo & Liang, Chao & Nazmul Karim, M & Falls, Matthew & Holtzaple, Mark. (2017). Mechanical pretreatment of biomass – Part I: Acoustic and hydrodynamic cavitation. *Biomass and Bioenergy*. 98. 135-141. [10.1016/j.biombioe.2017.01.007](https://doi.org/10.1016/j.biombioe.2017.01.007).

Ruly Terán Hilaes, Gabriela Faria de Almeida, Muhammad Ajaz Ahmed, Felipe A.F. Antunes, Silvio Silvério da Silva, Jong-In Han, Júlio César dos Santos, Hydrodynamic cavitation as an efficient pretreatment method for lignocellulosic biomass: A parametric study, *Bioresource Technology*, Volume 235, 2017, Pages 301-308, ISSN 0960-8524, <https://doi.org/10.1016/j.biortech.2017.03.125>.

Luo J., Cai M., Gu T. (2013) Pretreatment of Lignocellulosic Biomass Using Green Ionic Liquids. In: Gu T. (eds) *Green Biomass Pretreatment for Biofuels Production*. SpringerBriefs in Molecular Science. Springer, Dordrecht.

Kapoor M., Semwal S., Gaur R., Kumar R., Gupta R.P., Puri S.K. (2018) The Pretreatment Technologies for Deconstruction of Lignocellulosic Biomass. In: Singhanian R., Agarwal R., Kumar R., Sukumaran R. (eds) *Waste to Wealth. Energy, Environment, and Sustainability*. Springer, Singapore.

Ragauskas A.J., Huang F. (2013) Chemical Pretreatment Techniques for Biofuels and Biorefineries from Softwood. In: Fang Z. (eds) *Pretreatment Techniques for Biofuels and Biorefineries*. Green Energy and Technology. Springer, Berlin, Heidelberg.

Qin L., Li WC., Zhu JQ., Li BZ., Yuan YJ. (2017) Hydrolysis of Lignocellulosic Biomass to Sugars. In: Fang Z., Smith, Jr. R., Qi X. (eds) *Production of Platform Chemicals from Sustainable Resources*. Biofuels and Biorefineries. Springer, Singapore.

Bridgwater A.V. (2017) Biomass Conversion Technologies: Fast Pyrolysis Liquids from Biomass: Quality and Upgrading. In: Rabaçal M., Ferreira A., Silva C., Costa M. (eds) *Biorefineries*. Lecture Notes in Energy, vol 57. Springer, Cham.

Thormann L., Pizarro de Oro P. (2018) Fuels from Pyrolysis. In: Kaltschmitt M., Neuling U. (eds) *Biokerosene*. Springer, Berlin, Heidelberg.

Kataki R. et al. (2018) Waste Valorization to Fuel and Chemicals Through Pyrolysis: Technology, Feedstock, Products, and Economic Analysis. In: Singhanian R., Agarwal R., Kumar R., Sukumaran R. (eds) *Waste to Wealth. Energy, Environment, and Sustainability*. Springer, Singapore.

Xu C., Ferdosian F. (2017) Degradation of Lignin by Pyrolysis. In: *Conversion of Lignin into Bio-Based Chemicals and Materials*. Green Chemistry and Sustainable Technology. Springer, Berlin, Heidelberg.

Kundu K., Chatterjee A., Bhattacharyya T., Roy M., Kaur A. (2018) Thermochemical Conversion of Biomass to Bioenergy: A Review. In: Singh A., Agarwal R., Agarwal A., Dhar A., Shukla M. (eds) *Prospects of Alternative Transportation Fuels*. Energy, Environment, and Sustainability. Springer, Singapore.

Gvero P., Mujanić I., Papuga S., Vasković S., Anatinović R. (2017) Review of Synthetic Fuels and New Materials Production Based on Pyrolysis Technologies. In: Pellicer E. et al. (eds) *Advances in Applications of Industrial Biomaterials*. Springer, Cham.

Nachenius, Robert & Ronsse, Frederik & Venderbosch, Robbie & Prins, W. (2013). Biomass Pyrolysis. *Adv. Chem. Eng.*. 42. 75-139. [10.1016/B978-0-12-386505-2.00002-X](https://doi.org/10.1016/B978-0-12-386505-2.00002-X).

Thangalazhy-Gopakumar S., Adhikari S. (2016) Fast Pyrolysis of Agricultural Wastes for Bio-fuel and Bio-char. In: Karthikeyan O., Heimann K., Muthu S. (eds) *Recycling of Solid Waste for Biofuels and Bio-chemicals*. Environmental Footprints and Eco-design of Products and Processes. Springer, Singapore.

Stępień L., Ściążko M., Fluidization, AGH University, Department of Energy and Fuels, January 2015.

Meier D. (2017) Pyrolysis Oil Biorefinery. In: . *Advances in Biochemical Engineering/Biotechnology*. Springer, Berlin, Heidelberg

Xie, W. & Pan, WP. *Journal of Thermal Analysis and Calorimetry* (2001) 65: 669. <https://doi.org/10.1023/A:1011946707342>

- E. Brown, Michael. (1988). Evolved gas analysis (EGA). 86-98. 10.1007/978-94-009-1219-9_10.
- TGA Brochure, TA instruments, 2012.
- Ugol'kov L. Valery (2007) Instruments for Thermogravimetric Measurements. In: Thermal Decomposition of Solids and Melts. Hot Topics in Thermal Analysis and Calorimetry, vol 7. Springer, Dordrecht.
- Thomas L.C., Schmidt S.J. (2010) Thermal Analysis. In: Food Analysis. Food Analysis. Springer, Boston, MA.
- Nirav S. Thermal Methods of Analysis. Mod Appl Pharm Pharmacol. 1(2). MAPP.000509. 2017.
- Haines P.J. (1995) Thermogravimetry. In: Thermal Methods of Analysis. Springer, Dordrecht.
- M. Reichenbacher and J. Popp, Challenges in Molecular Structure Determination, DOI 10.1007/978-3-642-24390-5_1, Springer-Verlag Berlin Heidelberg 2012.
- Nölting B. (2009) Mass spectrometry. In: Methods in Modern Biophysics. Springer, Berlin, Heidelberg.
- Chu C.S., Lebrilla C.B. (2010) Introduction to Modern Techniques in Mass Spectrometry. In: Jue T. (eds) Biomedical Applications of Biophysics. Handbook of Modern Biophysics, vol 3. Humana Press, Totowa, NJ.
- Malainey M.E. (2011) Mass Spectrometry. In: A Consumer's Guide to Archaeological Science. Manuals in Archaeological Method, Theory and Technique. Springer, New York, NY.
- Kaltashov I.A., Bobst C.E. (2013) Mass Spectrometry. In: Allewell N., Narhi L., Rayment I. (eds) Molecular Biophysics for the Life Sciences. Biophysics for the Life Sciences, vol 6. Springer, New York, NY.
- Smith J.S. (2010) Evaluation of Analytical Data. In: Food Analysis. Food Analysis. Springer, Boston, MA.
- Smith J.S. (2017) Evaluation of Analytical Data. In: Nielsen S. (eds) Food Analysis. Food Science Text Series. Springer, Cham.
- Khan J.I., Kennedy T.J., Christian D.R. (2012) Chromatography and Mass Spectrometry. In: Basic Principles of Forensic Chemistry. Humana Press, Totowa, NJ.
- Shinde K.N., Dhoble S.J., Swart H.C., Park K. (2012) Methods of Measurements (Instrumentation). In: Phosphate Phosphors for Solid-State Lighting. Springer Series in Materials Science, vol 174. Springer, Berlin, Heidelberg.
- Zaharescu M., Mocioiu O.C. (2013) Infrared Spectroscopy. In: Schneller T., Waser R., Kosec M., Payne D. (eds) Chemical Solution Deposition of Functional Oxide Thin Films. Springer, Vienna.
- S. Petit, J. Madejova, Chapter 2.7 - Fourier Transform Infrared Spectroscopy, Editor(s): Faïza Bergaya, Gerhard Lagaly, Developments in Clay Science, Elsevier, Volume 5, 2013, Pages 213-231, ISSN 1572-4352, ISBN 9780080993645, <https://doi.org/10.1016/B978-0-08-098259-5.00009-3>.
- B. Stuart, Infrared Spectroscopy: Fundamentals and Applications, 2004, John Wiley & Sons, Ltd ISBNs: 0-470-85427-8 (HB); 0-470-85428-6 (PB).
- Doyle, W.M.. (1992). Principles and applications of fourier transform infrared (FTIR) process analysis. 2. 11-41.
- Ismail B.P. (2017) Basic Principles of Chromatography. In: Nielsen S. (eds) Food Analysis. Food Science Text Series. Springer, Cham.
- Harold M. McNair and James M. Miller, Basic Gas Chromatography, Second Edition, 2009 John Wiley & Sons, Inc.
- F. Poole, Colin. (2017). Mark F. Vitha: Chromatography: Principles and Instrumentation. Chromatographia. 10.1007/s10337-017-3447-3.
- Toor S.S., Rosendahl L.A., Hoffmann J., Pedersen T.H., Nielsen R.P., Søgaard E.G. (2014) Hydrothermal Liquefaction of Biomass. In: Jin F. (eds) Application of Hydrothermal Reactions to Biomass Conversion. Green Chemistry and Sustainable Technology. Springer, Berlin, Heidelberg.

- Fantini M. (2017) Biomass Availability, Potential and Characteristics. In: Rabaçal M., Ferreira A., Silva C., Costa M. (eds) Biorefineries. Lecture Notes in Energy, vol 57. Springer, Cham.
- A.R.K. Gollakota, Nanda Kishore, Sai Gu, A review on hydrothermal liquefaction of biomass, Renewable and Sustainable Energy Reviews, Volume 81, Part 1, 2018, Pages 1378-1392, ISSN 1364-0321, <https://doi.org/10.1016/j.rser.2017.05.178>.
- Daniel J.M. Hayes, Chapter 2 - Biomass Composition and Its Relevance to Biorefining, In The Role of Catalysis for the Sustainable Production of Bio-fuels and Bio-chemicals, edited by Kostas S. Triantafyllidis, Angelos A. Lappas and Michael Stöcker, Elsevier, Amsterdam, 2013, Pages 27-65, ISBN 9780444563309, <https://doi.org/10.1016/B978-0-444-56330-9.00002-4>.
- Gerd Brunner, Chapter 8 - Processing of Biomass with Hydrothermal and Supercritical Water, Editor(s): Gerd Brunner, Supercritical Fluid Science and Technology, Elsevier, Volume 5, 2014, Pages 395-509, ISSN 2212-0505, ISBN 9780444594136, <https://doi.org/10.1016/B978-0-444-59413-6.00008-X>.
- Meincken, Martina & Tyhoda, Luvuyo. (2014). Biomass Quality. 26. 169-187. 10.1007/978-94-007-7448-3_8.
- Li, Li & S. Rowbotham, Jack & Greenwell, Chris & W. Dyer, Philip. (2013). An Introduction to Pyrolysis and Catalytic Pyrolysis: Versatile Techniques for Biomass Conversion. New and Future Developments in Catalysis: Catalytic Biomass Conversion. 173-208. 10.1016/B978-0-444-53878-9.00009-6.
- Faik A. (2013) "Plant Cell Wall Structure-Pretreatment" the Critical Relationship in Biomass Conversion to Fermentable Sugars. In: Gu T. (eds) Green Biomass Pretreatment for Biofuels Production. SpringerBriefs in Molecular Science. Springer, Dordrecht.
- Rafiqul I.S.M., Sakinah A.M.M., Zularisam A.W. (2017) Hydrolysis of Lignocellulosic Biomass for Recovering Hemicellulose: State of the Art. In: Singh L., Kalia V. (eds) Waste Biomass Management – A Holistic Approach. Springer, Cham.
- Rana V., Rana D. (2017) Role of Microorganisms in Lignocellulosic Biodegradation. In: Renewable Biofuels. SpringerBriefs in Applied Sciences and Technology. Springer, Cham.
- Victor Martínez-Merino, María José Gil and Alfonso Cornejo, Chapter 5 - Biomass Sources for Hydrogen Production, In Renewable Hydrogen Technologies, edited by Luis M. Gandía, Gurutze Arzamendi and Pedro M. Diéguez, Elsevier, Amsterdam, 2013, Pages 87-110, ISBN 9780444563521, <https://doi.org/10.1016/B978-0-444-56352-1.00005-2>.
- Abramson M., Shoseyov O., Hirsch S., Shani Z. (2013) Genetic Modifications of Plant Cell Walls to Increase Biomass and Bioethanol Production. In: Lee J. (eds) Advanced Biofuels and Bioproducts. Springer, New York, NY.
- Favaro S.P., Miranda C.H.B., Machado F., Soares I.P., Jensen A.T., Medeiros A.M.M.S. (2018) Oleaginous Biomass for Biofuels, Biomaterials, and Chemicals. In: Vaz Jr. S. (eds) Biomass and Green Chemistry. Springer, Cham.
- Behrendt D., Schreiber C., Pfaff C., Müller A., Grobbelaar J., Nedbal L. (2018) Algae as a Potential Source of Biokerosene and Diesel – Opportunities and Challenges. In: Kaltschmitt M., Neuling U. (eds) Biokerosene. Springer, Berlin, Heidelberg.
- Junmeng Cai, Di Xu, Zhujun Dong, Xi Yu, Yang Yang, Scott W. Banks, Anthony V. Bridgwater, Processing thermogravimetric analysis data for isoconversional kinetic analysis of lignocellulosic biomass pyrolysis: Case study of corn stalk, Renewable and Sustainable Energy Reviews, Volume 82, Part 3, 2018, Pages 2705-2715, ISSN 1364-0321, <https://doi.org/10.1016/j.rser.2017.09.113>.
- Shurong Wang, Gongxin Dai, Haiping Yang, Zhongyang Luo, Lignocellulosic biomass pyrolysis mechanism: A state-of-the-art review, Progress in Energy and Combustion Science, Volume 62, 2017, Pages 33-86, ISSN 0360-1285, <https://doi.org/10.1016/j.peccs.2017.05.004>.
- Yanming Ding, Ofodike A. Ezekoye, Shouxiang Lu, Changjian Wang, Ru Zhou, Comparative pyrolysis behaviors and reaction mechanisms of hardwood and softwood, Energy Conversion and Management, Volume 132, 2017, Pages 102-109, ISSN 0196-8904, <https://doi.org/10.1016/j.enconman.2016.11.016>.

Daizo Kunii and Octave Levenspiel, CHAPTER 3 - Fluidization and Mapping of Regimes, In Fluidization Engineering (Second Edition), Butterworth-Heinemann, Boston, 1991, Pages 61-94, ISBN 9780080506647, <https://doi.org/10.1016/B978-0-08-050664-7.50009-3>.

Andrés Anca-Couce, Reaction mechanisms and multi-scale modelling of lignocellulosic biomass pyrolysis, Progress in Energy and Combustion Science, Volume 53, 2016, Pages 41-79, ISSN 0360-1285, <https://doi.org/10.1016/j.peccs.2015.10.002>.

Brennan Pecha and Manuel Garcia-Perez, Chapter 26 - Pyrolysis of Lignocellulosic Biomass: Oil, Char, and Gas, In Bioenergy, edited by Anju Dahiya, Academic Press, Boston, 2015, Pages 413-442, ISBN 9780124079090, <https://doi.org/10.1016/B978-0-12-407909-0.00026-2>.

X. Zhou, L.J. Broadbelt, R. Vinu, Chapter Two - Mechanistic Understanding of Thermochemical Conversion of Polymers and Lignocellulosic Biomass, Editor(s): Kevin M. Van Geem, Advances in Chemical Engineering, Academic Press, Volume 49, 2016, Pages 95-198, ISSN 0065-2377, ISBN 9780128097779, <https://doi.org/10.1016/bs.ache.2016.09.002>.

Abhishek Sharma, Vishnu Pareek, Shaobin Wang, Zhezi Zhang, Hong Yang, Dongke Zhang, A phenomenological model of the mechanisms of lignocellulosic biomass pyrolysis processes, Computers & Chemical Engineering, Volume 60, 2014, Pages 231-241, ISSN 0098-1354, <https://doi.org/10.1016/j.compchemeng.2013.09.008>.

Lina N. Samuelsson, Matthaus U. Babler, Rosana Moriana, A single model-free rate expression describing both non-isothermal and isothermal pyrolysis of Norway Spruce, Fuel, Volume 161, 2015, Pages 59-67, ISSN 0016-2361, <https://doi.org/10.1016/j.fuel.2015.08.019>.

Tao Kan, Vladimir Strezov, Tim J. Evans, Lignocellulosic biomass pyrolysis: A review of product properties and effects of pyrolysis parameters, Renewable and Sustainable Energy Reviews, Volume 57, 2016, Pages 1126-1140, ISSN 1364-0321, <https://doi.org/10.1016/j.rser.2015.12.185>.

Xiaoyan Jiang, Qiang Lu, Bin Hu, Ji Liu, Changqing Dong, Yongping Yang, Intermolecular interaction mechanism of lignin pyrolysis: A joint theoretical and experimental study, Fuel, Volume 215, 2018, Pages 386-394, ISSN 0016-2361, <https://doi.org/10.1016/j.fuel.2017.11.084>.

Jie Yu, Nigel Paterson, John Blamey, Marcos Millan, Cellulose, xylan and lignin interactions during pyrolysis of lignocellulosic biomass, Fuel, Volume 191, 2017, Pages 140-149, ISSN 0016-2361, <https://doi.org/10.1016/j.fuel.2016.11.057>.

Xiaolei Zhang, Weihong Yang, Wlodzimierz Blasiak, Kinetics of levoglucosan and formaldehyde formation during cellulose pyrolysis process, Fuel, Volume 96, 2012, Pages 383-391, ISSN 0016-2361, <https://doi.org/10.1016/j.fuel.2012.01.006>.

Xianglan Bai, Robert C. Brown, Modeling the physiochemistry of levoglucosan during cellulose pyrolysis, Journal of Analytical and Applied Pyrolysis, Volume 105, 2014, Pages 363-368, ISSN 0165-2370, <https://doi.org/10.1016/j.jaap.2013.11.026>.

Xiaolei Zhang, Weihong Yang, Changqing Dong, Levoglucosan formation mechanisms during cellulose pyrolysis, Journal of Analytical and Applied Pyrolysis, Volume 104, 2013, Pages 19-27, ISSN 0165-2370, <https://doi.org/10.1016/j.jaap.2013.09.015>.

Asuka Fukutome, Haruo Kawamoto, Shiro Saka, Kinetics and molecular mechanisms for the gas-phase degradation of levoglucosan as a cellulose gasification intermediate, Journal of Analytical and Applied Pyrolysis, Volume 124, 2017, Pages 666-676, ISSN 0165-2370, <https://doi.org/10.1016/j.jaap.2016.12.010>.

Yunyun Peng, Shubin Wu, The structural and thermal characteristics of wheat straw hemicellulose, Journal of Analytical and Applied Pyrolysis, Volume 88, Issue 2, 2010, Pages 134-139, ISSN 0165-2370, <https://doi.org/10.1016/j.jaap.2010.03.006>.

Shuai Zhou, Brennan Pecha, Michiel van Kuppevelt, Armando G. McDonald, Manuel Garcia-Perez, Slow and fast pyrolysis of Douglas-fir lignin: Importance of liquid-intermediate formation on the distribution of products, Biomass and Bioenergy, Volume 66, 2014, Pages 398-409, ISSN 0961-9534, <https://doi.org/10.1016/j.biombioe.2014.03.064>.

Pedro E. Sánchez-Jiménez, Luis A. Pérez-Maqueda, Antonio Perejón, José M. Criado, Limitations of model-fitting methods for kinetic analysis: Polystyrene thermal degradation, *Resources, Conservation and Recycling*, Volume 74, 2013, Pages 75-81, ISSN 0921-3449, <https://doi.org/10.1016/j.resconrec.2013.02.014>.

Vaz S. (2016) The Use of Analytical Chemistry to Understand Biomass. In: Vaz Jr. S. (eds) *Analytical Techniques and Methods for Biomass*. Springer, Cham.

Seyed Hadi SHAHCHERAGHI, Gholam Reza KHAYATI, Arrhenius parameters determination in non-isothermal conditions for mechanically activated Ag₂O-graphite mixture, *Transactions of Nonferrous Metals Society of China*, Volume 24, Issue 12, 2014, Pages 3994-4003, ISSN 1003-6326, [https://doi.org/10.1016/S1003-6326\(14\)63561-5](https://doi.org/10.1016/S1003-6326(14)63561-5).

Murillo, J. D., Biernacki, J. J., Northrup, S., & Mohammad, A. S.. (2017). BIOMASS PYROLYSIS KINETICS: A REVIEW OF MOLECULAR-SCALE MODELING CONTRIBUTIONS. *Brazilian Journal of Chemical Engineering*, 34(1), 1-18. <https://dx.doi.org/10.1590/0104-6632.20170341s20160086>.

Weixuan Wu, Yuanfei Mei, Le Zhang, Ronghou Liu, and Junmeng Cai , Effective Activation Energies of Lignocellulosic Biomass Pyrolysis *Energy & Fuels* 2014 28 (6), 3916-3923 DOI: 10.1021/ef5005896.

Xiaojie Zhang, Wiebren de Jong, Fernando Preto, Estimating kinetic parameters in TGA using B-spline smoothing and the Friedman method, *Biomass and Bioenergy*, Volume 33, Issue 10, 2009, Pages 1435-1441, ISSN 0961-9534, <https://doi.org/10.1016/j.biombioe.2009.06.009>.

R. Font, M.A. Garrido, Friedman and n-reaction order methods applied to pine needles and polyurethane thermal decompositions, *Thermochimica Acta*, Volume 660, 2018, Pages 124-133, ISSN 0040-6031, <https://doi.org/10.1016/j.tca.2018.01.002>.

Gamzenur Özsin, Ayşe Eren Pütün, Insights into pyrolysis and co-pyrolysis of biomass and polystyrene: Thermochemical behaviors, kinetics and evolved gas analysis, *Energy Conversion and Management*, Volume 149, 2017, Pages 675-685, ISSN 0196-8904, <https://doi.org/10.1016/j.enconman.2017.07.059>.

G. Santhosh, P.B. Soumyamol, M. Sreejith, S. Reshmi, Isoconversional approach for the non-isothermal decomposition kinetics of guanyurea dinitramide (GUDN), *Thermochimica Acta*, Volume 632, 2016, Pages 46-51, ISSN 0040-6031, <https://doi.org/10.1016/j.tca.2016.03.019>.

Peiyong Ma, Jing Yang, Xianjun Xing, Sebastian Weihrich, Fangyu Fan, Xianwen Zhang, Isoconversional kinetics and characteristics of combustion on hydrothermally treated biomass, *Renewable Energy*, Volume 114, Part B, 2017, Pages 1069-1076, ISSN 0960-1481, <https://doi.org/10.1016/j.renene.2017.07.115>.

Aaron Chee Ren Lim, Bridgid Lai Fui Chin, Zeinab Abbas Jawad, Kiew Ling Hii, Kinetic Analysis of Rice Husk Pyrolysis Using Kissinger-Akahira-Sunose (KAS) Method, *Procedia Engineering*, Volume 148, 2016, Pages 1247-1251, ISSN 1877-7058, <https://doi.org/10.1016/j.proeng.2016.06.486>.

Özge Çepelioğullar, Hanzade Haykırı-Açma, Serdar Yaman, Kinetic modelling of RDF pyrolysis: Model-fitting and model-free approaches, *Waste Management*, Volume 48, 2016, Pages 275-284, ISSN 0956-053X, <https://doi.org/10.1016/j.wasman.2015.11.027>.

Martí-Rosselló T, Li J, Lue L. Kinetic models for biomass pyrolysis. *Arch Ind Biotechnol*. 2016; 1(1): 4-7

Pedro E. Sánchez-Jiménez, Luis A. Pérez-Maqueda, Antonio Perejón, José M. Criado, Limitations of model-fitting methods for kinetic analysis: Polystyrene thermal degradation, *Resources, Conservation and Recycling*, Volume 74, 2013, Pages 75-81, ISSN 0921-3449, <https://doi.org/10.1016/j.resconrec.2013.02.014>.

Vyazovkin, S. *J Therm Anal Calorim* (2006) 83: 45. <https://doi.org/10.1007/s10973-005-7044-6>.

Ranjeet Kumar Mishra, Kaustubha Mohanty, Pyrolysis kinetics and thermal behavior of waste sawdust biomass using thermogravimetric analysis, *Bioresource Technology*, Volume 251, 2018, Pages 63-74, ISSN 0960-8524, <https://doi.org/10.1016/j.biortech.2017.12.029>.

Martí-Rosselló T, Li J, Lue L. Kinetic models for biomass pyrolysis. *Arch Ind Biotechnol*. 2016; 1(1): 4-7.

Brebu, Mihai & Vasile, Cornelia. (2010). Thermal degradation of lignin – A Review. *Cellulose Chemistry and Technology*. 44. 353-363.

Jiaxi Fang, Anna Leavey, Pratim Biswas, Controlled studies on aerosol formation during biomass pyrolysis in a flat flame reactor, *Fuel*, Volume 116, 2014, Pages 350-357, ISSN 0016-2361, <https://doi.org/10.1016/j.fuel.2013.08.002>.

Sijiang Xiong, Jiankun Zhuo, Beiping Zhang, Qiang Yao, Effect of moisture content on the characterization of products from the pyrolysis of sewage sludge, *Journal of Analytical and Applied Pyrolysis*, Volume 104, 2013, Pages 632-639, ISSN 0165-2370, <https://doi.org/10.1016/j.jaap.2013.05.003>.

E. Salehi, J. Abedi, and T. Harding, Bio-oil from Sawdust: Pyrolysis of Sawdust in a Fixed-Bed System, *Energy & Fuels* 2009 23 (7), 3767-3772, DOI: 10.1021/ef900112b.

Sevgi Şensöz, Dilek Angın, Pyrolysis of safflower (*Charthamus tinctorius* L.) seed press cake: Part 1. The effects of pyrolysis parameters on the product yields, *Bioresource Technology*, Volume 99, Issue 13, 2008, Pages 5492-5497, ISSN 0960-8524, <https://doi.org/10.1016/j.biortech.2007.10.046>.

Tevfik Aysu, M. Maşuk Küçük, Biomass pyrolysis in a fixed-bed reactor: Effects of pyrolysis parameters on product yields and characterization of products, *Energy*, Volume 64, 2014, Pages 1002-1025, ISSN 0360-5442, <https://doi.org/10.1016/j.energy.2013.11.053>.

Won Chan Park, Arvind Atreya, Howard R. Baum, Experimental and theoretical investigation of heat and mass transfer processes during wood pyrolysis, *Combustion and Flame*, Volume 157, Issue 3, 2010, Pages 481-494, ISSN 0010-2180, <https://doi.org/10.1016/j.combustflame.2009.10.006>.

Jun Shen, Xiao-Shan Wang, Manuel Garcia-Perez, Daniel Mourant, Martin J Rhodes, Chun-Zhu Li, Effects of particle size on the fast pyrolysis of oil mallee woody biomass, *Fuel*, Volume 88, Issue 10, 2009, Pages 1810-1817, ISSN 0016-2361, <https://doi.org/10.1016/j.fuel.2009.05.001>.

S Şensöz, D Angın, S Yorgun, Influence of particle size on the pyrolysis of rapeseed (*Brassica napus* L.): fuel properties of bio-oil, *Biomass and Bioenergy*, Volume 19, Issue 4, 2000, Pages 271-279, ISSN 0961-9534, [https://doi.org/10.1016/S0961-9534\(00\)00041-6](https://doi.org/10.1016/S0961-9534(00)00041-6).

Wan Nor Roslam Wan Isahak, Mohamed W.M. Hisham, Mohd Ambar Yarmo, Taufiq-yap Yun Hin, A review on bio-oil production from biomass by using pyrolysis method, *Renewable and Sustainable Energy Reviews*, Volume 16, Issue 8, 2012, Pages 5910-5923, ISSN 1364-0321, <https://doi.org/10.1016/j.rser.2012.05.039>.

Thilakavathi Mani, Pulikesi Murugan, Jalal Abedi, Nader Mahinpey, Pyrolysis of wheat straw in a thermogravimetric analyzer: Effect of particle size and heating rate on devolatilization and estimation of global kinetics, *Chemical Engineering Research and Design*, Volume 88, Issue 8, 2010, Pages 952-958, ISSN 0263-8762, <https://doi.org/10.1016/j.cherd.2010.02.008>.

Kwang Ho Kim, In Yong Eom, Soo Min Lee, Donha Choi, Hwanmyeong Yeo, In-Gyu Choi, Joon Weon Choi, Investigation of physicochemical properties of biooils produced from yellow poplar wood (*Liriodendron tulipifera*) at various temperatures and residence times, *Journal of Analytical and Applied Pyrolysis*, Volume 92, Issue 1, 2011, Pages 2-9, ISSN 0165-2370, <https://doi.org/10.1016/j.jaap.2011.04.002>.

Alina Rahayu Mohamed, Zainab Hamzah, Mohamed Zulkali Mohamed Daud, Zarina Zakaria, The Effects of Holding Time and the Sweeping Nitrogen Gas Flowrates on the Pyrolysis of EFB using a Fixed-Bed Reactor, *Procedia Engineering*, Volume 53, 2013, Pages 185-191, ISSN 1877-7058, <https://doi.org/10.1016/j.proeng.2013.02.024>.

Selim Ceylan, Dilek Kazan, Pyrolysis kinetics and thermal characteristics of microalgae *Nannochloropsis oculata* and *Tetraselmis* sp., *Bioresource Technology*, Volume 187, 2015, Pages 1-5, ISSN 0960-8524, <https://doi.org/10.1016/j.biortech.2015.03.081>.

A. Soria-Verdugo, L.M. Garcia-Gutierrez, L. Blanco-Cano, N. Garcia-Hernando, U. Ruiz-Rivas, Evaluating the accuracy of the Distributed Activation Energy Model for biomass devolatilization curves obtained at high heating rates, *Energy Conversion and Management*, Volume 86, 2014, Pages 1045-1049, ISSN 0196-8904, <https://doi.org/10.1016/j.enconman.2014.06.074>.

Khan Muhammad Qureshi, Andrew Ng Kay Lup, Saima Khan, Faisal Abnisa, Wan Mohd Ashri Wan Daud, A technical review on semi-continuous and continuous pyrolysis process of biomass to bio-oil, *Journal of Analytical and Applied Pyrolysis*, Volume 131, 2018, Pages 52-75, ISSN 0165-2370, <https://doi.org/10.1016/j.jaap.2018.02.010>.

Abhishek Sharma, Vishnu Pareek, Dongke Zhang, Biomass pyrolysis—A review of modelling, process parameters and catalytic studies, *Renewable and Sustainable Energy Reviews*, Volume 50, 2015, Pages 1081-1096, ISSN 1364-0321, <https://doi.org/10.1016/j.rser.2015.04.193>.

Manoj Tripathi, J.N. Sahu, P. Ganesan, Effect of process parameters on production of biochar from biomass waste through pyrolysis: A review, *Renewable and Sustainable Energy Reviews*, Volume 55, 2016, Pages 467-481, ISSN 1364-0321, <https://doi.org/10.1016/j.rser.2015.10.122>.

Tao Kan, Vladimir Strezov, Tim J. Evans, Lignocellulosic biomass pyrolysis: A review of product properties and effects of pyrolysis parameters, *Renewable and Sustainable Energy Reviews*, Volume 57, 2016, Pages 1126-1140, ISSN 1364-0321, <https://doi.org/10.1016/j.rser.2015.12.185>.

Antonio Soria-Verdugo, Elke Goos, Nestor García-Hernando, Uwe Riedel, Analyzing the pyrolysis kinetics of several microalgae species by various differential and integral isoconversional kinetic methods and the Distributed Activation Energy Model, *Algal Research*, Volume 32, 2018, Pages 11-29, ISSN 2211-9264, <https://doi.org/10.1016/j.algal.2018.03.005>.

Garima Mishra, Jitendra Kumar, Thallada Bhaskar, Kinetic studies on the pyrolysis of pinewood, *Bioresource Technology*, Volume 182, 2015, Pages 282-288, ISSN 0960-8524, <https://doi.org/10.1016/j.biortech.2015.01.087>.